Tectonic Deformation of the Oceanic Lithosphere at Ridge Transform Intersections

RRS Charles Darwin Cruise 100
Cruise Report

April-May 1996

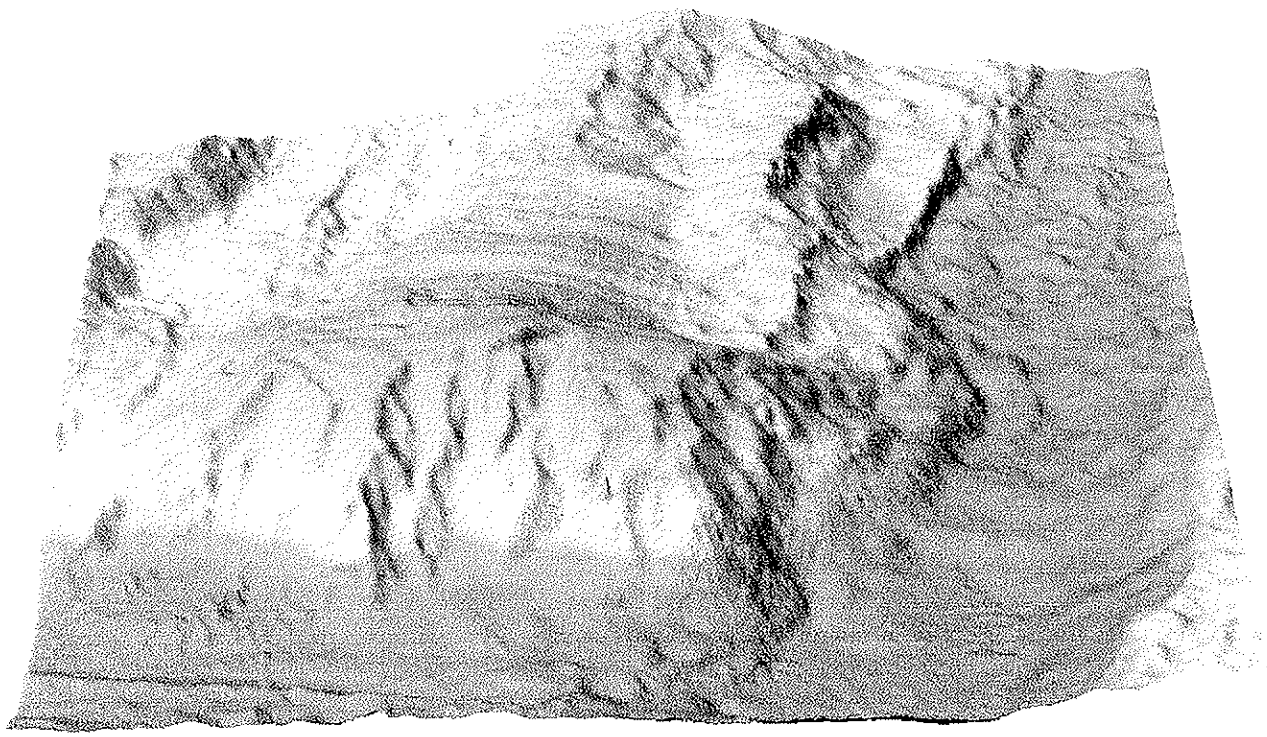

Contents

CD 100
NOBSKA

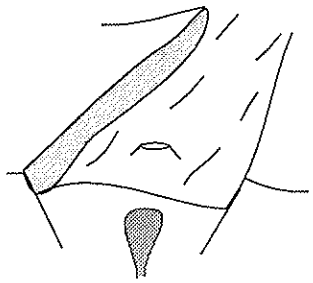

Section 1.0 Overview

Tectonic-volcanic control on segment morphology and lithospheric scale deformation.

1.1 Summary of Results

1.1.1 Scientific summary

The scientific work during RRS Charles Darwin Cruise 100 took a somewhat different course than had been planned because of problems with the Tobi deep-towed side-scan sonar vehicle and with the Shrimp camera system. It focussed eventually on three different areas and their associated problems: (a) the full length of the Nobska spreading segment and its volcanism and tectonics, (b) the southern end of the Broken Spur segment and the landslide zones at its inside corner, and (c) the Atlantis transform and the nature of its inside and outside corners.

(a) The NOBSKA Segment

The NOBSKA (North of Broken Spur, Kane to Atlantis) segment, is about 100km long, and is bounded by the Atlantis Transform Fault at the north, and by the non-transform offset separating it from the Broken Spur segment to the south. The segment has an asymmetric longitudinal axial profile, with the greatest axial depths at the north end because of the presence of the transform, but with the shallowest depths paradoxically near to the north end rather than to the south end. Towards its southern end, the segment is symmetrical in cross section, with a median valley floor bounded by major fault zones with a throw of hundreds of metres, but to the north, the throw of the faults on the west side reduces until it is difficult to define the median valley floor. On the east side there is still a significant boundary fault even at the north end.

The style of volcanism is consistent along the whole segment. The most recent volcanism, judged by the brightness of the sonar return, forms an axial volcanic

ridge within the median valley floor. Most of this ridge is constructed of hummocky flows, and these hummocky regions often contain strings of hummocks defining the location of eruptive fissures. There are numerous point sources of eruption forming small seamounts. These are almost all coated with smooth lava, and have smooth flat tops. Some are surrounded with a flat smooth halo, defining the greatest extent of lava flowing from the source. The abundance of smooth flat seamounts on the axial volcanic ridge is unusual; previous surveys of other segments showed that most point source eruptions form hummocky heaps (Smith et al., J. Volc. Geotherm. Res., 1996).

As the axial volcanic ridge approaches the southern end of the segment, it becomes smaller, and the thickness of sediment on the valley floor increases, until it is possible to define sporadic single flow units newly-erupted onto much older sedimented flows. Towards the northern end of the segment, near to the transform fault, the volcanism shows no signs of decreasing in vigour, and a major volcanic ridge extends into the transform domain. This ridge curves markedly to the east within 10km of the transform, showing its response to the stress field around the ridge-transform intersection.

One conspicuous feature of the segment is Yellow Mountain, which rises to within1km of the surface on the eastern rim of the median valley near its N end. The morphology of the mountain, with its radiating finger ridges, suggests that it may be a near-axis volcano, perhaps similar to the near-axis volcanoes of the Juan de Fuca Ridge. Its side nearest to the median valley is covered with debris flow material, and from these flows several dredges of basalt were made. Geochemical analysis will give some further clues to its nature.

The style of faulting shows great contrasts from side to side and from end to end of the segment. At the southern end, the inner corner of the NTO is marked by a major steep fault scarp up to 1km high, from which we dredged dolerites that may be part of a sheeted dyke unit. Further N, at the centre of the segment, the faulting is nearly symmetrical, with large faults with a throw of hundreds of metres on each side. At this position are some small, but apparently significant, faults in the middle of the axial volcanic ridge, possibly representing early stages in the growth of the next major median valley wall fault. Towards the N end of the segment, the faults on the western side become smaller and less abundant, until there is no clear tectonic boundary to the median valley floor. Tobi images show that the volcanics become gradually more sediment-covered, and hence older, to the west, suggesting progressive accretion of volcanic crust without sudden breaks related to faulting. This progressive disappearance of faults as the transform is approached seems to run counter to current ideas that more strain is accommodated by faulting near to transform faults.

(b) Broken Spur segment

CD100 was in many ways a follow-up to CD65, which worked in the Broken Spur segment among others, and, when Tobi was not working in the Nobska segment, we came south to dredge the landslide area that we had identified on CD65. This lies at the inside corner at the south end of the Broken Spur segment, and shows a wide range of debris flow morphologies on previous Tobi images. Four successful dredges were made there to supplement the one we made previously, and brought back a range of basalts, gabbros, pyroxenites and

wholly or partly serpentinised peridotites, emphasising the heterogeneous nature of the landslide material, and the inorporation within it of rocks from upper crust, lower crust and upper mantle.

(c) Atlantis Transform Fault

Transform domains are complex environments about which much has been writen, but which have not before been studied in detail at the intermediate scales possible with Tobi, and with the enhanced topographic visualisation possible on CD100. The transform fault itself could be identified as a single fault strand in the transform valley, running from the transform wall at the end of one segment to the same position at the other, and hence running obliquely across the transform valley. Tobi images showed that at the west end it splits into extensional splays linking through to the Nobska segment. Bathymetry shows it to be a simple single fault at its east end as well, but to be more complex in its central section.

The two ridge-transform intersections were at very different stages of evolution. The western RTI is volcanically robust, with a ridge of young volcanics running across the nodal deep to the transform wall on the other side. West of the volcanic ridge are progressively older volcanics, unbroken by any major fault, showing a long-continued volcanic robustness in this part of the transform. At this western end of the transform there is no currently-active inside corner high. The inside corner is separated from the southern extension of the nodal deep by a fault, and within the inside corner area bathymetry shows irregular hills up to a few hundred metres high, which Tobi images show to be covered with different types of debris flow sonar facies. Two dredge hauls were made in this area: one brought up basalts and the other serpentinised peridotites.

At the other end of the transform, the eastern RTI is volcanically starved. There are no fresh volcanics in the area of the nodal deep, nor for 20km from there up the median valley axis. There is a robust volcanic ridge on the outer corner, but it is sedimented, and separated from the nodal deep by two large faults. The inside corner at the eastern RTI has a large active inside corner high rising to within 1000m of the surface. The highest part of this lies closest to the transform, and is made up of serpentinites and gabbros to judge from dredge hauls. A few kilometres further N there is a wide corrugated surface, curved into a cylinder with a horizontal axis, striated on top of the corrugations. The corrugations and striations run parallel to the spreading direction. This surface runs underneath a large slipped block of crust with hummocky volcanic morphology on its upper surface. Dredge hauls indicate that this is made of basaltic material, while serpentinised peridotite was recovered from the striated surface itself.

A fossil inside corner high on the southern side of the transform valley possesses a similarly corrugated and striated surface, again striated parallel to the spreading direction. This surface is nearly horizontal, dipping at a very low angle to the south. Basalts and serpentinite were recovered from this block, with the serpentinite coming from a dredge haul on the striated surface. Another fossil inside corner high to the north of the transform shows spreading-parallel corrugations on a surface dipping down into the transform valley.

Both the active and fossil inside corner highs, and the walls of the transform valley between them, show extensive signs of landsliding both from bathymetry and from Tobi, and large amounts of landslide material are being fed into the transform valley, potentially making up a large part of the crust there.

1.1.2 Operational summary

Operations on the ship were enhanced by the first class teamwork involving everyone on board. All individuals made important contributions to the success of the whole venture, and showed great professional dedication even when circumstances were at their most difficult. Everyone deserves the heartiest congratulations for their hard work.

Operational difficulties arose from instrumental problems and from a prolonged spell of unexpectedly rough weather for the location and the time of year. Both types of problem resulted in substantial modifications to the planned programme of work. On the other hand, the modifications also provided new opportunities for science, and opened up the most interesting developments arising from the cruise.

The shipboard computing system operated very well indeed. We were able to integrate our own powerful science system into the onboard network and transfer files from one to the other. This allowed us to conduct a substantial part of our data reduction on board ship, and to generate very high quality output from the data. In this we were assisted substantially by the efforts of the CD99 scientists in setting up the system in the first place, and through the loan of their hardware and software.

The Simrad system produced first class data which were transferred through the network to the science system. The overall quality of the maps and images was substantially higher than on previous surveys of the region, and contributed significantly to the scientific insights. It would be appropriate to give the Simrad operators who do not have the specific skills some training in basic data processing through the Neptune system to increase the interest and productivity of the otherwise very tedious Simrad watchkeeping.

Tobi was plagued by problems in the early part of the cruise, was always subject to unexplained noise of variable intensity, and did not perform to specification in its phase bathymetry. The quality of the side scan images was rarely as good as we had obtained four years previously on CD65. To some extent this meant that CD100 was another extension of the string of Tobi trials cruises rather than an application of the technology to science. Many of the failures were of simple components such as connectors and seals which had functioned well previously but were now not satisfactory, partly, perhaps, because of enhanced power loading putting unanticipated stress on these components. At an early stage in the cruise we disabled the Tobi gyro because of its potential effect on slip ring failures at the depressor swivel. Far range oscillatory noise in the side scan images was never traced to its source, and affected the image quality significantly at times. Phase bathymetry was always poor on the port side. After an indexing problem had been solved, the phase information of the starboard side looked good, but the problems of turning these rather noisy data into bathymetric maps remain severe, mainly because of the difficulty of maintaining

phase wrap identification against a background of significant noise. Further efforts on noise reduction will be important if bathymetry is to be obtained on a routine basis.

The modified Whips software proved to require substantial effort in rewriting and editing before being useful, despite the efforts put into this area by the CD99 scientists. Some of the routines were based on a poor appreciation of actual operating practice, and modifications were hampered by poor commenting.

The prototype Shrimp camera system was plagued by problems. The first two stations were nearly unproductive because of winding-on problems caused, apparently, by friction between the film spool and the camera case. On the third station, conducted in poor weather, the battery pack on the instrument became detached from its mounting, and escaped from the frame, thus preventing any further use of the camera system. Some photographs were obtained on stations 1 and 3.

Most dredge stations went very smoothly indeed, thanks to the professional cooperation between bridge officers and winch drivers. Two dredges were lost in very difficult terrain during bad weather, when very sudden stresses were put on the weak links. A pipe dredge was lost from a dredge bag in similarly difficult terrain.

The proton magnetometer and the gravity meter functioned very well throughout, yielding data of high quality. The Japanese 3-component magnetometer continued to operate for most of the criuse, though the data became more and more noisy with time. Interpretation of the data will be the responsibility of the Japanese group.

1.2 Personnel

The personnel listed below formed the scientific and support party on Leg 100 in the North Atlantic. Specific responsiblities of each person is highlighted.

Scientific Personnel	Ship board role
Johnson R. Cann Dept. of Earth Sciences, University of Leeds Leeds LS2 9JT. j.cann@earth.leeds.ac.uk 0113 233-5204 0113-233-5259 (fax).	(Principal Investigator)
Donna K. Blackman (co. PI) Dept. of Earth Sciences, University of Leeds Leeds LS2 9JT. dkb@earth.leeds.ac.uk 0113 233-XXXX 0113-233-5259 (fax)	(TOBI Bathymetry)
Deborah K. Smith Dept. of Geology & Geophysics Woods Hole Oceongraphic Institution, Woods Hole, MA 02543. d.smith@humm.whoi.edu	(Sidescan)
Eddie McAllister Rock Deformation Research, Dept. of Earth Sciences, University of Leeds Leeds LS2 9JT. e.mcallister@earth.leeds.ac.uk 0113 233-5208 0113-233-5208 (fax).	(Processing TOBI data)
Bob Janssen Dept. of Earth Sciences, University of Leeds Leeds LS2 9JT. b.janssen@earth.leeds.ac.uk 0113 233-6624 0113-233-5259 (fax).	(Navigation)
Rachel Pascoe Dept. of Earth Sciences, University of Leeds Leeds LS2 9JT. r.pascoe@earth.leeds.ac.uk 0113-233-5259 (fax).	(Magnetics)

Sidney Mello (Simrad bathymetry)
Dept. of Earth Sciences,
University of Leeds
Leeds LS2 9JT.
s.mello@earth.leeds.ac.uk
0113-233-5259 (fax).

Mike Avgerinos (Simrad bathymetry)
Dept. of Earth Sciences,
University of Leeds
Leeds LS2 9JT.
e.avgerinos@earth.leeds.ac.uk
0113-233-5259 (fax).

Support Personnel	Role
Chris Flewellen Duncan Mathew Dave Edge Ocean Technology Division Southampton Oceanographic Centre University of Southampton Southampton	TOBI Team SHRIMP
Martin Beney Rod Pearce	Ship computing network/navigation Simrad processing
Chris Paulson Chris Hunter	Underway geophysics
Kevin Smith Jason Scott David Dunster	Winch operators

Research Vessel Services,
Southampton Oceanographic Centre,
European Way,
Empress Dock,
Southampton.

1.3 Scientific Objectives

1.3.1 Background

Charles Darwin Cruise 100 set out to investigate two related problems: (a) Can observed patterns of crustal deformation over a wide range of scales at the ends of spreading segments be simulated by numerical modelling, thus giving constraints on mantle dynamics beneath mid-ocean ridges? (b) Are the major scarps characteristic of inside corner highs at segment terminations low angle detachment faults or are they low angle failure surfaces in serpentinite extruding from diapirs rising along steep faults? If they are serpentinite failure slopes, what is the role of serpentinite in oceanic crustal construction? To answer these questions CD100 set out to undertake a programme of field observations of the NOBSKA (North of Broken Spur, Kane to Atlantis) Segment of the Mid Atlantic Ridge with the upgraded TOBI sidescan sonar instrument (newly equipped with swath bathymetry) and with the Simrad EM12 multibeam echosounder, and through a programme of dredging and camera work.

The principal aims of this work are:

- To quantify the mantle dynamics that lead to crustal deformation at a wide range of scales in a spreading segment at a slow spreading ridge, especially at and close to transform and non-transform offsets.
- To discriminate between two contrasting hypotheses for the major low angle scarps near inside corner highs at segment terminations, that they are either (a) low angle detachment faults separating the lower crust from the upper crust, or (b) failure slopes of the surfaces of serpentinite diapirs that rise along steep lithosphere-penetrating normal faults.

Other aims are:

- To quantify the volcanic constructional topography of a single spreading segment, and to relate this to models of volcanic plumbing beneath a spreading axis
- To determine the patterns of faulting that accompany crustal construction in a spreading segment and to compare these with patterns seen in continental rifting.
- To examine the interplay between faulting and volcanism on the median valley floor.
- To link measurements of the magnetic field at the surface and near the sea floor with volcanic and tectionic processes.
- To compare crustal generation in the Kane-Atlantis region with those at 45 N on the Mid-Atlantic Ridge.

These aims require the following objectives:

1. To make a detailed survey of a single major spreading segment adjacent to a transform fault, collecting bathymetry, high-resolution deep-towed side-scan sonar images, measurements of gravity at the surface, and of magnetic field at the surface and at the sea floor.

2. To obtain ground truth for this survey through dredging and photography.

3. To correlate and coanalyse these observations through a programme of image processing and image analysis.

4. To conduct numerical modelling of crustal deformation to examine the following questions:

(a) What are the processes and system parameters that control along-strike variation in stress and related strain in the lithosphere at slow spreading centres?

(b) What are the effects of mantle flow, including regional flow in the asthenosphere, geometrically induced flow, and buoyancy induced flow, near to segment boundaries on crustal deformation?

(c) How can the contrasting effects of deformation seen near transform and non transform segment boundaries be explained in terms of the magnitude and nature of the offset?

The modelling will follow the collection of information during the cruise.

1.4 Instrumentation

1.4.1 TOBI (Towed Ocean Bottom Instruments)

TOBI is a deep-tow stable platform designed primarily to carry high resolution sidescan, high resolution swath bathymetry, a bottom profiler and a three component magnetometer. Additional instrument packages include a Conductivity Temperature Density (CTD) probe, a Gyro and a sensor on the vehicle movements: pressure, pitch, heading. Data is transferred upstream via a armoured co-axial conducting tow cable.

The vehicle has an open aluminum frame under syntactic foam buoyancy blocks. It is approximatley 4 metres in length and 2 metres wide and weighs 2.5 tonnes in air, although in water it is very slightly positively buoyant. TOBI is separated from the conductive cable by a 200 m long neutrally buoyant umbilical cable, which is linked to a 600 kg depressor weight. The depressor weight dampens any sudden movements in the towed cable, most common in large sea swells.

Operational towing speed during surveying is 1.5 to 2 kts, with towing height of approximately 500 m of the seafloor. The sidescan operates at a frequency of approximately 30 kHz on the port and 32 kHz on the starboard side, this produces a sidescan swath width of 6000 metres, 3000 metres to either side, with a resolution of 3 x 3 metres per pixel in the near range and 30 x 2 metres at the far range.

Data logging and on-line displays are controlled by 3 pentium PC's and a PS/2. The data is logged every 4 seconds, displayed on a bank of moniters, and stored onto a 1.2 Giga bytes magneto-optical cartridge (approx. 18 hours of data). The main on-line displays are: 1. a slant-range corrected sidescan image; 2. a vertical profile below the vehicle; 3. a display of the phase information; 4. vehicle sensor data.(See "TOBI Processing" on page 95. for a full discussion of the TOBI data stream and processing route carried out).

1.4.2 SIMRAD

The RRS Charles Darwin is equipped with the SIMRAD EM 12S - 120 Hydrographic echosounder (Simrad Subsea A/S, Horten, Norway). The echosounder's technical specifications are summarised in the following:

- Operation frequency 13 kHz.
- Angular coverage of 90°, 105° and 120° with 81 beams spaced at 1.125°, 1.3125° and 1.5° respectively. In the EM 12S - 120 a software option extends the coverage to 120° gaining 4-5 km in swath width at depths of 3000-6000 m. This is reduced automatically when the vessel's roll is excessive.
- Precise swath mapping of full ocean depths (up to 11,000 m). -Typical accuracy (after processing) of 0.25% of the water depth and swath capability up to 3.5 times the water depth.
- Separate transducer arrays for transmission and reception, mounted in the vessel's hull in a cross-shaped configuration.
- Sea surface sound velocity sensor, located in an isolated tank within the hull too.
- Bottom detection largely based on phase (interferometric principle) or on amplitude for near normal incidence.
- Simrad's data logging system is MERMAID.
- Simrad's post processing system is NEPTUNE.

During the RRS Charles Darwin Cruise 100 EM 12 was mostly working in DEEP MODE, which sets the transmitter pulse length to 10 ms to allow maximum transmitted energy. This permits the use of narrower filters in the receiver, thus improving noise reduction. The transmission sector is tailored to the angular coverage sector, stabilised for roll (±15°) and pitch (±10°) and covered by several beams within each ping. The reception beams are roll stabilised and the sampling interval in each beam is 240 cm in range. The transmission and the reception athwartships beamwidths are 1.8° and 3.5° whereas the alongship beamwidths are 1.8° and 20° respectively. Compensation for the vessel's pitch and roll ensure accurate beam steering towards the ocean, obtaining maximum bottom echo and keeping a regularly sampled coverage of the seafloor.

The wide coverage sectors of EM 12S-120 would normally result in an across-track increase of sounding spacing from the centre with equi-angle beam spacing, however the beam spacing of the EM 12S - 120 is set to be equidistant in horizontal spacing rather than angle (EDBS mode, EquiDistant Beam Spacing) to enable regular sampling of the seabed and easier post-processing.

The coverage sector is automatically chosen according to depth, bottom conditions and number of beams validly detected. During rough weather conditions the system switches to narrow the total swath angle to 105 or even 90 deg under extreme conditions.

To fully exploit the system's capabilities, calibration for a varying sound velocity (SV) through the water column is necessary, otherwise considerable errors both in depth and in horizontal distance are unavoidable. Correction of the sound velocity along a vertical profile was done by the use of the a SV

Probe(SVP 16) at the beginning of the cruise within the survey area; the profile was entered in the system after the measurement was finished. This SV profile was cross-checked by launching Expendable Bathy-Thermographs (XBT's) daily.

The EM 12 controls the direction of each beam based on the sea surface SV measured by the OTS probe located in a tank in which the sea water is continually flowing. In rough seas the sound velocity value was entered manually because the sensor was giving incorrect measurements due to air entering the tank.

1.4.3 SHRIMP

No results were obtained due to persistent failures.

1.4.4 Dredging

Dredging was conducted with a standard RVS dredge which consists of a chain dredge bag, an inner polypropylene net bag, and a pipe dredge towed behind the net. A 10 m length of chain was towed in front of the dredge to provide extra weight to hold the dredge on the sea-floor. A series of weak links allowed the dredge first to pivot onits arm, and then to come free, throttled by a wire strap, before the whole dredge assembly was lost if the final 5 ton weak link failed. The dredge was run with a pinger 100 m above the bag, and was lowered on the end of a cable until the pinger was 50 of the bottom. Monitering of the pinger weight above the bottom was on the SIMRAD echosounder console.

At each dredge site the ship held position until the pinger was 500 m of the bottom and then the ship would start to move slowly(0.3 - 1.0 kts) in the required direction. The wireout was controlled to keep the pinger close to a 50 m separation for a distance of 1 mile, at which point the dredge was hauled in. At this point most of the bites occurred, and most rocks collected. Constant monitering of ship position, wireout and number of bites enable us to constrain the location of the drege hauls to within a few hundred metres (See "Dredge Hauls" on page 82. for a report of the dredge results).

1.4.5 Scientific Computing System

The computing system used for scientific purposes on board was a small network of Sun Unix workstations: an Ultra-Sparc 140, a Sparc 20, a Sparc 10 and two Sun IPC's (supplied and maintained by RVS). The configuration of each workstation is as follows:

Sun Ultra Sparc 140: 17 in graphics monitor, 128 megabytes of memory, 1 gigabyte internal disk storage and 36 gigabytes of external disk storage, a Dat drive and a CDROM drive.

Sun Sparc 20: 17 in. graphics monitor, 64 megabytes of memory, 2 gigabyte internal disk storage, 1 gigabyte external storage, an internal CDROM, internal floppy drive and an external DAT drive.

Sun Sparc 10: 20 in. graphics monitor, 32 megabytes of memory, 500 megabyte internal disk space and 1 gigabyte external disk space, an internal floppy drive and an external CDROM and exabyte drive.

2 Sun IPC- 17 in. graphics monitors, 16 & 24 megabytes of memory, 1.5 & 4 gigabytes of disk space.

All Suns were linked via a 10base10 ethernet network using NFS(Network File System) to allow access across the network. The primary processing workstation was the Ultra Sparc which was used to process all TOBI data, majority of the SIMRAD data, and to server the main data store disk stack.

1.4.6 Ship Board Computer System

The RRS Charles Darwin is equipped with a standard data logging, archive and processing system common to all NERC ships. It is a three layer system comprising firstly of a microprocessor associated with each data source, secondly a VME OS9 based system that acts as a data concentrator and archive and thirdly a network of 4 Sun UNIX workstations and a Viglen 486 PC. The primary purpose of the system is to log the underway geophyiscal data which includes the following:

Navigation:

GPS: Trimble 4000SX
Transit: Magnavox MX 1107RS.

Echosounder:

Simrad EM12 operating in a continuous single ping/await return pulse mode. Bottom detected automatically and logged every ping.

Magnetometer:

Varian proton precession magnetometer V75, towed 150 m behind the ship. Effective resolution of ± 1nT over a range 20,000 - 100,000nT.

Gravimeter:

LaCoste and Romberg digital S84 with a 4 minute damping applied. This was tied into the gravity base station at Ponta Delagada and Cadiz with a Texas Instruments Worden portable land gravimeter.

Time reference:

DMW IRIG B clock system.

Daily processing is performed to derive the best navigation data and to derive the gravity and magnetic anomalies.

1.5 Seminar summaries

A series of on-board seminars were held on a daily basis in the scientific plot, below is a summary of each seminar, in order of presentation.

1.5.1 Variation in Lithospheric Stress Along Ridge-Transform Plate Boundaries.
Donna Blackman

Three-dimensional numerical models of asthenospheric flow and deformation in the oceanic lithosphere predict variability in the stress field that reflects the geometry of the ridge-transform boundary. Comparison of the predicted lithospheric deformation and the patterns of faulting and morphology observed along oceanic spreading centers can provide constraints on the relative importance of mantle vs crustal processes in creating seafloor relief. The series of 3-D Boundary Element calculations performed in this study show how spreading rate, transform offset and segment length each influence the flow and stress fields that develop during plate driven asthenospheric flow beneath a ridge-transform plate boundary. The predicted patterns of stress-supported seafloor relief generally follow those observed: median valleys are predicted at slow-spreading ridges vs small axial highs at fast spreading ridges; nodal deeps occur at ridge-transform intersections for offsets greater than 25 km; longer segments have more along-axis deepening than short segments which do not shoal much in their center. The predicted amplitude of the stress supported topography is about one third to one half that observed for an assumed asthenospheric viscosity of 5×10^{19} Pa s and a weak lithosphere (local compensation).

Application of the calculated flow stresses to the base of an elastic lithosphere model suggests that the variable plate thickness, in combination with the free-surface effect at the seafloor, may contribute to the development of the inside corner highs that are often observed at ridge-transform intersections. A pattern of axial tension switching to compression just off-axis and then back to vertical tension further away is predicted for the elastic plate model in the vicinity of the intersection. Thus, even though vertical normal stresses at the base of the plate would not directly result in the local formation of inside corner highs or transverse ridges, the response of a variable thickness plate with strength to these loads is more complex and may be conducive to formation of such features.

1.5.2 Geometry and Evolution of Boundary Wall Faults along the Mid-Atlantic Ridge (24-29°N).
Eddie McAllister)

The major faults that bound the median valley on slow spreading ridges form a staircase that migrates upwards and outwards from the valley floor like a slow escalator. Each boundary wall fault is generated at the margin of the median valley at about 2 km from the spreading axis. Boundary wall faults that appear to be single scarps on the resolution on the relatively low resolution Seabeam

multibeam echosounder amps are shown by high resolution TOBI sidescan sonar images in some cases to be single faults, but in others to be complex anstomosing fault zones. The major faults in such zones are often scalloped in plan view. There is no systematic relation between fault zone geometry and segment type.

We conclude that during the growth of boundary wall faults the strain is first accommodtred over a wide area, in which an array of small faults dissects the volcanic surface. However, with time, and with continued extension, the strain becomes organised into increasingly narrower zones of deformation until a major boundary wall fault wall develops. Faults grow by propagation and linkage with other nearby faults. The early stages of linage include tilted ramps, but at later stages brittle faults cut across the ramps, and eventually become part of a scalloped fault trace. In some places, linkage is through zones of small-scale diffuse faulting, rather than through a single fault. Fault capture and linkage can occur over lateral distances (perpendicular jto the mean azimuth of the faults) of up to 1.5 km.

This deformation takes place within a fault growth window fixed relative to the spreading axis, through which the lithosphere passes as seafloor spreading continues. Most of the growth of each boundary fault takes place before the next fault is initiated. We conclude that the location and size of the narrow fault growth window is controlled by the changing mechanical properties of the ocean lithosphere as it spreads away from the axis. Its inner boundary represents the position at which a normal fault reaches the sea floor after originating at the base of the lithosphere at the spreading axis. Its outer boundary is interpreted as the point at which the strength of the boundary wall fault, increasing as the lithosphere ages and thickens, becomes greater than the strength of the lithosphere at the spreading axis, when a new fault is generated. The process of fault generation ay mid-ocean ridges has relevence to fault generation in other extensional environments.

1.5.3 What Do We Know About Segment 18 at this Point? Debbie Smith

The axial morphology of a slow spreading ridge is characterized by a median valley. The inner valley floor is the site of constructional volcanism. Volcanism is mostly in the form of seamounts and short flows which commonly combine to form larger axial volcanic ridges. Faults cut the crust in the valley walls and crestal mountains as it moves away from the spreading axis. From Sea Beam bathymetry data previously collected by Purdy et al. we know that Segment 18 exhibits these characteristics. As well there is a large along-axis change in bathymetry. The segment shallows ~2/3's of the way toward the Atlantis transform, yellow mountain occurs eastward of the valley floor at this spot. Surface magnetic data collected at the same time as the seabeam bathymetry data show that there is an along axis variation in crustal magnetization. Crustal magnetization highs occur at the ends of segment 18, and a low occurs at the segment center. In addition, gravity data reduced to mantle Bouguer anomaly show a large negative anomaly offset to the east of the valley floor adjacent to the magnetic low. Morphologic patterns suggest that landslide zones are common in segment 18. Collection of TOBI side-scan sonar data will provide

ground truth for the bathymetery data, and in combination with dredges and camera runs will allow us to answer many questions concerning the processes acting at segment 18.

1.5.4 Strain Modelling
Bob Janssen

Most of the earth's crust is or has been subject to strain as is expressed by pervasive faulting and jointing at a wide range of scales. Seemingly rigid masses of crustal rock can deform over geological time-periods according to some rheology. A plastic rheology is probably appropiate for time-scales covering tens of millions of years but a linear elastic behaviour is a good first approximation for shorter periods.

Rheology describes a material's flow behaviour as well as the appropriate stress-strain relations. In case of the earth's crust, stress-measurements tend to be momentaneous and localised views of the ambient stressfield. Transient and heterogeneous stress fields can therefore be elusive. Strain and strain rates however, are recorded in deformed rocks. Geologists observe fault slip reates which are the expression of discrete strain. Geodesists observe strain by measuring position changes between fixed points.

The majority of strain in continental crust appears to be accommodated by a relatively small number of major faults. The San Andreas fault shows in the order of 300 km offset whilst the Garlockfault in eastern California shows many tens of kilometers of slip. The numerous smaller faults that occur over wide regions accommodate typically display slip in the order of 10-100m.

This assumption and the approximation of linear elasticity allows us to propose a simple model in which the crust is represented by a thin elastic plate and major faults are represented by dislocation elements. The plate sits on an inviscid fluid and drag from underlying material is not taken into account.

A Boundary Element method is used to numerically describe this model. When the model is deformed,, the dislocations/faults will ideally accommodate the majority of strain. Some remaining strain is accommodated by continuous strain throughout the model plate. This simple technique allows us to simulate the deformation of the earth's crust and the slip of major faults simultaneously. This method has been applied successfully to the Walker Lane belt of the western Basin and Range. Some important constraints on fault slip and strain migration were obtained. Extension of this method to mid-ocean ridges may not be straightforward as the assumption of linear elastic behaviour may not be valid, given the high strain rates and influence of upwelling mantle material.

1.5.5 Serpentinites and crustal construction at the Mid-Atlantic Ridge
Joe Cann

Though the current view of ocean crustal structure is that the crust is basaltic, excluding serpentinite as a major component, Hess's early model that the lower crust is made of serpentinised peridotite still has adherents, and serpentinites have been extensively dredged and drilled from the Mid-Atlantic Ridge, even

from the tops of the crestal mountains. This has led to the idea that diapiric intrusion of serpentinite along major fault zones may play a significant part in crustal construction. Our recognition, on Charles Darwin Cruise 65, that landslides might play an important role in modifying the fault patterns on the MAR, especially at non-transform inside corners, gave a new twist to those concepts. If serpentinite could intrude diapirically up deeply penetrating fault zones, then it might fail by landslipping when extruded at the surface. Serpentinite landslide flows from extruding diapirs have been described from California, and the same could happen at the ocean floor. Tobi side scan textures and sonar facies lend strong support to this view, since what have been interpreted from bathymetry as low angle detachment faults have all the appearance on the Tobi images as being failure surfaces of landslides. In the Broken Spur segment we recovered serpentinite from an area of such sonar facies, and debris flows from this region reach out on the floor of the median valley to the edge of the zone of active volcanism. Clearly here it would be possible for debris flow material to lie stratigraphically between lava flows; in several deep-sea drill holes heterogeneous units dominated by serpentinite have been found in the upper part of the basalt sequence. It seems likely, therefore, that serpentinite brought diapirically to the sea floor be more important in crustal construction than has recently been considered, and that concepts of crustal structure may need to be modified accordingly.

1.5.6 Modelling of instabilities of hydrothermal flow at mid-ocean ridges
Rachel Pascoe

An overview was given detailing the history of the discovery of hydrothermal vents on the seafloor, from the Galapagos Spreading Centre, through the East Pacific Rise, Juan de Fuca Ridge to the more recent discoveries on the Mid-Atlantic Ridge. There are three main types of venting observed at these sites, the most spectacular being the high temperature (~350°C) black smoker vents. These usually emerge from chimney-like structures constructed by the precipitation of sulphides and other metallic minerals. Also emerging from chimney structures are the lower temperature white smokers (~150°C). The third type of venting is the low temperature diffuse flow which emerges from large patches throughout the vent fields. This is thought to contribute a large amount to the heat flux from a field and is the most important biologically being of lower temperature and less toxic. There are several lines of evidence that suggest that the flow at these ventfields is unstable, in that it varies with time. These include the finite lifetimes of vents, brecciation of sulphides, formation of megaplumes (or event plumes) and the fine-scale re-routing of pathways within a given vent system. The work carried out in my thesis set out to produce simple pipe models of hydrothermal flow in an attempt to gain a better understanding of these instabilities.

In a pipe model, the downflow (recharge), cross-flow (heater) and upflow (discharge) limbs of the system are modelled as pipes filled with porous material through which water flows. Each limb of the model can be assigned a different resistance to flow which depends on the permeability and cross-sectional area of that limb. Although they have their limitations they provide a simple and transparent method of investigating complicated systems.

The first set of models concerned the production of diffuse flow by including an extra discharge pipe to allow cold seawater to mix with the hot rising hydrothermal fluid. It was found that for low temperatures to be observed at the surface, the upper part of the circulation for that part of the discharge has to be relatively permeable, and that the deeper sections of the upflow must be much more impermeable. The model suggests that the early stages of evolution of a hydrothermal system are characterized by widespread diffuse flow and that black smokers develop as subsurface precipitation reduces the permeability of the upper section of the crust.

The second set of models included a cross-limb which allowed fluid to either by-pass the heater limb altogether or to allow fluid to re-circulate after passing through the heater. The stability of the system was investigated as a function of two of the model parameters (the temperature of the heat source and a dimensionless number relating the heat input and resistance to flow). In this plane regions of stable and unstable behaviour could be defined and predictions made about the effect other parameters had on the system.

1.5.7 Tectonics and Volcanism of the Mid-Atlantic Ridge at 45N
Sidney Mello

The Mid-Atlantic Ridge (MAR) at 45° N has a long history of investigation, including extensive geological and geophysical research by the Bedford Institute (Canada), a GLORIA survey and a DSDP site (Leg 49 - hole 410). Simrad multibeam swath bathymetric data was recently collected along the ridge axis, and this provides a reason for a reevaluation of the area.

The ridge at 45° N is part of a 1300 km long MAR section lacking major transform faults, between the Azores at 39° N and the Charles-Gibbs Transform at 51 N. Previous work has shown that this area is unusual for two reasons: (a) The whole area shows a high positive regional free-air gravity anomaly on satellite gravity maps, even though it lies at normal oceanic depths (b) The basalts from this area are abnormally enriched in incompatible trace elements compared with normal MORB, indicating that the mantle feeding this ridge segment has an unusual composition.

The ridge crest morphology in the region is similar to others sections of the MAR. It is characterized by an axial valley (9 to 18 km wide) striking 019° with water depths to the median valley floor between 3000 and 3500 m. The ridge section surveyed can be divided into three spreading segments. The southernmost segment (Segment A), which extends from 45° 15'N to 45° 23'N, contains an axial volcanic ridge (AVR) about 400m high and trending 010 . The AVR is 18 km long and 3 Km wide and its nothern part has a flat top. It is flanked by two structural basins. At 45° 23'N occurs a typical ridge axis discontinuity (RAD), defined by two subparallel basins around 3000 m deep, which clearly offsets right-laterally by 5 km the whole of Segment A. Segment B starts at 45° 24'N and contains a conspicuous AVR (+/-500m high) which also strikes at 010 . It shows much more rugged morphology than the AVR in Segment A and it is about 5 km wide and 30 km long. Through its entire length the AVR of Segment B is flanked by two structural basins deeper than 3000 m. However at its northern tip around 45° 40'N the eastern basin gradually

disappears. At this location occurs a new RAD, which once more seems to offset right-laterally the ridge axis topography. From 45° 50'N a major structural basin dominates the axial valley extending towards the north end of the survey area. This large (10 km) and deep (> 3500 m) valley defines the third segment (Segment C), in which there is no apparent AVR . The floor of this segment rises to a high at 45° 50'N where the median valley is almost blocked by two mountains that encroach on the valley from east to west.

Dredge hauls have recovered, besides the E-MORB basalts, deeper crustal lithologies including metabasalts, gabbros and serpentinites. The sea floor spreading magnetic anomalies are very clear over the region as far as anomaly 5 (10 my) . The central magnetic anomaly lies over the axial valley with amplitudes of 500 nT and seems to be offset by the RAD at 45° 40'N. This anomaly shows maxima associated with the two structural basins to the west of the AVRs of the two southern segments.

The next steps on this study will be to prepare a detailed structural map in order to characterize fault style variation along and across the axial zone, and spatial and temporal variation of the ridge morphology. Magnetic anomalies will be modeled to allow dating of events and structures as well as to reconstruct the geology back through the last 8 my. The Canadian gravity survey will be reinterpreted in the light of new concepts.

1.5.8 Interplay between tectonics and volcanism in the Mid-Atlantic Ridge (MAR) between the Kane and the Atlantis Fracture Zones. Mike Avgerinos

The extensional strains observed at all mid-oceanic ridges areaccomodated partially by faulting and partially by dyke intrusion. Weintend to investigate within the setting of the median valley of MAR:

1 the degree of coupling between the two processes of stress relief.
2 the controls of the evolution of rifting
3 the controls of the quantitative parameters of faults
4 the controls of the relative positions of the axial volcanic ridgeand faults
5 the effect of stress generated or relieved by volcanism onfaulting and vice versa

In particular, we seek to understand the processes by which new medianvalley wall faults nucleate and grow. Each new fault must form within the volcanically active median valley floor, cutting of a section of the floor to make a new step on the median valley walls.

The primary tools for this study are high resolution bathymetric maps, generated by the Seabeam and Simrad multibeam bathymetry systems, and sidescan sonar images generated by TOBI. We focus on fault tips away from segment ends and on the relative position of faults and AVR's. Faults which end within a segment are believed to be either parts of inactive complex en-echelon fault arrays, which have probably ceased propagating, or newly nucleated and propagating faults. Several examples of possible fault nucleation (eg. segment 14, 43° 56'W 28° 00'N, Broken Spur, 43° 10'W 29 14'N), propagation (eg. segment 6, 45° 25'W 25° 08'N) and linkage (eg. segment 11, 44° 38'W 26° 42'N, segment 7, 45°

23'W 25° 27'N), as well as varied fault system patterns (eg. Broken Spur, 43° 07'W 29 °10'N, segment 15, 47° 43'W 28° 31'N, segment 17, 43° 11'W 28° 56'N to 29° 05'N) have been examined within the median valley. As it propagates, a new median valley wall fault cuts off a segment of the AVR and, at the same time, the locus of volcanism will shift. To test this concept equally spaced W-E topographic profiles intersecting the AVR are drawn within a window three minutes of latitude wide, both to the north and to the south of fault tips. The profiles are then aligned, adjusting for the orientation of the segment axis, and then stacked. The variation of the cross-sectional area of the AVR in the stacked profiles may reflect the relative age of the AVR (assuming magma is supplied at constant rate). New information from RRS Charles Darwin Cruise 100 will be used to develop such models further.

CD 100
NOBSKA

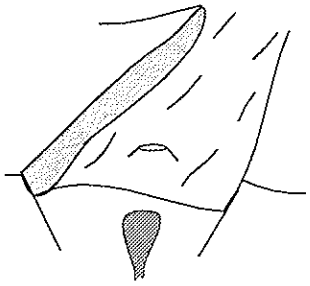

Section 2.0 Daily Narrative

Life on the ocean waves

2.1 Abstract of activities, CD 100

99 / 8 April 1996 (Easter Monday)

Science party flies to Ponta Delgada.

100 / 9 April

Charles Darwin arrives in Ponta Delgada. Debriefing of CD99 science party starts.

101 / 10 April

Debriefing continues together with preparations for leaving.

102 / 11 April

CD 100 sails from Ponta Delgada at 1300, underway to work area at 30 N, 42 W. Science meetings and boat drill held. Cool brisk wind from the N.

103 / 12 April

Stream magnetometer and PES fish, and switch on Simrad EM12 and shipboard 3 component magnetometer at Portuguese 200 mile limit. Set track to parallel CD99 inbound track to give broad Simrad track coverage. Blackman seminar on modelling stresses in plates near ridge-transform intersections. Wind now light, but air cool.

104 / 13 April

Continue along track towards work area. McAllister seminar on generation, growth and linking of boundary wall faults. Brisk, warm humid wind from the south.

105 / 14 April

Continue passge to work area. Meeting to discuss processing of Tobi and Simrad data. Fluellin seminar on Tobi phase bathymetry. Warm sun, little wind, swell from SW.

106 / 15 April

Arrive on site 1030. Sound velocity dip 1045 - 1345. Transit to Tobi launch site for line 1. At lauch site 1445, depresssor weight at 1530, first side scan images 1730. Side scan poor but usable, bathymetry poor. Images of transform wall and neovolcanic zone at the RTI. Smith seminar on use of Tobi and bathymetry to interpret segment processes, emphasising Segment 18. Weather warm with light winds, but a large swell from the W or SW.

107 / 16 April

Continue Tobi survey, with similarly poor images until Tobi fails at 1650. Depressor weight on board 1915, Tobi on board 2000. Slip ring failure diagnosed. Transit to Dredge 1 site, 2010 - 2040. Dredge 1 over side at 2140, pinger on at 2204, dredge onboard, 0049/108. Cann seminar on serpentinite in ocean crust. Clear weather with occasional rain showers.

108 / 17 April

Transit to Tobi restart (0100 - 0230). Tobi overside at 0315, does not work, and is recovered by 0800. Transit back for dredging (0830 - 1000). Dredge 2 overside at 1005, pinger on at 1016, and back on board at 1235. Dredge 3 overside at 1320, the pinger is on at 1330, and back on board at 1615. Dredge 4 overside at 1650 and back on board at 1925. Transit back to Tobi restart (1935 - 2100). Tobi launched at 2110, the depressor at 2147, and fails again. Hauling starts at 2335. Janssen seminar on Basin and Range. Clear day with little wind.

109 / 18 April

Tobi on board at 0145. Transit to Dredge Station 5 (0230 - 0410). Dredge 5 overside at 0419, pinger on at 0428, dredge back on board 0630. Dredge 6 overside at 0715, pinger on at 0721, dredge on board at 1016. Dredge 7 overside at 1045, pinger on at 1056, dredge back on board at 1300. Start Atlantis RTI Survey 1315, and continue the survey for the rest of the day. Pascoe seminar on modelling instability of hydrothermal systems. Sunny and very warm day.

110 / 19 April

Atlantis RTI survey continues until1745. Tobi deployed at 1815, depressor weight in at 1900. Divert Tobi towards shallow water after failure in deep water at 2200. Mello seminar on 45 N survey. Cool day with NW wind and rain showers.

111 / 20 April

Tobi excursions in the night bring it onto shallow line at 0800. Poor signal in the side scan forces hauling in at 0950, with Tobi on board at 1320. Resume Atlantis RTI survey.Avgerinos seminar on volcano/tectonic interactions at mid-ocean ridges. Warm sunny day with light wind and rain in evening.

112 / 21 April

Complete Atlantis RTI survey at 0645. Start Tobi deployment 5 at 0826, with the depressor over at 0848. Tobi fails again. Start hauling at 1015, bringing Tobi on board at 1150. Circle to see if quick fix possible. Set out at 1413 towards S end of Seg 18. Start Tobi deployment 6 at S end of line 4 at 1850, with the depressor out at 1910. Tobi fails; start hauling at 1940, on board again at 2015. Set out for S end of Segment 17 2025. On site for Dredge 8 at 2313, pinger over at 2325. No seminar. Weather clear and sunny with a cool breeze.

113 / 22 April

Dredge 8 onboard 0235. Dredge 9 over at 0315, pinger on at 0322, onboard at 0645. Camera station 1 over the side 0905, ends 1530. Dredge 10 overboard at 1625, pinger over at 1635, dredge on board again at 1952. Dredge 11 overboard at 2022, pinger on at 2030, dredge onboard again at 2310. Part 1 of Donna seminar on Agar and Klitgord paper. Excursion in rubber boat. Weather sunny and warm with a breeze.

114 / 23 April

Tobi survey for Roger Searle starts 0000, with the depressor weight over at 0020. Pass E end of Line P at 0110, and the W end at 0900. Pass W end of Line R at 1045 and its E end at1530. Tobi on board again at 1913. Camera run 2 starts at 2022, first leg ends 2325. Part 2 of Donna's seminar on Agar and Klitgord. Weather grey at first, gradually increasing, first from the W, then from the NW, to a gale with a large swell.

115 / 24 April

Second leg of camera run 2 starts 0056/115, camera onboard 0316/115 in worsening weather. Transit to start of Tobi line 4 (0330 - 0630), but weather too bad to launch. Simrad survey 0830 - 1300. Dredge 12 overboard at 1400, pinger on at 1405, dredge on board 1628. Transit 1640 - 1810. Dredge 13 over at 1820, pinger on at 1830, dredge on board at 2130. Transit to start of Tobi line 4 (2140 - 2250). Tobi over at 2305. Depressor over at 2330. McAllister seminar on Escartin and Lin. Gale in morning moderates to evening, though swell is still high.

116 / 25 April

Tobi continues down. Surface reflection at 0030, floating magnetometer out at 0035 and bottom images at 0120. Tobi continues along Line 4 all day. Debbie Smith seminar on Cannat. Cool, breezy day with a high swell.

117 / 26 April

Tobi fails at 0030. Hauling in brings depressor on board for checking (0415). Wait for light, then recover Tobi (0915). Repairs to Tobi (0930 - 1400). Return close to failure place an redeploy Tobi (1420). First Tobi signals at 1715. Floating magnetometer out at 1730. Continue Tobi Line 4. Cann seminar on Neumann and Forsyth. Weather good, but still with a swell.

118 / 27 April

Long turn to Line 5 takes much of the night. On Line 5 by 0700. Run along transform to the end of Line 5 (1800), and turn onto Line 6, along S wall of transform by 2000. Jansen seminar on Krafla event in Iceland. Weather rainy then sunny, with light winds.

119 / 28 April

Tobi continues along S wall of transform and across median valley axis. Start the very long turn onto Line 7 at 1200, and finish it at 1730. Line 7 runs S down the axis of the median valley. Weather good, with brisk N wind and swell, and patchy sun annd cloud.

120 / 29 April

Tobi survey continues on Line 7, starting the turn to Line 8 at 1900, and finishing it to start Line 8, up the west side of the median valley, at 2200. Weather grows worse as the day goes on, with a low approaching from the W, and wind increasing from the W to a gale. Pascoe seminar on inversion of deep towed magnetic anomalies.

121 / 30 April

By 0400 blown off line 8. Try to turn to Line 9, but blown of that too. Set course downwind across median valley. Stern slamming prevents that, so haul Tobi to 500m and turn into wind (1200 - 1400). Try 015 course and fail. Try diagonal across valley towards W, and fail. At 1845 start to haul Tobi to 500m and give up science, and wait for weather to improve. Mello seminar on magnetic anomaly signals of hydrothermal alteration.

122 / 1 May

Weather moderating by 0800. Set course at 070 at 1000, and start lowering Tobi again at 1035, and it records images again at 1200. Make track towards Yellow Mountain line, crossing median valley, and turn to cross Yellow Mountain on Line 10A. Weather stays the same after the initial improvement, with 25-30kt winds from the W. Avgerinos seminar about structure of MAR transforms.

123 / 2 May

Turning to Line 10A at midnight, and passing the top of Yellow Mountain at 0430. Line 10A continues until 1402, when Tobi swivel fails. Tobi inboard by 1645. Transit to camera station 3, with a start point of 29 49.1'N 42 41.4' W, at 1650m. Camera over at 1957, and on bottom at 2056. Swell forces station to be abandoned at 2152. Camera on board at 2240, without battery cases. Set out for dredge 14 site. Seminar from Cann on basalt geochemistry. Weather as the day

before, 25-30kt winds from just W of N, a large (but not so large) swell, and mixed sunshine and clouds.

124 / 3 May

Dredge 14 overside 0109, pinger on 0109, back on board 0208; dredge lost. Dredge 15 overside 0358, pinger on at 0408, brought back in because of wire trouble. Dredge overside again at 0530, pinger on at 0540, dredge back on board 0819. Dredge 16 overside 0859, on bottom 0859, back on board 1108; dredge lost. Rigging new dredges, 1115-1230. Dredge 17 overside at 1255, on bottom at 1335, inboard again at 1450. Dredge 18 overside at 1552, pinger on at 1600, dredge on board at 1856. Dredge 19 overside at 2016, pinger on at 2020, dredge on board 2350. Blackman seminar on phase bathymetry. Winds still strong, 25-30kt, but moving round to NW in afternoon.

125 / 4 May

Dredge 20 overside at 0107, pinger on at 0117, dredge back on board at 0435. Simrad minisurvey 0500-1500. Transit to Tobi launch site 1500-1650. Tobi in water 1710, depressor weight in 1730, first images 1910, magnetometer out 2012. Start Tobi Line 11. McAllister seminar on sub-seismic faults. Weather improving, wind out of NW, less than 20kt.

126 / 5 May

Tobi Line 11 ends 0930, turning to Line 12. Start of line 12 (Tobi) 1230. No seminar. Weather moderating to light wind from N. Barbecue evening.

127 / 6 May

Tobi Line 12 ends with turn to transit Line 13 across transform valley and start of Line 14. Line 14 ends 1500. Turn to Line 15. Line 15 (starts 1800) across furrows and striations to end and turn at top of Rose (2330). Smith seminar on past work in Atlantis. Weather fine with light breeze.

128 / 7 May

Tobi Line 16 starts at 0100, ends at 0800. Turn to Line 17. Line 17 runs from 1130 to 1400. Turn to Line 18. Line 18 runs from 1630 to1915. Turn to Line 19. Line 19 starts 2315. Janssen seminar on maps. Weather fine and warm, with a light breeze.

129 / 8 May

Tobi finishes Line 19 and is on board at 0415. Dredge 21 overboard at 0500, pinger over at 0508, dredge on bottom at 0608 and onboard again at 0833. Dredge 22 overboard at 0909, pinger on at 0912, dredge on bottom at 0957 and back on board at 1130. Dredge 23 over side at 1236, on bottom at 1409 and back on board at 1620. Dredge 24 overside at 1745, pinger on at 1755, and dredge back on board at 2021. Dredge 25 over side at 2100, pinger on at 2104, dredge on bottom at 2132, and back on board at 2238. Dredge 26 over side at 2302, pinger on at 2307, dredge back on board at 0010/130. Hot and very still day. Rides in the rubber boat and swim call.

130 / 9 May

Dredge 27 overboard at 0042, pinger on at 0049, dredge on the bottom at 0014 and back on board at 0206. Dredge 28 overboard at 0233, pinger on at 0241, dredge on bottom at 0258 and on board again at 0400. Ship sets sail for Cadiz. Cann seminar on preliminary results. Weather fine with a light wind.

2.2 CD 100 Cruise Narrative

8 April 1996, Easter Monday, Julian Day 99

The science party flies out to the Azores via Lisbon. The plane lands through cloud almost low enough to be fog, and we transfer to the Hotel Azores Atlantico.

9 April, 100

The science party assembles to meet the Darwin coming in from CD 99. Roger Searle briefs us on the events of his cruise, and Peter Slootweg begins an intensive process of educating us about all that happened to the computer system on CD 99. We arrange for the Matlab licence to be transferred from the ailing Durham Sparc 20 onto the Durham Sparc 10. Joe Cann and Roger Searle give interviews to the local papers. HMS Hecla arrives in Ponta Delgada shortly after Darwin, smartly white and dressed with flags. The Master and Chief Officer of Cruise 99, with Roger Searle and Joe Cann, attend a cocktail party on board together with local dignitaries and British expats: gins and nibbles. Some of the science party sneak off to the Sete Cidades caldera for the afternoon.

10 April, 101

Peter Slootweg continues his struggles with the computer system, while others work with him, or go shopping, or get their hair cut, and all of the other normal pre-cruise activities. Another party goes to Sete Cidades, and comes back claiming that it did not rain on them very much, an assertion doubted by the others who had been soaked by rain even in Ponta Delgada, and had seen the clouds pressed low on the hills. Debbie Smith showed Joe Cann the nature of true assertiveness by holding a picnic in the bar of the San Pedro Hotel during a rain storm.

11 April, 102

Joe Cann gives an interview live to the local breakfast radio show from a van parked on the quay. As the interview proceeds, it becomes clear that the interviewer has a daily slot, which has to be filled, anyhow. Donna Blackman has been picked out by him on the promenade already, when out running, and she has sent him on to the ship. Peter Slootweg arrives for his last two hours on the computer system, leaving only just as the gangplank is to be raised. The ship sails at 1300 (delayed because pilots were needed for a Russian sail training ship coming in. The wind is brisk from the N, cool and strong, and there is a swell on the quarter, not a comfortable experience for those without sea legs yet. The ship wallows in a difficult way. We are underway to the Portuguese 200 mile

limit before streaming gear. There are meetings of the science party at 1100, 1230 and 1730 concerned with safety, shipboard life. First fire drill at 1600.

12 April, 103

In the morning we continue to run through Portuguese waters. Work continues on configuring the computer network. Chris Fluellin and Chris Turner set out to rewire the Tobi transducers so that they have an impedance more matched to the rest of the circuitry, and thus a better signal to noise ratio. Dave Edge replaces the faulty parts of the Shrimp camera system. At 1230, permission comes through for us to work in Portuguese waters ....too late for us to collect data near the Azores, since we are about to leave their waters. At 1430, at the 200 mile limit, we stop to stream the PES fish and the proton magnetometer, and turn on the Simrad EM12 and the shipboard three component magnetometer. Donna gives a seminar at 1330 on modelling the stresses near to the spreading axis, and especially at slow-spreading ridge-transform intersections, where the models predict large tensional and compressional stresses under realistic conditions. The weather is sunny during the day, with light winds, but the air is still cool. Since streaming Tobi we have followed Roger Searle's inbound track to the Azores, about 2.5 km offset to the west, to collect a broad swath of data, and continue to do so through the night.

13 April, 104

We continue all day to run along the track towards the work area, with Simrad and the magnetometers operating. There is a brisk, warm, humid wind blowing from the south, with a tropical feel to it. Chris Fluellin and his team continue to work on the Tobi transducers, refilling the first set with oil and proceding to the second. There are continuing problems with Erdas, but these are eventually solved by reconfiguring the memory, which Martin Beney and Rod Pearce do amazingly fast. Eddie gives a seminar on fault patterns in the median valley floor, discussing the generation, growth and linking of the major bounding faults, and suggesting that fault activity is confined to the first or first and second wall faults. Donna and Joe spend time planning tracks with Eddie and Debbie. This results in some changes from the original plan, but a sense that much will be decided when we reach the work area. The area around the inside corner is clearly critical, and tracks are needed to cover that. There is much discussion of what we will be able to see with Tobi when we try to scan the transform valley walls. Later another discussion develops about the processing scheme, when it becomes clear that we will have to structure carefully our approach to ensure that critical information, such as the Tobi navigation files, is available when needed. This requires more systematic airing.

14 April, 105

We continue our passage into the work area at 10.5 kt, in warm sun, little wind and a swell from the SW. The first stages are replanned to allow for a sound velocity dip in 5000m of water in the Atlantis Fracture Zone, followed by a deployment of Tobi at the north end of Line 1. Line 1 is examined carefully to ensure that we obtain the best possible side scan, and at the same time insonify some possible dredge targets in case Tobi needs attention. Donna and Eddie move it around, and end up replacing it where it was at first, with a small

deviation in the middle, to ensure that one of the median valley wall faults is properly insonified. Chris Fluellin gives a seminar at which he explains the intricacies of ambiguous and unambiguous phase, and how the use of both can lead to well-controlled Tobi phase bathymetry. The science party meets to discuss the structure of data processing, and identify a network of data transfers which will allow the most efficient flow towards processed data. How this will turn out remains to be seen. Most of the stages in the procedure are tested with data from the previous cruise.

15 April, 106

In the morning ending passage to work area. Weather warm, with a light breeze, but a large swell from the W or SW. Recover proton magnetometer at 1000. Arrive on site for sound velocity probe at 1030. Velocity probe onboard again at 1345. Transit to Tobi launch site. On site for Tobi launch 1445. Depressor weight away 1530. First useful Tobi data 1730. Track runs S along E side of the Segment 18 median valley from the N side of the transform wall, to image Yellow Mountain, fault zone S of it, and E side of AVR. Tobi side scan images are poor in quality. There is a lot of speckle, fringes at far range, and short-period oscillations that distort lines on the image. Phase information for bathymetry has much noise, both speckle and oscillations that give bands across the image. All the same there are good images of the transform wall and of the neovolcanic zone in the RTI. Debbie Smith gives a seminar on slow spreading ridges, and what she has seen in Segment 18 from Seabeam bathymetry.

16 April, 107

Continue Tobi survey, with technically relatively poor images, as previous day, but with good images of the W side of Yellow Mountain, the major fault zone to the S of it, and curving hummocky ridges on the AVR in the centre of the median valley floor. Most spectacular is the image of a large debris flow coming down over a faut scarp just S of Yellow Mountain, perhaps connected with the 1985 earthquakes in the area, and containing some chunks of relatively coherent rock. At 1650 Tobi stops operating, apparently from slip ring problems. Depressor weight on board 1915. A check shows that the slip rings have gone. Tobi is inboard by 2000. Decide to start a series of dredge hauls on the slopes of Yellow Mountain, at sites imaged by the first Tobi run, while Tobi is being attended to. First is Dredge 1, at 29 46.0'N 42 44.5' W, 2400 - 2000 m, sited on the large debris flow imaged earlier. Transit to Dredge 1 site starts 2010 and ends 2140. Dredge overside 2140, pinger on 204, large bites from 2330 - 2350. Dredge onboard 0049 / 108. Joe Cann gives a seminar on the possibility of serpentinite intrusions and extrusions forming a major part of the crust at inner corner highs. Good clear weather with occasional rain showers.

17 April, 108

Dredge 1 on board 0049, with a large haul of basalt fragments ranging from aphyric to phyric. The haul also contains two small red shrimp (juvenile vent shrimp??). After the haul is on board, start transit back to the point where the Tobi line had stopped so as to restart it, since the slip rings had now been replaced (0100 - 0230). To reduce slip ring problems we decide to disable the gyro. Tobi is over the side by 0315, but very soon it is clear that it is not

working, and at 0600 hauling in starts, with Tobi inboard by 0800. Not clear what is wrong at this stage. Further work eventually shows that the connexion at the inboard end of the umbilical has failed. Transit back to Yellow Mountain area for further dredging (0830 - 1000). Dredge 2 (29 47.0'N 42 43.3' W, 2150 - 2000m), sited on the fault scarp or debris flow underlying the fresh debris flow sampled in dredge 1, is over the side at 1005, the pinger on at 1016, there are bites from 1118 - 1145, and the dredge is back on board at 1235. There is a large haul of basalt fragments, with some deep water coral pieces, a whole gastropod shell and one glacial erratic. Dredge 3 (29 49.8'N 42 4.9' W, 2190 - 2000m), sited on the cliffs on the W side of Yellow Mountain overlooking the median valley, is over the side at 1320, the pinger is on at 1330, and is back on board at 1615. This haul contains several hundred blocks of basalt, mostly very porphyritic, with some indurated ooze and fragments of basalt glass breccia. Dredge 4 (29 49.9'N 42 43.9' W, 1600 - 1500m) is targeted at a bright patch in the Tobi image near to the top of Yellow Mountain. The dredge went over at 1650, and was back on board at 1925. It contained 42 pieces of basalt, and a number of chunks of indurated ooze. Some of the smaller fragments appear to be of metabasalt, and one contains a quartz vein. Tobi is by now repaired. Transit back to the Tobi restart position takes from 1935 to 2100. We decide this time to disable the port bathymetry, in case the bathymetry problems are caused by cross talk between the two sides. This turns out not to be the case, since the same interference is present on the starboard side bathymetry even with the port side switched off. Tobi is over the side by 2110 and the depressor weight over at 2147. Tobi fails again; there are severe oscillations in the side scan circuits which lead to failure and to destruction of some of the on board programming. Start hauling in at 2335. Bob Janssen gives a seminar about deformation of continental crust in the Basin and Range. It is a bright clear day with little wind.

18 April, 109

Tobi is on board at 0145. Again it is not at first clear what has happened, but further work shows that it is another connexion that has failed, this time the connexion within the depressor weight leading to the umbilical, but the damage is more serious, and takes much longer to fix. Transit to Dredge 5 from 0230 - 0400. Dredge 5 (29 49.6'N 42 42.9' W, 1350 - 1200m) is at the top of Yellow Mountain. The dredge is over at 0410, the pinger at 0428, and the dredge back on board at 0630. It contains 16 fragments of basalt pillows, all rather weathered with palagonitic rinds, and manganese oxide coatings. Three of the fragments are attached to indurated ooze. There are fragments of coral and sponge. Dredge 6 (29 52.5'N 42 44.3' W, 2650 - 2500m) is sited on a fissured bulge imaged by Tobi on the W flanks of Yellow Mountain above the median valley. It goes overboard at 0714, the pinger at 0721, and is back on board at 1016. The bag contains a large haul of basalt pillow fragments, moderately weathered, but with much fresh glass. Dredge 7 (29 53.2'N 42 42.4' W, 2200 - 2100m) is on one of the finger ridges that run N from Yellow Mountain, the closest to the Tobi line, imaged on Tobi line 1. It is over at 1044, the pinger is in at 1056, and the dredge is on board again at 1300. It contains a good haul of basalt fragments, moderately weathered with palagonite rinds and marked coating by manganese oxide. Rachel Pascoe gives a seminar on her thesis work,

modelling instability of hydrothermal flow. At 1330 start the transit to the start point of a bathymetric survey of both ridge-transform intersections of the Atlantis Fracture Zone, using the Simrad system, and collecting magnetic and gravity data too for future interepretation. The track lines are oriented ENE - WSW, and the bridge is told to make rounded turns at the end of each track line to asist with smoother gravity measurements. Details of this survey can be found in the waypoint catalogue as the Atlantis RTI survey. Waypoint S1 is passed at 1501, and the survey continues for the rest of the day. Weather is sunny and very warm with light winds.

19 April, 110

The Atlantis RTI Survey continues through the night, and into the next day as Tobi repairs continue. The Tobi team identify surges of power in the main power supply, and discover that the inboard connector in the main lab is in poor condition, which may account for much, but tests show that swath bathymetry is not working at all on the starboard side, though it is working on the port side (which had been switched off on the previous deployment). Sidney Mello gives a seminar on his work on the 45N area using the Simrad and the Canadian data from earlier. The Atlantis RTI survey comes to a convenient point at 1745 to break off and to deploy Tobi at the E end of the main E-W cross line in the transform valley. Start to deploy Tobi at 1815, with the depressor weight in at 1900. By 2200 it is clear that there are major problems with Tobi. Major oscillations in the side scan start up as Tobi sinks deeper. These are first diagnosed as unstable circuits that are temperature sensitive, and we come to shallower levels, when they disappear. We now set out to tow Tobi over to try a survey on a shallower E-W line on the S side of the transform valley. The wind was high in the night of 109/110, with clouds and rain showers, but decreased as the day went on and the showers became less frequent. The wind is from the NW, cool.

20 April, 111

The ship (and Tobi) go on major excursions in the night, with first a wide turn towards the shallow line, then a steering problem that takes it far away, followed by a near encounter between Tobi and the bottom, avoided by rapid winching and acceleration of the ship. Tobi eventually comes onto the shallow line at 0800, running to the west. It is working, but the signal for side scan is unacceptably noisy, with fog at far range, and even moderately clear signal only over half of the swath. This becomes clear as we go over a major mountain/ fossil inner corner high, and we decide to pull Tobi at 0950. Tobi is on board at 1320. The ship resumes the Atlantis RTI survey with a new series of waypoints. Because of the suspicion of temperature effects, the Tobi team take the circuits into the scientific cold store at 3 C. But they quickly find it is an earthing problem, probably exacerbated by cooling and pressure effects in the deep ocean. They set about putting insulation in at critical places. Mike Avgerinos gives a seminar on the interaction between volcanism and tectonism. It is a warm sunny day with light wind and some rain in the evening.

21 April, 112

The Atlantis RTI survey is finished at 0645, and their ship turns to reach the Tobi deployment point at the N end of Tobi line 4. The magnetometer is recovered by 0750, and Tobi is over the side at 0826, with the depressor weight going in at 0848. It is soon clear that the port side is not transmitting or receiving. The signal, including the surface reflection and TVG noise is clear on the starboard side, but nothing comes through at all on the port side. Start hauling Tobi in at 1015. It is possible that the fault is a simple one in a connector that can be put right rapidly on deck, so the ship is set to circle slowly to return to the deployment point in an hour or so. Tobi is on board at 1150. No easy answer is obvious, and the fault may be caused by a failed transducer, which will take a while to repair. We decide to take the ship down to the S end of Segment 18, where we can dredge the cliffs at the inner corner of the non-transform offset, using the CD 76 images as a rough guide. Eddie discovers strange features of the Whips processing system, and especially that the supposed filtered version of the Tobi altitude is sometimes apparently that, and other times DC shifted from the raw value by up to 300m. This is the result of 3 succesive filters that seem to destroy signal as well as noise. By 1630, Tobi has been repaired, so we go to the S end of Tobi line 4, ready to run the line in the reverse dirction. Tobi goes over on its 6th deployment at 1850, and the depressor weight at 1910. By 1940 it is clear that though the port transducers may be transmitting, the port array is not receiving, even though the port array was picking up ship noise on deck. Start to haul Tobi, which is on board at 2015. In yet another change of plan, we decide to move down to Segment 17, since this is close by; we can dredge there on CD 65 side scan targets, and can, if Tobi works, also pick up one of Roger Searle's lines there. Debbie and Joe spend a hectic hour and a half correlating CD 65 images with Roger Searle's new bathymetric map, and select sites for dredging and camera stations. We are on station for Dredge 8 at 2313. No seminar today. Weather is clear and sunny, though with a cool breeze from the E, and a moderate swell.

22 April, 113

Dredge 8 (28 56.4'N 43 16.6W, 3400 - 3100m) is on a domal feature in the slide zone at the Segment 17 SW inner corner high, N of CD 65 Dredge 34. The dredge went over at 2313/112, the pinger at 2325/112 and the dredge was on board again at 0235/113. The dredge contained hundreds of rocks, including pillow fragments, dolerites, gabbros, some of them apparently metamorphosed. Dredge 9 (28 59.2'N 43 15.1' W, 3400 - 3200m) is on a steep part of the flow zone near its N end just to the W of W Seamount. The dredge went over at 0322, the pinger on at 0322, and the dredge on board again at 0645. It contained about 100 fragments of serpentinised harzburgite, serpentinised dunite, and dolerite. Camera run 1 starts at 0905 at 28 58.8'N, 43 13.3' W in 3500m and finishes at 28 59.5'N, 43 15.7' W. It is targeted to run across the hummocky volcanics just to the W of W Seamount, and then go up the slide slope and through the site of Dredge 9 to the top of the slope. It is set up with black and white film to check exposures with the camera, but there is a wind-on problem. Only the first 30 or so frames come out, showing talus breccia, and then there is no more winding-on. The camera frame brought back two fragments of

porphyritic basalt with manganese oxide encrustations. Dredge 10 (28 54.3'N, 4 18.0' W, 3150 - 3000m) was placed on a domal feature on the slide zone SW of CD 65 Dredge 34. The dredge went over the side at 1625, and the pinger at 1635. It was back onboard again at 1952. The dredge bag contained an enormous haul of pillow basalt fragments, serpentinites and pyroxenites or wehrlites. Dredge 11 (28 53.3'N 43 19.6' W, 2840m) is along the horizontal bench that forms a local top to the slide zone, as imaged on CD 65 Tobi. It is over the side at 2022, and the pinger is on at 2030. The dredge is back onboard again at 2310. It contains pillow fragments with spectacular devitrification structures, and lava shelf and stalactite features. We move to deploy Tobi at the first of Roger Searle's lines. Donna gives the first part of a two part seminar on the paper by Sue Agar and Kim Klitgord on the detachment structure near Agros in Cyprus. Weather is fine and warm, with a breeze from the NE. The rubber boat is exercised, and several members of the science party go out for rides on a choppy sea with the Chief Engineer, returning very happy, very wet, and very impressed by the size of the ship .... not its large size, but its small size.

23 April, 114

Tobi is in the water for its 7th deployment at the start of Roger Searle's line P at 0000, and the depressor weight in at 0020. The survey of Line P starts at 0110, and Tobi goes through the end of Line P at 0900. Tobi passes the W end of Line R at 1045, and the east end of Line R at 1530. Hauling in starts at 1535, and Tobi is inboard at 1913. Tobi operates satisfactorily over the whole pair of lines, giving images similar to those obtained by Roger Searle on CD 99. The along axis jiggle we trace to instability of the bottom detection used for the side scan slant range correction. This can be compensated for if we can get a properly filtered and accurate bottom depth. Sidney and Mike create a good colour palette to use for the area, with pale colours that grade stably into each other. Eddie produces a remarkable illuminated, contoured map of the Atlantis RTI survey, showing some astonishing features, including giant furrows on a 10 slope above the inner corner high at the E intersection, suggesting a huge slip into the median valley floor. We agree that we have to make some more observations there before we leave the area. Donna finishes her two-part seminar on the Agar and Klitgord paper. The weather is grey at first, with a wind gradually increasing from the west, and then moving around to the north-west. After the Tobi line is over, we move to Camera station 2, which is designed to look at the volcanics around and at the top of W Seamount, and to peer into its crater. The survey is in two lines, one from 29 00.0'N, 43 12.3' W to 29 00.2'N, 43 13.3' W, and the second from 28 59.6'N, 43 12.3' W to 28 59.8'N, 43 13.3' W. Both lines run into the now strong wind, and the ship drifts back from the end of one line to the start of the next with the camera above the seafloor. In the middle of the first line the camera passes over the centre of the crater of W Seamount, and the altitude pinger measures its depth as 125m. The camera is overboard at 2022, and the first photograph is at 2158. The first line ends at 2325, the second line starts at 0056/115, and the end of the line is at 0200/115. The camera is back on deck at 0316/115. Because of a broken connector, the flash is not synchronised with the shutter, and no photographs result. Three pieces of volcanic glass come up on the camera frame.

24 April, 115

The day starts with the end of camera run2 (see above), onboard at 0316 in worsening weather. We set out for the S end of Tobi Line 4 in Segment 18, arriving there at 0630 in a gale and a steep nasty swell. The ship heaves to until light. The weather does not moderate, and launching of Tobi is not possible, or even moving Tobi across the deck. Tobi is across the A frame at the stern, and, until we move it, even dredging is not possible. We decide to run N along the W side of the median valley, hoping that Simrad sidescan will allow us to identify dredge sites on slide zones at the SW end of the segment. There is little relation that is obvious between what we see on the Simrad side scan and the Tobi images from CD 76, so we turn at 1145 to close on dredge site 12. The weather is moderating, and Tobi can be moved to clear space on the deck, even though it is too rough to launch it. Dredge 12 (29 22.7'N 42 59.7' W 3000m) is at the southwest edge of the major steep scarp that sits near the SW end of Segment 18. We heave to to move Tobi at 1310, and put the dredge over the side at 1400, with the pinger on at 1405. The dredge is back on board at 1628. It contains one huge block of rock, about 50 ten-cm sized fragments, and smaller cobbles, of basalt and a coarse doleritic or gabbroic rock. We set out for the start of Line 4 again, but the Tobi team report that there is a faulty connexion in the swivel on the depressor, and we turn towards the site of dredge 13. Dredge 13 (29 25.0'N 42 57.4' W 3300m) is near the foot of the major scarp at the SW end of Segment 18, about one third of its length from its E end. The dredge is overboard at 1820, the pinger on at 1830, and the dredge back on board at 2130. It contains about 3 kg of cobbles and pebbles of metabasalt, a modest and retiring haul that brings cheers from the assembled scientists watching it come on deck; it is the smallest yet, but entirely satisfactory for petrology. After the dredge is on board, we set out for the start of Tobi line 4 again. Tobi is over the side for its 8th deployment at 2305, and the depressor weight at 2330. Eddie gives a seminar on the paper by Escartin and Lin on the gravity signal of low-angle faulting at inner corner highs. Weather starts as a gale with high swells and moderates as the day goes on, but is still not pleasant at the evening.

25 April, 116

The surface reflection from Tobi is visible at 0030, so the floating magnetometer is deployed at 0035, and by 0120 bottom features are seen. Tobi continues along Line 4 all day, showing on the side scan, among other features, the sliced-off fault block from which dredges 12 and 13 came, several flat-topped seamounts, a hummocky volcanic ridge made up largely of fissure-fed flows and a major fault zone along the west side of the median valley. The quality of the side scan is as before, with the along-axis jiggle that is caused by the instability of the bottom detection, and the fringing at far range. The signal of the phase bathymetry is unusually clear, especially because Chris Fluellin has discovered the cause of the striping that was running across the record, which came from an indexing problem in the software. The signal disappears abruptly about half way across the record, suggesting to Chris that there may be a problem with getting sound out to the far range, perhaps because of the transducer design. Debbie gives a seminar on Mathilde Cannat's paper on the structure of slow-spreading crust. The weather is cool and breezy, with a high swell still running.

Debbie and Donna point out that, if Yellow Mountain is discounted, the northern end of Segment 18 has almost no median valley, since the level of the valley floor rises, while the flanking mountains remain at the same level. It is a cool breezy day with a large swell.

26 April, 117

At 0030 there is a voltage surge in Tobi, and it fails. Tobi is hauled in, and the depressor weight is taken on board. Tests indicate that the fault is further into the system, and the swell is too high in the dark for Tobi to be recovered. The depressor weight is put out again, and 200m of wire, and Tobi is left until daybreak, while the ship return slowly to the place where Tobi records stopped. Tobi is brought on deck at 0915. Further tests show that the fault is in the swivel on the depressor after all. When the swivel is stripped down, the oil inside is milky with water leaking in. The Tobi team decide to replace a unit of the swivel that contains a seal that may have failed with a replacement unit from a spare, which requires machining the spare to match the part that is being replaced. All is ready by 1410, and by 1420 Tobi is overboard. It takes a long time to acquire the first Tobi signals from the bottom which arrive at 1715, and the floating magnetometer is put out at 1930. The signals seem as bfore, though the port sidescan image is noisy at far range. There are occasional bursts of noise on the port side swath bathymetry, but these do not affect the other channels. More flat-topped seamounts come by. Joe and Debbie bet about the nature of the median valley floor next to Yellow Mountain. Debbi wins. Joe gives a seminar about the Neumann and Forsyth paper on the origin of the topography of the median valley. The weather is good, with a light wind and patchy sunshine, but still with a marked swell.

27 April, 118

The long turn from Line 4, up the axis of the median valley, to Line 5, the line along the transform fault, takes most of the night, though there are Tobi images of the crust on the N side of the transform in the course of it. The ship steadies on the new line about 0700, and crosses the neovolcanic zone of Segment 18 at about 0800. Shortly after, as we cross the nodal deep, we can see splays of the transform fault cutting across the track. Side scan noise levels start to increase, and the range of visibility closes down. Further on, the transform can clearly be seen as a single fault trace. The sediments on the floor of the transform trough are patterned like melted chocolate. Tobi starts to turn onto the parallel Line 6, on the south wall of the transform vally, at 1800, and completes the turn by 2000. As Tobi rises the noise decreases, gradually on the starboard side and abruptly on the port side. Any improvement in phase bathymetry is "more subtle" (quoting Chris Fluellin, which means that the rest of us cannot see it at all). The track is now over the finger ridges that run down the transform wall, spines of rocky crags, with sediment-covered valleys betweeen them, that, on the Simrad map, have the geometry of debris flows. Eddie finds that the Whips altitude smoothing routine uses pressure change as an indicator of changing altitude, assuming terrain following tracks, which we do not use. He takes this out. Bob Janssen gives a seminar on the Krafla spreading event in N Iceland in 1975-1982. The weather is very dull and rainy at first, changing sudddenly to a bright sunny day in the early afternoon, with light winds.

28 April, 119

Tobi continues through the night on Line 6, over more finger ridges and the valley between them. Around 0700 we pass over a strange cirque-like feature, mantled with sediment, but with a bright floor, perhaps a dome leading to a flow. Interference reappears at 0715 on both port and starboard sidescan simultaneously, stronger on port than on starboard. Tobi is descending, and we wonder if the noise is a tempoerature effect. We descend into the median valley, though flying high to try to avoid the fog, and pass across it onto sedimented basalt before starting to make the turn onto Line 7 at 1200. The starboard side scan noise decreases gradually, but the port noise stays high. Line 7 is the central line in the median valley floor, going south. By 1400, the ship has turned east on a 5 mile leg before turning S. The volcanics W of the median valley are very highly sedimented even close to the neovolcanic zone. The start of Line 7 is passed at 1730. As Tobi nears the bottom, the port sidescan picks up, but is still dim compared with the starboard side. We puzzle over how few faults there are on the whole section at the N end of Segment 18, including both the inner and outer corners. We image a major fault at the E side of the median valley, and fresh volcanics to the west.. Eddie makes a plot of Simrad sidescan for the RTI survey, which shows a lot of textural differences, including faults and sediment ponds very clearly. No seminar today as it is Sunday. The wind is brisk from the N, with patchy sun and cloud, and a large swell.

29 April, 120

Tobi continues throught the night on Line 7, imaging the debris flows from Yellow Mountain, which stop exactly at the track of Tobi, and then a varied range of vlocanic features down the axis of the valley, as well as some young faults, with intricate fracture patterns of linking segments even though the throw of the faults is below the resolution of the Simrad bathymetry. There are 3 fault arrays of this kind, each about 10km long. Towards the S end of the segment there are interesting textures of volcanics and sediments, with individual lava flows clearly visible, and strange pits in the sea floor, one of which, if it is a pit, seems to have lava ooozing out of it. Opinions differ. We start the long turn to Line 8 at 1900, which is difficult because of large wire angles, and the turn is only complete at 2200. There is a poor weather forecast of a rapidly approaching low, and, after a bright and breezy start, as the day goes on the wind comes around to the W and increases steadily, so that by midnight it is a stiff gale. Rachel Pascoe gives a seminar on inversion of deep-towed magnetic profiles.

30 April, 121

The storm becomes very bad in the night, with winds over 30kt and a steep swell. By 0400 it is clear that we cannot hold onto Line 8, and we start to turn towards the wind, with the aim of turning eventually onto Line 9, a diagonal line running SE across the median valley. The part of Line 8 that we complete shows the scarp from which we dredged metabasalts on dredges 12 and 13, as well as the fault structure N of that which may be part of a slide zone. As the ship reaches the start of Line 9, it becomes clear that the wind and swell will not allow us to hold that line either; it is too far off the wind. We modify the line to

be more directly down wind, but the weather grows worse, and soon the stern is slamming down hard on the swells every few minutes. We decide to abandon any attempt to run down wind, to haul Tobi in to 500m, and then make a turn into the weather. We start to haul at 1200, and have hauled in to 500m by 1400, by now some way E of the median valley. We try to set a course of 015 , to run parallel to the median valley, and join on to a line we plan over Yellow Mountain, but the wire angle on this course is very bad, so we modify this to a diagonal course across the median valley towards the end of our E-W lines. As we pay out wire on this course, the wire starts to snatch in the A-frame block, going alternately slack and tight in great jerks because of the swell. At this point (at 1845) we decide that the weather is too bad to do any science at all, and to haul in to 500m, while setting a course into the wind and wait for the weather to improve. Sidney Mello gives a seminar on the modelling of the effect of hydrothermal alteration on axial magnetic anomalies.

1 May, 122

By 0800 the weather is moderating a bit, and the swell is much less steep. We are by now far to the W of the survey area. The wind is at 25-30kt from just N of W. We decide that our highest priorities lie at the N end of the segment, and that we should make our way back there as soon as we can. At 1000 we turn to see if the ship can hold a course that will take us to the line over Yellow Mountain, with the wind and sea following. Though uncomfortable, this is far better than the day before, and we decide to lower Tobi and collect data as we make our way across. This is line 9M (M for May Day). We start to lower Tobi at 1035, and by 1200 are seeing the bottom, though the record is quite noisy, especially on the port side. As we continue across the crestal mountains on the way to the median valley, it is noticeable how few faults there are, compared, say, with the off axis line in Segment 17, even this far from the transform. And it is clear from the bathymetry that there are even fewer faults as the transform is approached. By 2000 we are still just holding the track, though with a poor wire angle, and are coming into the median valley. As we climb the major fault that marks the E edge of the median valley, we try to turn onto a track at 015 , but are defeated by poor wire angle, and the need to haul fast up the cliff, so we run on further, and turn further into the wind to cross Yellow Mountain at an acute angle and run for the W end of the E-W cross tracks (Line 10A). After the inital moderation, the weather stays constant all day, blowing 25-30kt from the W, with a large swell, and at times sunny skies. Mike Avgerinos gives a seminar on the crustal structure of North Atlantic fracture zones.

2 May, 123

As we start Line 10A, we are pushed NE by the wind, but still make a good course over Yellow Mountain, which we pass at 0430. The top is a jumble of features, which will need to be superimposed on the bathymetry to make sense. We make an interesting diagonal track across the median valley, and have nearaly reached the end of Line 10A when the Tobi swivel fails at 1402. Tobi has worked continuously since 1420 on 117, for 6 days, even in really bad weather. We haul Tobi in, and the depressor weight is in at 1600, and Tobi is on board after a difficult recovery at 1645. The swell is still high, making the whole process rather marginal. The flotation is chipped, the fenders bent, and

one of the swath bathymetry tubes is split during recovery, so that oil runs from it out onto the deck. The failure is apparently caused by breaking of the cable at the swivel just where it enters the umbilical, perhaps by working to and fro during all of the bad weather. There is no question of deploying Tobi again until after the bad weather is over, so we decide to go for a camera station on the top of Yellow Mountain, to see if it is a large volcano, and to test the camera system to se if it is working now. Just before launching, Dave Edge reports that the wind-on problems have been caused by friction between the film spools and the camera cover. Camera station 3 starts at 29 49.1'N 42 41.4' W, at 1650m and is planned to finish on the summit plateau of Yellow Mountain. The camera goes over at 1957, and is at the bottom by 2056. Once the camera reaches the bottom it becomes clear that control of its height is very difficult, since it has to be 3-7m above the bottom, and the swells are as high as that, to say nothing of the irregularities of the bottom. The camera takes pictures, but continually collides with the bottom. We decide to abandon the station in view of these difficulties at 2152. When the camera is back on board at 2240, its battery packs have become dislodged, and have fallen out of the frame. There are no spare battery packs on board, so we are now without a camera. We set out on transit to make dredge 14. The weather remains the same all day. The wind occasionally drops to 20-25kts, but then rises again, and remains constant in direction, The swell is not as bad as at the height of the storm. Joe Cann gives a seminar explaining how basalt geochemistry can give information about magmatic processes below the ridge axis, and how the answers may be largely controlled by the model you start with.

3 May, 124

The day is spent dredging. Dredge 14 (29 57.3'N 42 30.4' W 1800m) is in the cirque at the NW corner of Hinge Mountain, at its S side, designed to find out the composition of this large slab of rock. It goes over the side at 0101/124, the pinger is out at 0109, the dredge is on the bottom at 0154, and the remains back on board at 0258. After 15 minutes on the bottom there is a sudden and enormous bite, up to 7 tonnes. When the wire is reecovered, the dredge chain comes on board, but the dredge is not there. It is clearly a hungry mountain. Dredge 15 (29 55.1'N 42 30.0' W, 1550m) is in the middle of the flat block of Hinge Mountain, where we later see strong lineations, partly covered by sediment, from Tobi. It goes over the side at 0358/124 and the pinger is on at 0408. There is a problem with the swivel on the pendant, and the dredge has to be brought back on board for the wire to be sorted out. The dredge is over the side again at 0530, the pinger is on at 0540, and the dredge on the bottom at 0655. There are large bites, and the dredge is brought in slowly , then off the bottom at 0722, and back on board at 0819. It is a small haul of indurated ooze, with one angular fragment of basalt, and two small rough lumps of serpentinised harzburgite. Dredge 16 (29 57.6'N 42 30.3' W 1850m) is again in the cirque at the NW corner of Hinge Mountain, this time on its E side. The dredge is over the side at 0859/124, and is on the bottom at 0948. By 1000 the dredge is firmly stuck on the bottom, and the ship, dredging downwind, cannot get back fast enough over the dredge. Tension stays high until there is a 7 tonne bite, and the chain comes free. The chain is back on board at 1108, with no dredge, another victim of the hungry Hinge Mountain. Dredge 17 (29 55.0'N 42 26.9' W

2000m) is on the large fault bounding Hinge Mountain to the east, targeted about half way up the fault to collect some talus. The dredge is over the side at 1255/ 124, and on the bottom at 1335. There are one or two bites including one very large twitch, and we start to haul in at 1405, bringing the dredge back at 1450. The pipe dredge has been torn from the dredge bag, ripping two holes in the corner of the bag. The dredge contains two fragments of weathered basalt, one of them with a skin of indurated ooze. Dredge 18 (30 00.0'N 42 25.0' W 3200m) is on the finger ridge that runs down into the transform valley from the NE corner of Hinge Mountain. The dredge is over at 1552/124, and the pinger is on at 1600. The dredge is back on board at 1856, containing two fragments of weathered pillow basalt with a thick coating of manganese oxide. Dredge 19 (30 02.6'N 42 37.6' W 4250m) is on a rounded bulge of the topography close to the western RTI of the Atlantis Transform, showing bright on Tobi. The dredge is over the side at 2016/124, the pinger is on at 2020, and the dredge is back on board at 2350. This virgin dredge frame is seriously bent by the time it arrives back, and it and the pipe dredge contain a small haul of peridotite, gabbro and pyroxenite. Donna gives a seminar on phase bathymetry, starting from basic levels, and including some of her latest insights. The weather continues rough, with 25-30kt winds, and a large swell, but the winds come round to the NW in the afternoon, giving promise of calmer weather to come.

4 May, 125

Dredge 20(30 01.7'N 42 41.2' W 4100m) is on a fissured slope imaged by Tobi close to the western RTI. The dredge is over at 0107/125, the pinger is on at 0117, and the dredge back on board at 0435. The dredge contains about 20 chunks of pillow basalt, moderately weathered and with a thin coating of manganese oxide. After the dredge is on board, we set out on a mini-Simrad survey to fill in the west end of our previous survey, which stops a bit short there, and to add a bit to the north. This starts at 0500 and runs on until the Tobi team tell us at 1410 that they have Tobi back together again and testing well. At 1500 we reach the end of the latest line of the survey and head for the Tobi deployment site at the E end of Line 11. The deployment goes smoothly. Tobi is in the water at 1710, the depressor weight is in at 1730 and the first images of the bottom appear at 1900. The floating magnetometer is deployed at 2012. The Tobi images first show thick sediments with rocks poking through, and then go up the fault scarp to the top of Hinge where the most amazing striations appear parallel to the furrows that show up faintly on the topography. They run parallel to the course we are following. The longest set is 1-2 km long, and there is a shorter set at an angle to this. It is difficult to see how they can be anything else except striations on a fault or slip surface. Further to the west the striations are covered with sediment, but can still be seen faintly across the whole of the flat block. The weather is getting better. The wind is below 20kt for the first time in over 4 days, and is in the NW. Temperatures are cool, but the motion is much reduced. Eddie gives a seminar on fault damage zones and subseismic faults in the North Sea.

5 May, 126

Tobi Line 11 ccontinues through the night, coming down off the top of Hinge over a fault dusted wih sediments, and then over slide-like topography towards

the median valley. The slides continue into the narrow deep that cuts into the end of the median valley, while the west half of that deep contains bright volcanics. To the west of the deep, young volcanics continue for a while, and then sediment gradually begins to cover them. The end of Line 11 is reached at 0930, and the start of Line 12 is passed by Tobi at 1230. Tobi has risen onto a major ancient volcanic ridge running towards the transform valley, showing as lumpy topography poking up through mud. Towards the median valley we cross a muddy plain before coming onto young volcanics near the median valley. At this point it becomes clear that the starboard swath bathymetry has stopped working (the port swath bathymetry had not been working for some time). Then it reappears for 5 minutes before vanishing again. As we cross the median valley, spectacular lavas show up, and then slide material comes in on the other side of the valley floor, with one small, conspicuous cirque from which a bright flow emerges. The line goes over the N end of Hinge, over rather broken terrain, though there do seem to be some striations there. The cirque in which we lost two dredges looks very innocuous. No seminar today. The weather is on the mend, with a brisk wind in the morning, dying down as the day goes on. We have a barbecue in the evening, to celebrate the end of bad weather, and, crossing fingers, the fact that Tobi is still working. Various events happen, perhaps better remembered (and they were pretty memorable) than recorded, assisted by some smoothly slurpable, but astonishingly strong, punch. Afterwards we agree that to have another barbecue would be an anticlimax after this one.

6 May, 127

Continue to the end of Line 12 with Tobi, then make a rapid crosing of the transform valley (Line 13) to start Line 14 diagonally NE along the NW side of the block that makes up Rose. Port sidescan is weak, especially looking down hill. Starboard side swath bathymetry came back some time in the night, and is looking good. Side scan records are noisy at far range. No clear furrows are seen on this run, which is west of the main furrowed area, but several axis-parallel features show up. Towards the end of Line 14 is a good image of the fault that lies at the back of the N end of the slide area. Line 15 starts at 1800, and climbs up onto the slipped block first, showing good hummocky volcanic topography on the top of it, and then rises onto the furrowed surface, on which are excellent striations, especially on its upper part, parallel to the topographic furrows. On the top of Rose are areas of slabby outcrop, cut in one place by a small corrie. Line 15 ends at 2330, with the start of the turn to Line 16. Debbie gives a seminar on previous work in the Atlantis fracture zone. The weather has become very fine and warm, with a light breeze and much sunshine.

7 May, 128

Line 16 starts at 0100 and runs along the S edge of Rose, before descending to cross the median valley. On the edge of Rose it images finger ridges running down into the transform valley, with gullies between. The descent into the median valley is a long sheet of bright talus, interspersed with small crags. The median valley floor has no recent volcanism on it at all; it is thickly sedimented. The line goes up the scarp opposite, and onto sedimented hummocky volcanics. Line 16 ends at 0800. There is a long turn to Line 17, which Tobi starts at 1130.

The volcanics on the ridge seem less sedimented than on Line 16 further N, and are separated from the nodal deep by a fault. Tobi flies high over the nodal deep so as to make the start of Line 18 at 1830. This line runs at the base of the steep slope coming down from the inside corner high. On one side the slope is a bright debris flow/talus pile, and on the other the median valley floor is thickly sedimented and cut by faults and fisssures. Further N there are recognisable volcanic landforms which are moderately sedimented, and N again the sediment looks thinner and the volcanism more recent. The turn to Line 19 starts at 1915, and Tobi passes the start of Line 19 at 2315. On this last line, there are good images of faults, volcanics and debris flows as Tobi climbs the shoulder of Rose. Bob Janssen gives a seminar on maps, and especially on the Universal Transverse Mercator Projection. Weather has become very fine with a light breeze.

8 May, 129

Line 19 finishes by imaging more striations on the upper part of Rose, and then is recovered, with Tobi on deck at 0415. Dredge 21 (30 05.8'N 42 03.3' W 2900m) is sited on the very bright debris flow material on the eastern slopes of Rose, just above an outcropping scarp, imaged on Tobi Line 16. The dredge is over the side at 0500, the pinger is on at 0508, and the dredge is on the bottom at 0608. It becomes stuck at 0651, and the ship comes round to pull from the other direction. At 0729 the dredge is off the bottom. and is on board, empty at 0833, with the pipe dredge lost on the bottom. Dredge 22 (30 06.0'N 42 03.6' W 2550m) is just up the slpe from Dredge 21, on the same bright sheet of debris. The dredge is over the side at 0909, the pinger on at 0912, and the dredge on bottom at 0957. The dredge is stuck at 1015, and the ship comes around again to pull the dredge free, which it does at 1055. The dredge is back on board at 1130 with a large haul of gabbroic and ultramafic rocks (in the broad sense) with a variety of grain sizes and textures. There appear to be no deformed gneissic rocks in the dredge haul, and no harzburgites. Dredge 23 (30 08.5'N 41 59.6' W 4200m) is on the debris flow coming down from the down-slipped block, near to the median valley floor, and imaged on Tobi Line18. The dredge is over the side at 1236, the pinger is on at1245, the dredge is on the bottom at 1409, and the dredge is back on board at 1620. This dredge brings up a large haul of pillow fragments, many fragments of coarser rock that may be fragments of dykes, one piece of serpentinite, one gneissic gabbro and two fragments of breccia. Dredge 24 (30 05.7'N 42 06.6' W 2250m) in targeted at a stone chute in one of the gullies running down from the top of Rose, imaged by Tobi on Line 16. It is over the side at 1745, the pinger is on at 1755 and the dredge is back on board at 2021. The dredge contains 7 rock fragments: one gabbro and six serpentinites. Dredge 25 (30 10.1'N 42 07.2' W 1650m) is targeted at the striations running across the smooth surface at the N of Rose. It is over the side at 2100, the pinger is on at 2104, the dredge is on the bottom at 2132, and is back on board at 2238. It is a difficult dredge across bare rock, and only brings back two small pieces of rock, both serpentinised harzburgite. Dredge 26 (30 08.4'N 42 06.7' W 1200m) is in a small corrie near the top of Rose. It is over the side at 2302, the pinger is on at 2307 and the dredge is back on board at 0010/130. There is a large bite shortly after the dredge reaches the bottom, whoich suggests that the dredge is strangled, but when it is brought back it has not strangled, and also has nothing

in it. The day is hot, sunny and almost glassy calm. The engineers have the rubber boat out from 0800 to 1500, and give rides across the sea away from the ship, which rolls behind shining swells. At 1700, just before dredge 24, we have a swim call for 20 minutes, and Debbie catches and removes jellyfish from the swimming area.

9 May, 130

Dredge 27 (30 08.4'N 42 06.7' W 1200m) is again in the small corrie near the top of Rose. The dredge is over the side at 0042, the pinger is on at 0049, the dredge is on the bottom at 0114 and back on board at 0206. The only product of this dredge is a delicate, pink, branching coral. We give up the corrie and try to sample the top of Rose. Dredge 28 (30 07.8'N 42 07.3' W 900m) is on the summit plateau. It is over the side at 0233, the pinger is on at 0241, the dredge is on the bottom at 0258, and back on board at 0400. It brings back a small piece of limestione and a small angular clast of basalt. Immediately the ship sets sail for Cadiz, and the magnetometer is streamed at 0415. The weather is still good, with a light head wind. Joe Cann gives a seminar setting out tentatively his ideas about the interpretation of the ridge-transform intersection surveys.

CD 100
NOBSKA

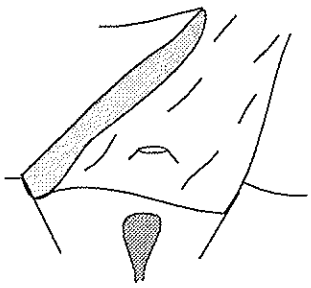

Section 3.0 Transit to Survey Area

Ponta-Delgada to Segment 18 on the Mid-Atlantic Ridge

3.1 Outward journey

The transit survey started at the 200 m limit to the Azores. At 1430 the surface magnetometer was deployed and the three-component flux-gate magnetometer, and the SIMARD multi-beam bathymetry started. The following waypoints were given to the bridge:

35 23.63 N	30 35.60W
35 08.06N	31 35.60W
34 08.71N	33 09.31W
33 07.82N	35 11.20W
31 09.71N	37 07.39W
31 10.69N	39 03.03W
30 41.18N	40 00.85W
30 11.6N	42 38.7W

The route taken to the survey area was defined to parallel the route taken by CD99, on their leg from Lisbon to the Broken Spur segment, increasing the available multi-beam swath data to ~20 km wide. **Figure 3.1** shows the transit from the Azores to the survey area, with the SIMRAD multibeam swath underlying the track. On the return leg to Cadiz, a small deviation in the track was made to pass over the Gorringe Bank with Simrad, providing a single swath of multibeam data.

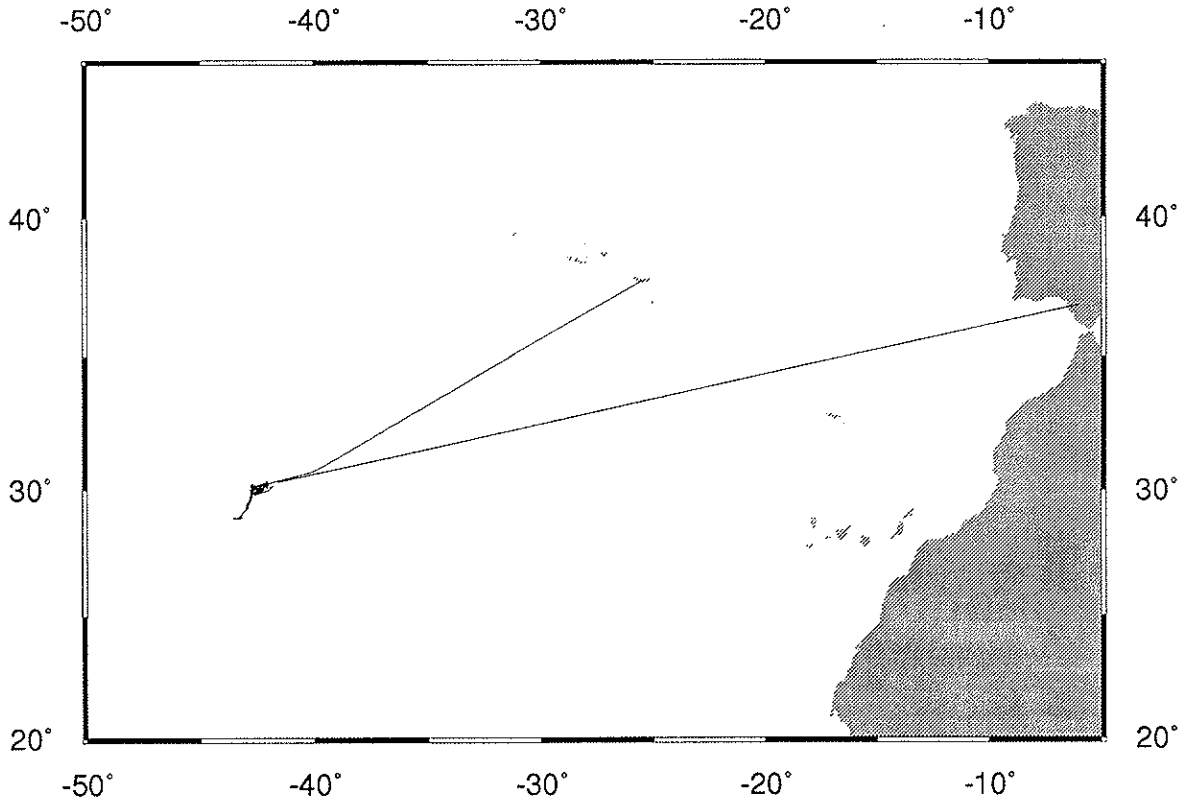

FIGURE 3.1

Transit route from Azores to the NOBSKA survey area and from survey area to Cadiz. The start of data logging commenced at the 200 m limit from the Azores. The simrad swaths are ~10 km wide (3 x water depth).

CD 100
NOBSKA

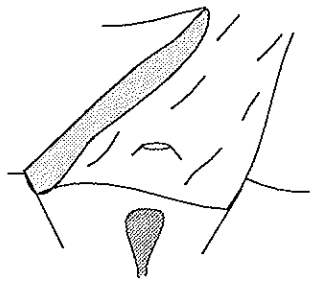

Section 4.0 Survey Results

North of Broken Spur Kane to Atlantis

4.1 Introduction

This section presents the results of the complete survey carried out during cruise 100. After reviewing the know geology of the three areas of the survey, we present the data gathered, starting with the TOBI sidescan data, through SIMRAD bathymetry and sidescan to the under-way geophysical data.

4.2 Geological Overview

There are 18 tectono-volcanic spreading segments betwen the Kane Transform and the Atlantis Transform, each from 10 to 100km long. The Broken Spur and Nobska spreading segments are the two most northerly segments, and the Nobska segment terminates in the Atlantis Transform. The Broken Spur segment, studied during CD65 by many of those on the ship for CD100, has an ideally typical morphology. It has a straight, narrow median valley, with a well-defined axial volcanic ridge, and is offset from the segments north and south by non-transform offsets of about 15km. The CD65 survey showed it to contain some classic small volcanic seamounts, and an extensive area of landsliding at its southern inside corner, perhaps associated with serpentinite diapirism. The Broken Spur hydrothermal vent site lies at its centre of this segment, and has been the subject of intense study. A microearthquake survey was made in the southern end of the segment.

The Nobska Segment to the north is less classical in form. It is bordered by a non-transform offset to the south and by the Atlantis transform fault to the north. At its southern end it is symmetrical, with major faults on each side bordering a median valley floor containing an axial volcanic ridge, but to the north the cross-axis profile becomes asymmetrical, with a large fault on the east side, but only

minor faults to the west. At its northern end the western faults are so small that it is difficult to define the edge of the median valley at all. The shallowest depth on the longitudinal profile of the median valley floor would be expected to be south of the centre because of the presence of the transform fault to the north. It is, however well towards the north of the segment centre, close to a major seamount on the eastern wall of the median valley, which we term Yellow Mountain, and at about the place where the western wall of the median valley vanishes. It seems that excess volcanism at this place may have filled up the median valley, and may be responsible for Yellow Mountain, too, which has well-developed ridges resembling volcanic rift zones radiating from its summit.

The Atlantis Transform is the southernmost of a group of transforms that offset the MAR as it approaches the Azores. It has a relatively small offset for a transform, about 80km, and a correspondingly simple morphology. The trace of the transform can be identified from bathymetry as a single fault trace for most of the length of the transform valley. The two ridge-transform intersection at each end have very different characters. That at the west, where the Nobska segment reaches the transform, is volcanically very robust, with a major volcanic ridge reaching across to the far side of the transform valley. At this end of the transform, there is no inside corner high, but an area of hills with a height of a few hundred metres. At the eastern end of the transform, the nodal deep shows little sign of recent volcanism, and there is a major inside corner high reaching to within 1000m of the surface

4.3 TOBI Sidescan

The original survey plan was to have 3 km spaced ship tracks running parallel to the NOBSKA segment, allowing for dual insonfication of the median valley and part of the offaxis region. However due to the time lost as a result of TOBI problems the survey was ammended (See "CD 100 Cruise Narrative" on page 30.). The calculated TOBI route for the whole survey of the NOBSKA segment, Atlantis Transform and the inside corner high of segment1 north of Atlantis, are presented in **Figure 4.1**. More detailed tracks can be found within the relevent sections.

TOBI images for the complete survey are shown in **Figure 4.3** through **Figure 4.15**, the source file for these images are shown at the top of the figures along with the starting and finishing time and location. The order of images reflects the order in which they were collected.

The images presented have been heavily sub-sampled from the original 8000 pixels across, 4000 port and starboard to 200 pixels across. A discussion of the TOBI sampling rate and original resolution can be found in Section 1.4.1 on page 13. . Detailed images, are highlighted by a white box on the sub-sampled sidescan images, and a discussion of the geology interpreted from the sidescan images are presented in the next section.

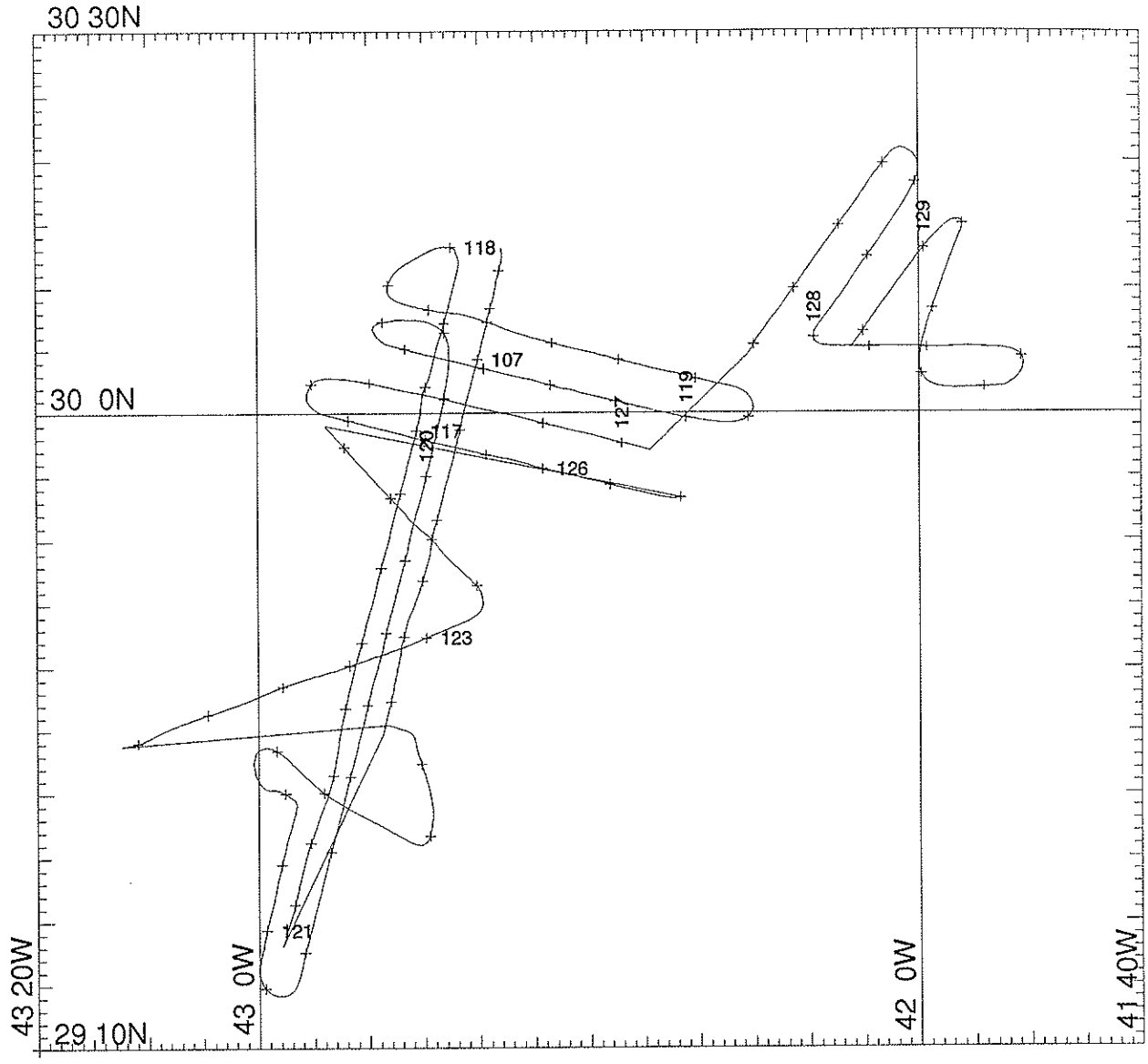

FIGURE 4.1

Tobi survey track over the NOBSKA segment, the Atlantis Transform and segment 1 north of Atlantis. Crosses represent 3 hour time markers and the Julian day is plotted at midnight.

MO: 431
Start: 30.2177°N -42.6317°W
Time106/16:11

End:29.7990°N - 42.7457°W
Time:107/08:06

MO: 432
Start:29.7944°N - 42.7474°W
Time:107/08:19

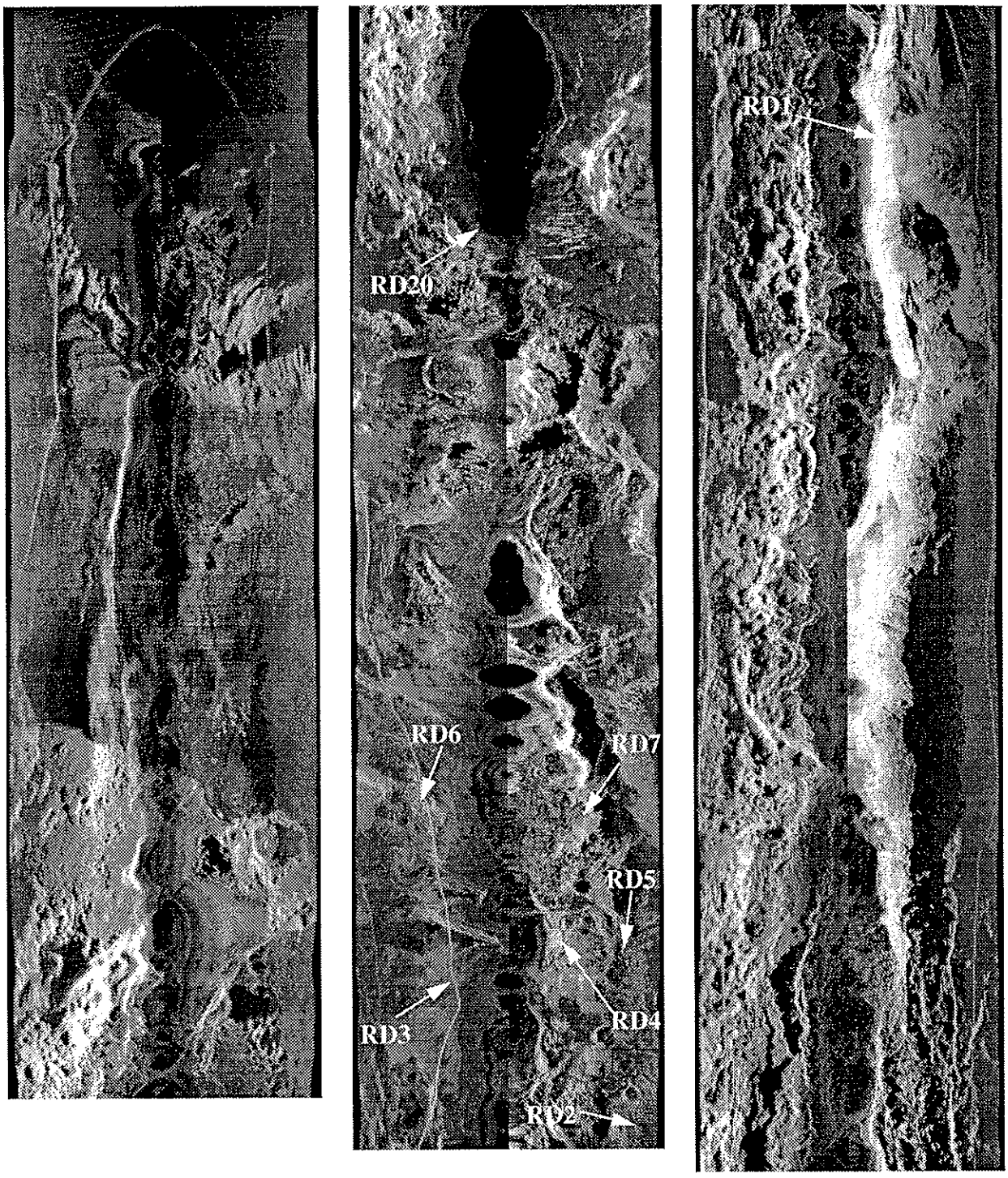

FIGURE 4.2

TOBI images. Time progresses from left to right and from top to bottom in each tile. The original 8000 pixels across have been subsampled to 200 pixels across. The start and end for time and location have been defined for each magneto-optical disk (and compact disk). Dredge haul locations and detailed images are indicated on the tiles.

MO: 435-436

Start: 29.5707°N -42.8786°W
Time: 115/23:37

End: 29.9974°N -42.7546°W
Time: 116/10:35

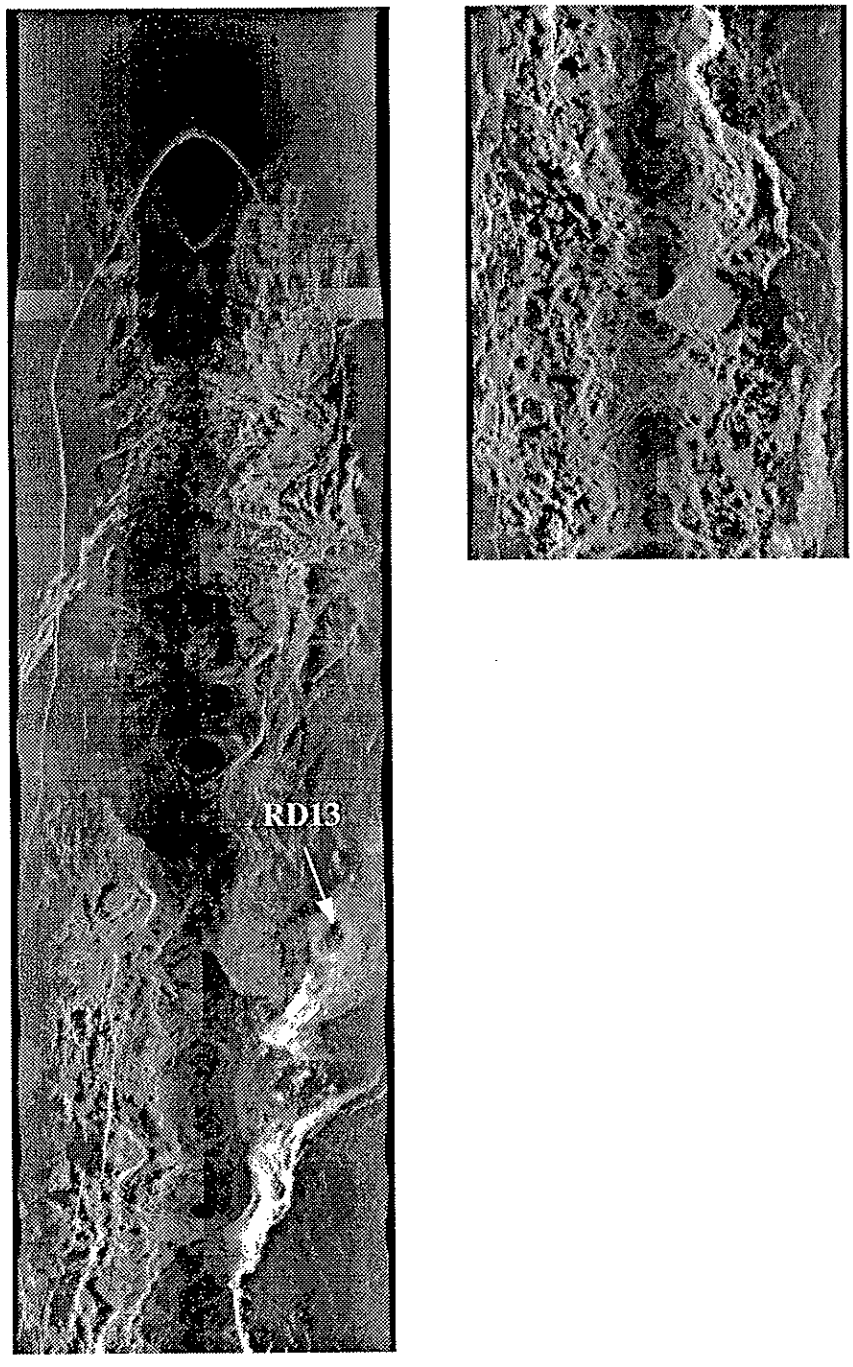

FIGURE 4.3 TOBI sidescan images from julian day 115

MO 437
Start: 29.5707°N -42.8786°W
Time: 117/14:38

End: 30.1337°N -42.7192°W
Time: 118/06:46

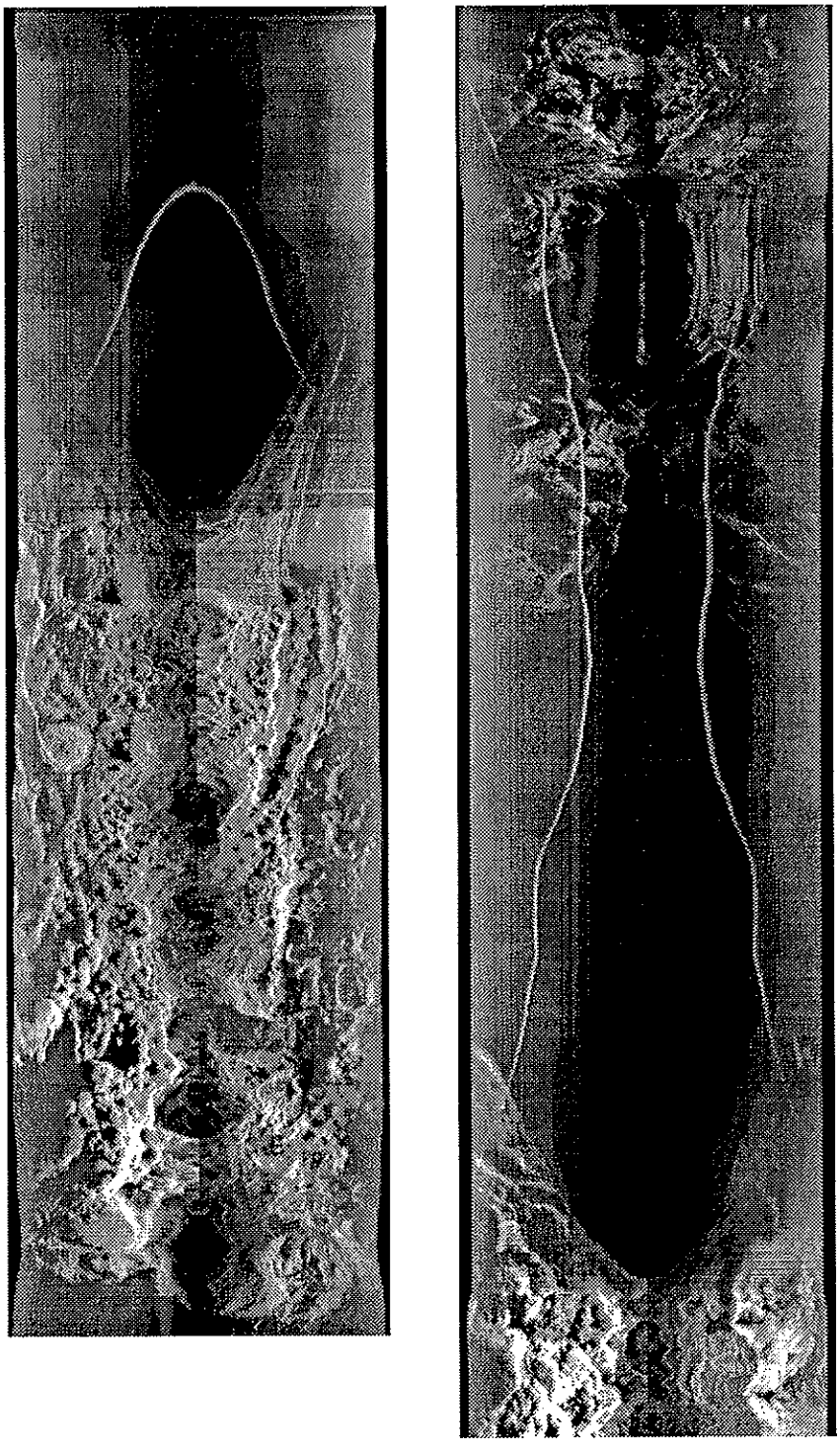

FIGURE 4.4 TOBI sidescan images from julian day 117

MO: 438
Start: 30.1337°N -42.7192°W
Time: 118/06:46

End: 29.9881°N-42.3191°W
Time: 118/22:55

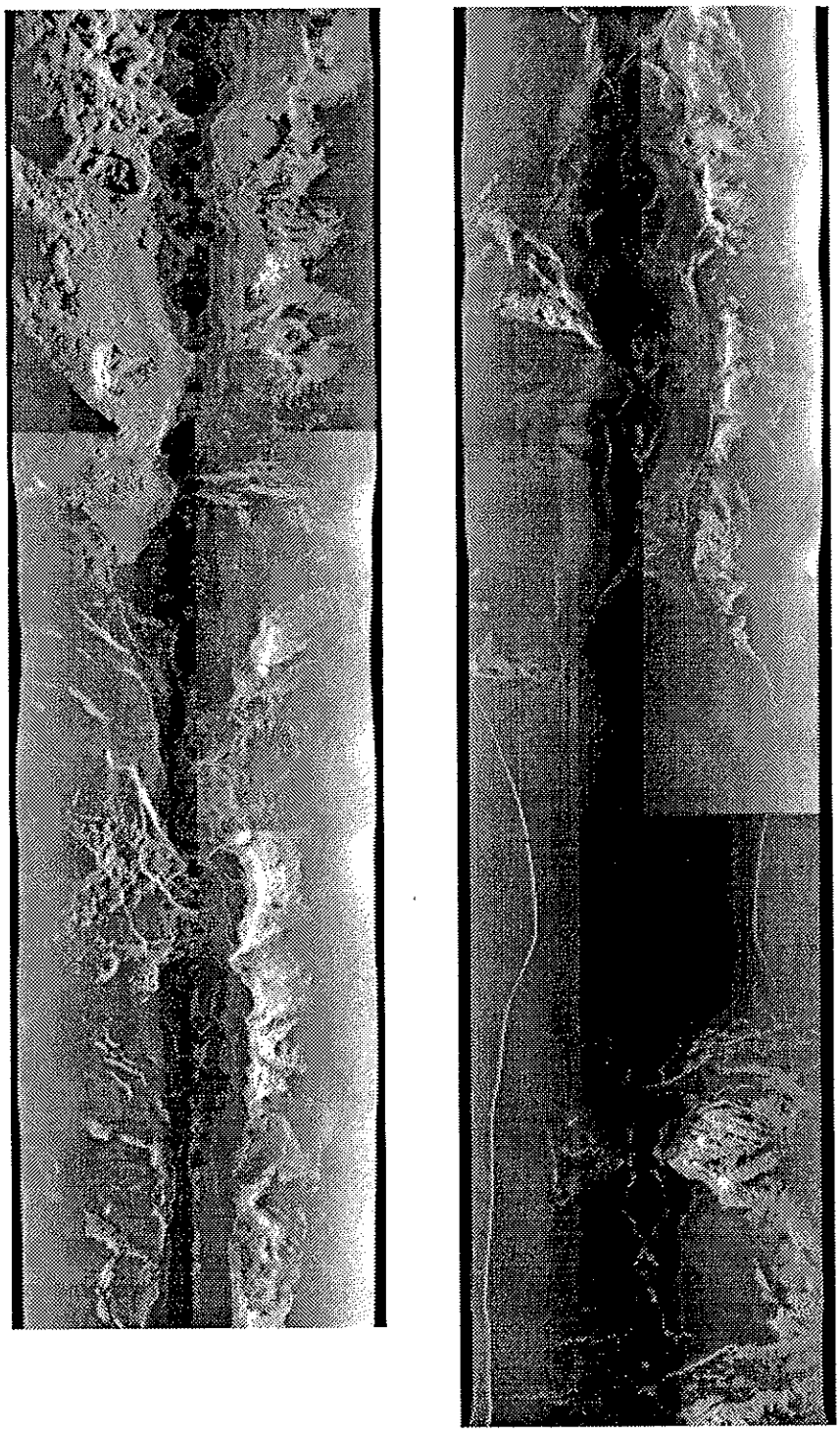

FIGURE 4.5

TOBI sidescan images from julian day 118.Time progresses from left to right and from top to bottom in each tile. The original 8000 pixels across have been subsampled to 200 pixels across. The start and end for time and location have been defined for each magneto-optical disk (and compact disk). Dredge haul locations and detailed images are indicated on the tiles.

MO: 439
Start: 29.9881°N -42.3191°W
Time: 118/22:55

End: 29.9881°N - 42.3191°W
Time:119/15:04

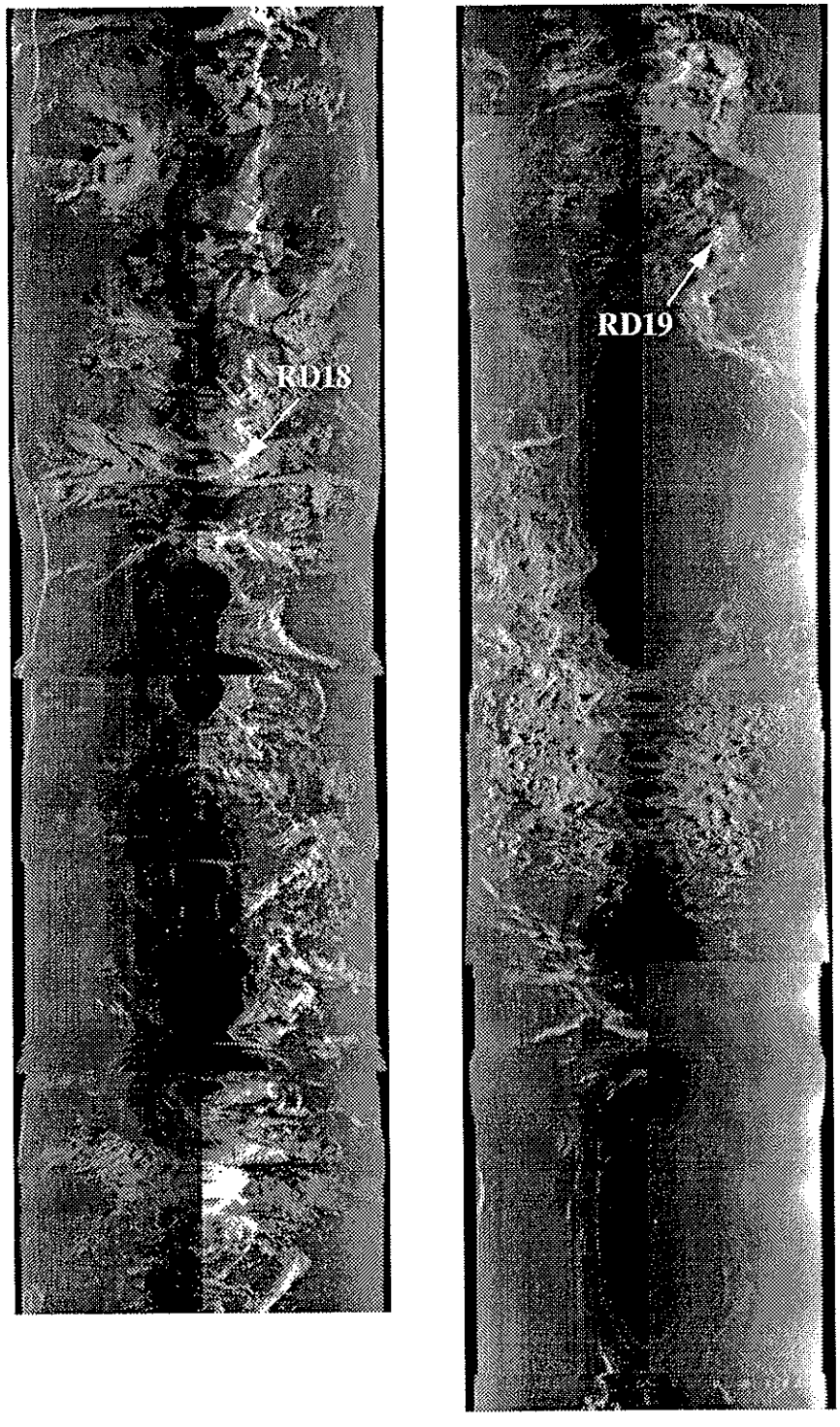

FIGURE 4.6 TOBI sidescan images from julian day 118

MO: 440
Start: 29.9881°N -42.3191°W
Time: 119/15:04

End: 29.6735°N -42.817°W
Time: 120/07:14

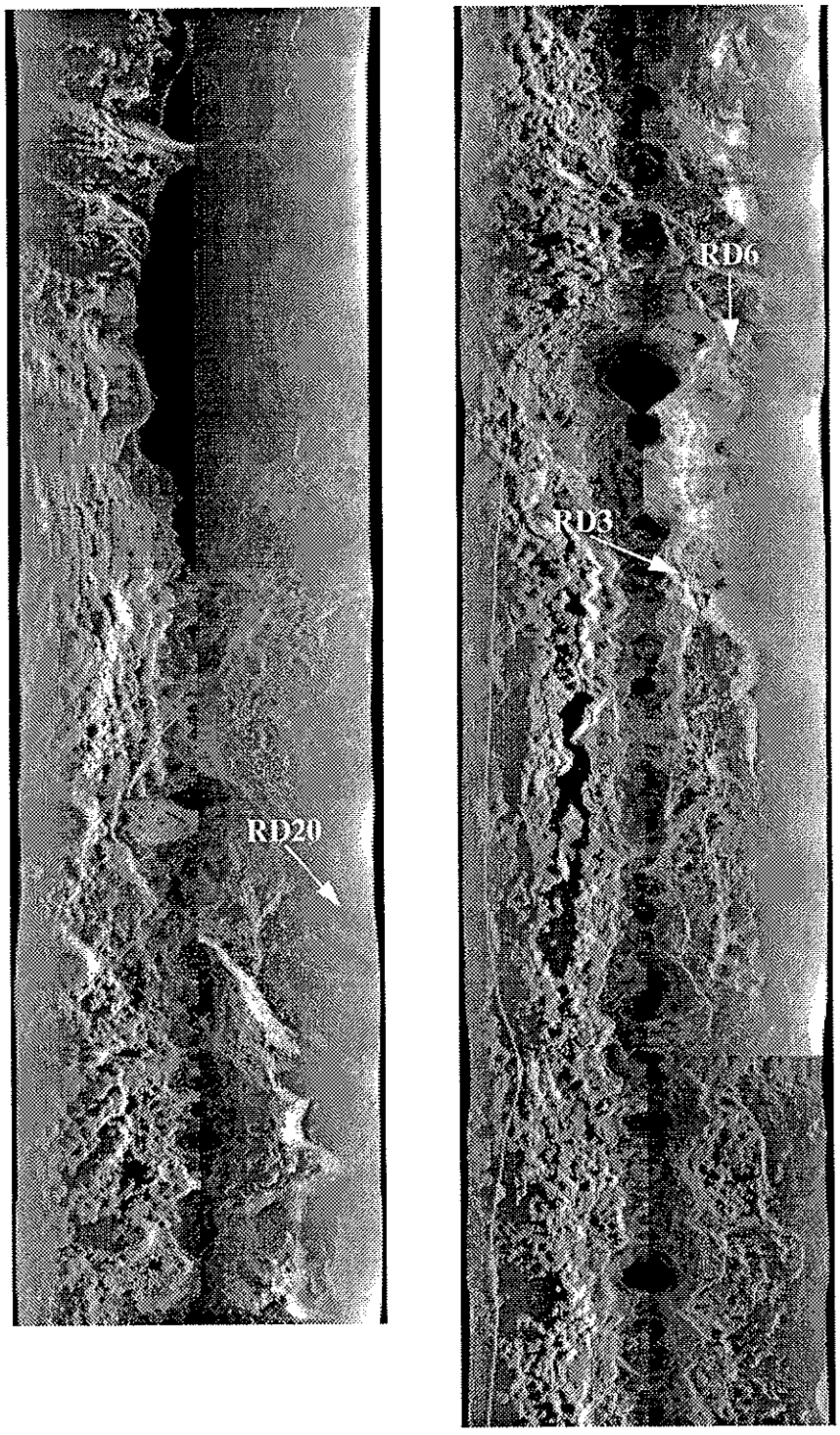

FIGURE 4.7

TOBI sidescan images from julian day 119.Time progresses from left to right and from top to bottom in each tile. The original 8000 pixels across have been subsampled to 200 pixels across. The start and end for time and location have been defined for each magneto-optical disk (and compact disk). Dredge haul locations and detailed images are indicated on the tiles.

MO: 441
Start: 29.6735°N -42.8178°W
Time: 120/07:14

End: 29.3053°N-42.9924°W
Time: 120/23:23

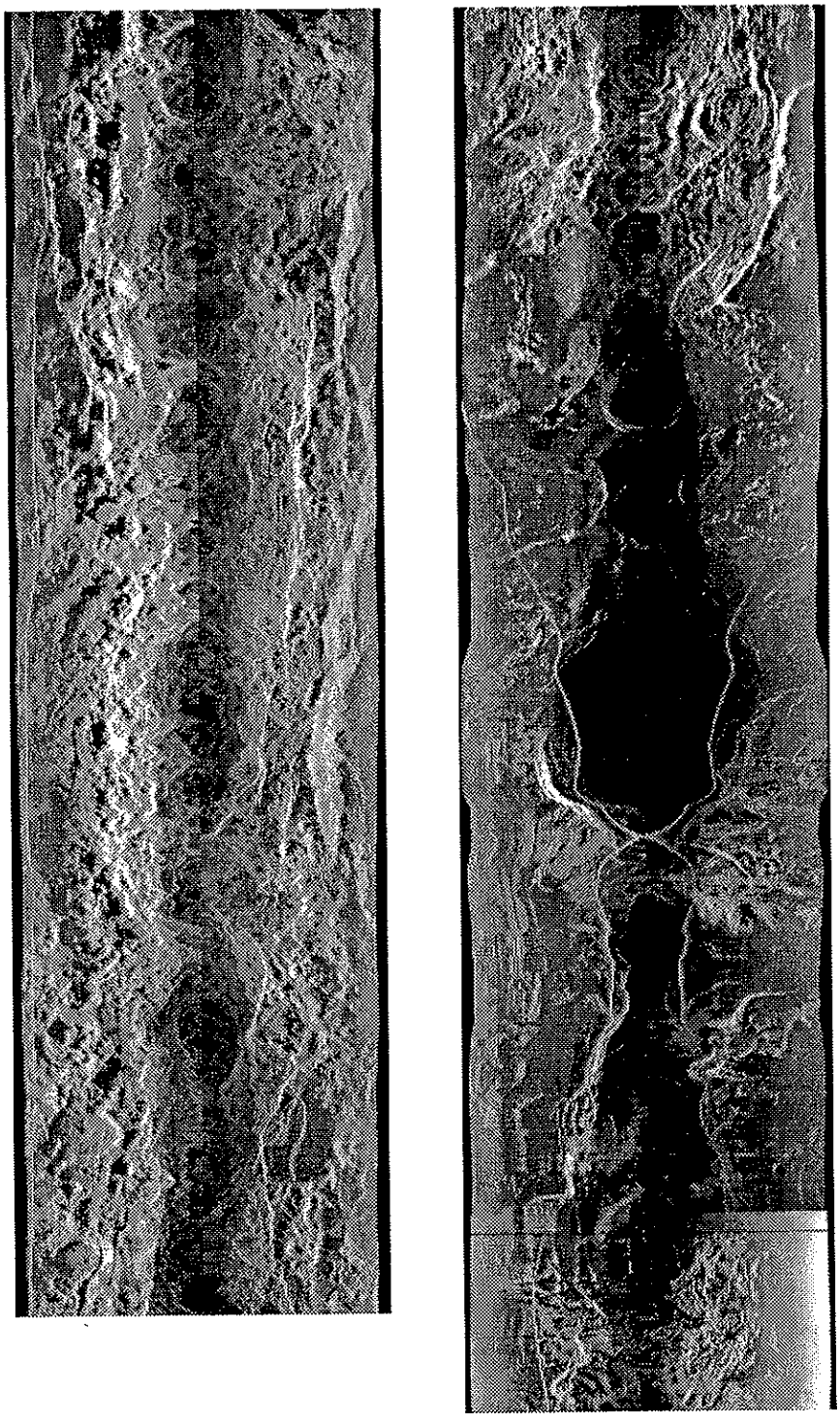

FIGURE 4.8 TOBI sidescan images from julian day 120.

MO: 442
Start: 29.3053°N -42.9924°W
Time: 120/23:23

End: 29.3053°N -42.9924°W
Time:121/15:35

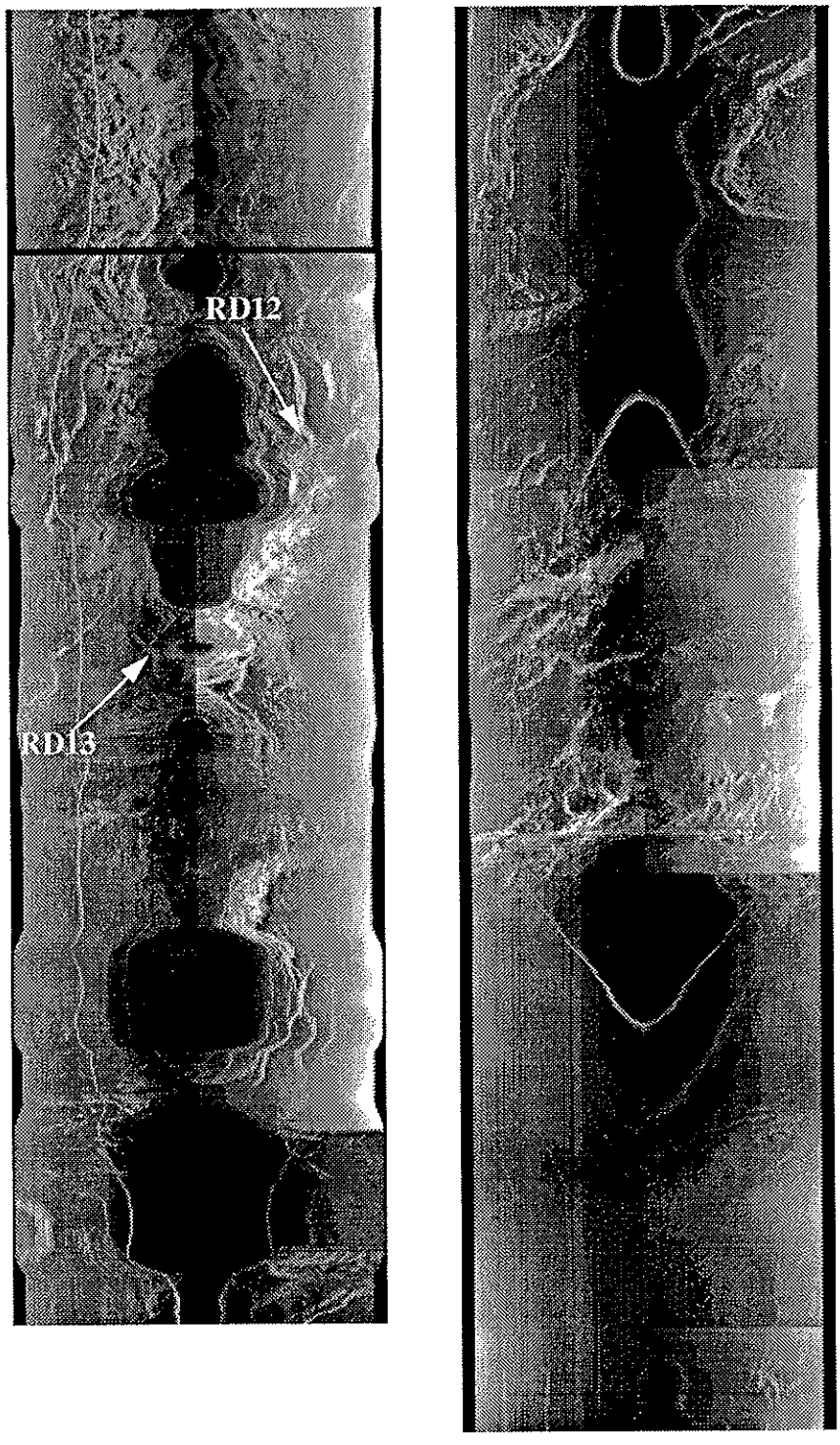

FIGURE 4.9

TOBI sidescan images from julian day 120.Time progresses from left to right and from top to bottom in each tile. The original 8000 pixels across have been subsampled to 200 pixels across. The start and end for time and location have been defined for each magneto-optical disk (and compact disk). Dredge haul locations and detailed images are indicated on the tiles.

MO: 443
Start: 29.3053°N -42.9924°W
Time: 121/15:35
End: 29.5935°N -42.8128°W

MO: 443_2
Start: 29.5649°N -43.204°W
Time: 122/10:55

End: 29.6857°N -42.8076°W
Time: 122/22:36

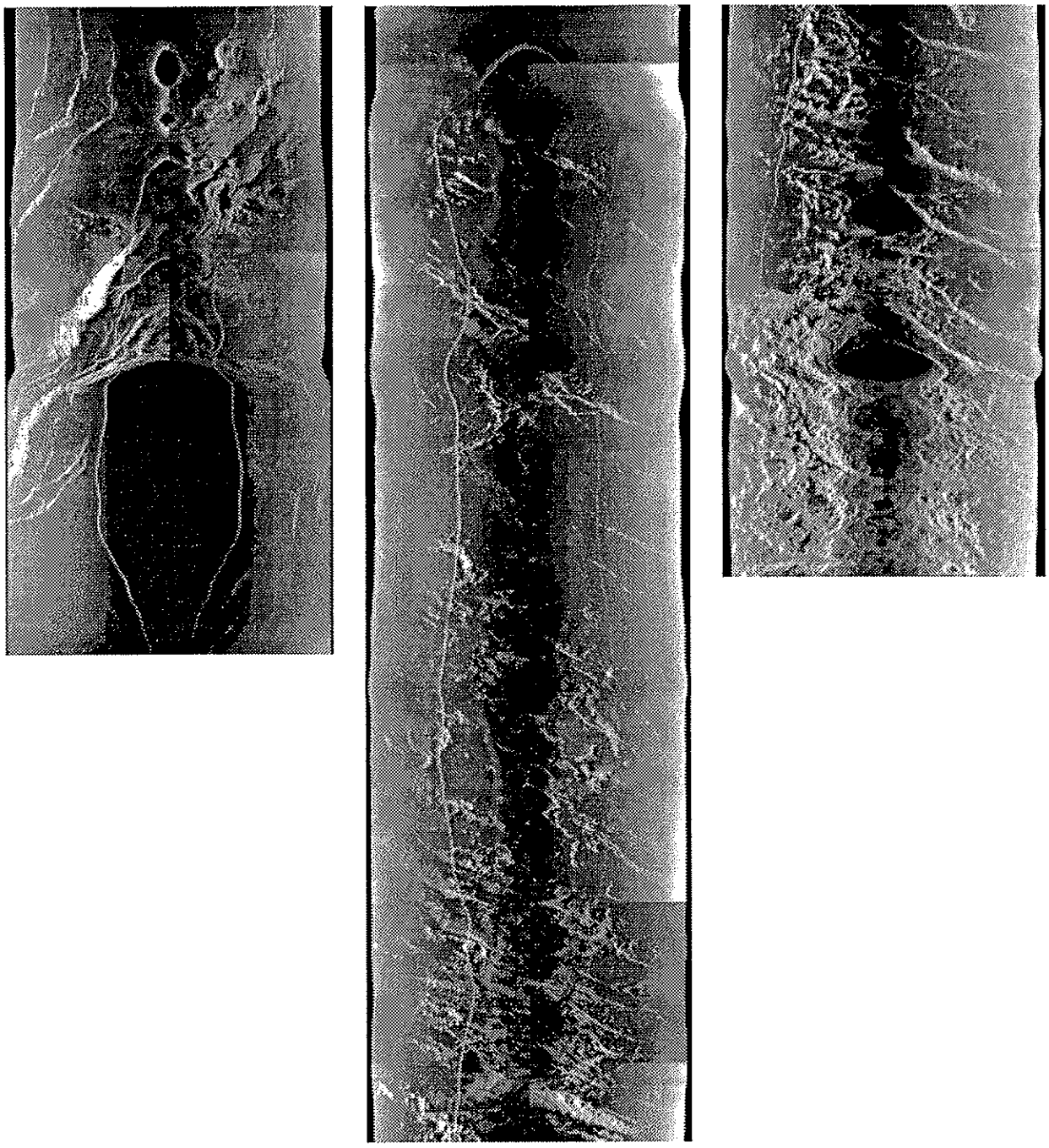

FIGURE 4.10 TOBI sidescan images from julian day 121.

MO: 444
Start: 29.6857°N -42.8076°W
Time: 122/22:36

End: 29.9903°N -42.9051°W
Time: 123/13:29

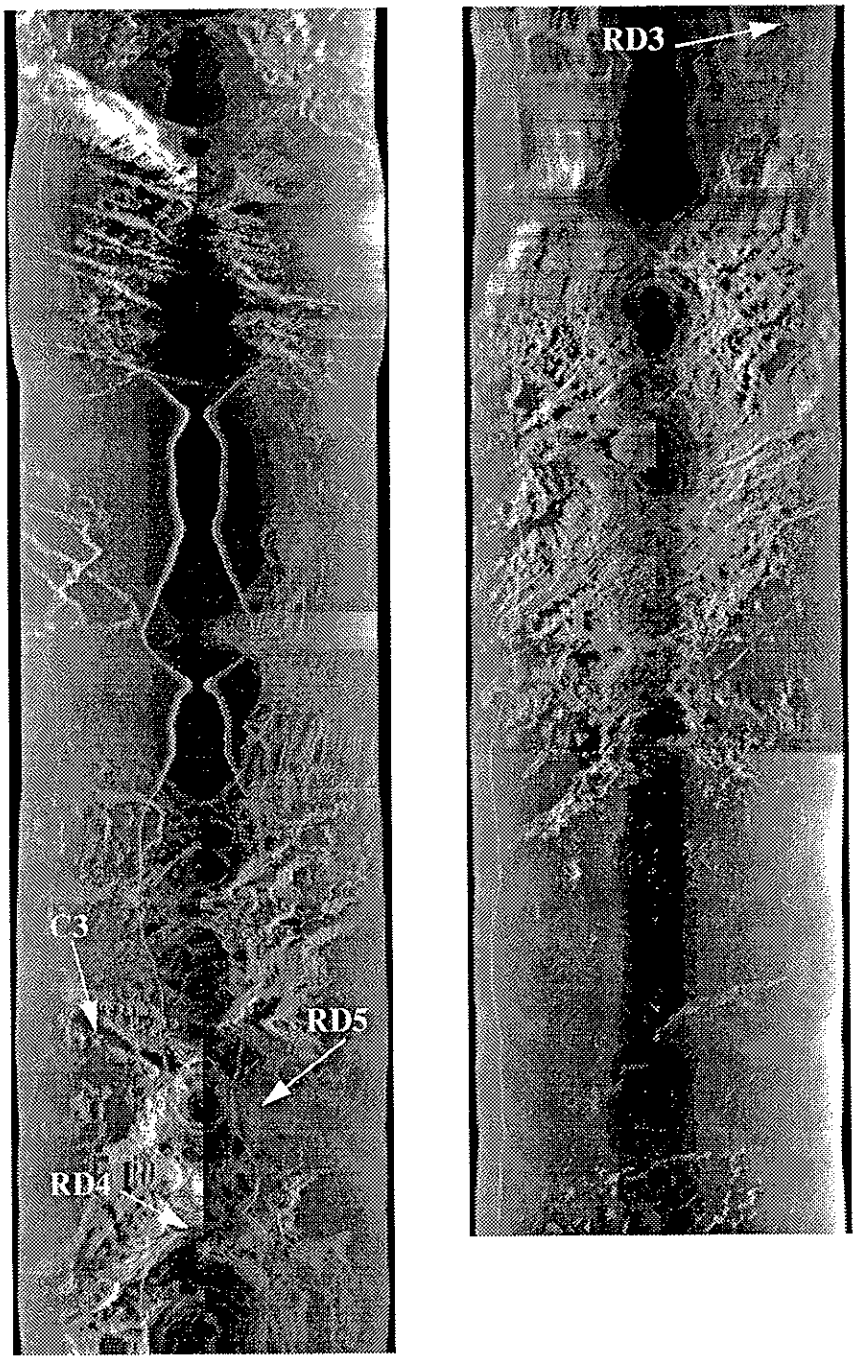

MO: 445
Start: 29.9903°N -42.9051°W
Time: 125/17:49

End: 29.9991°N -42.901°W
Time: 126/09:58

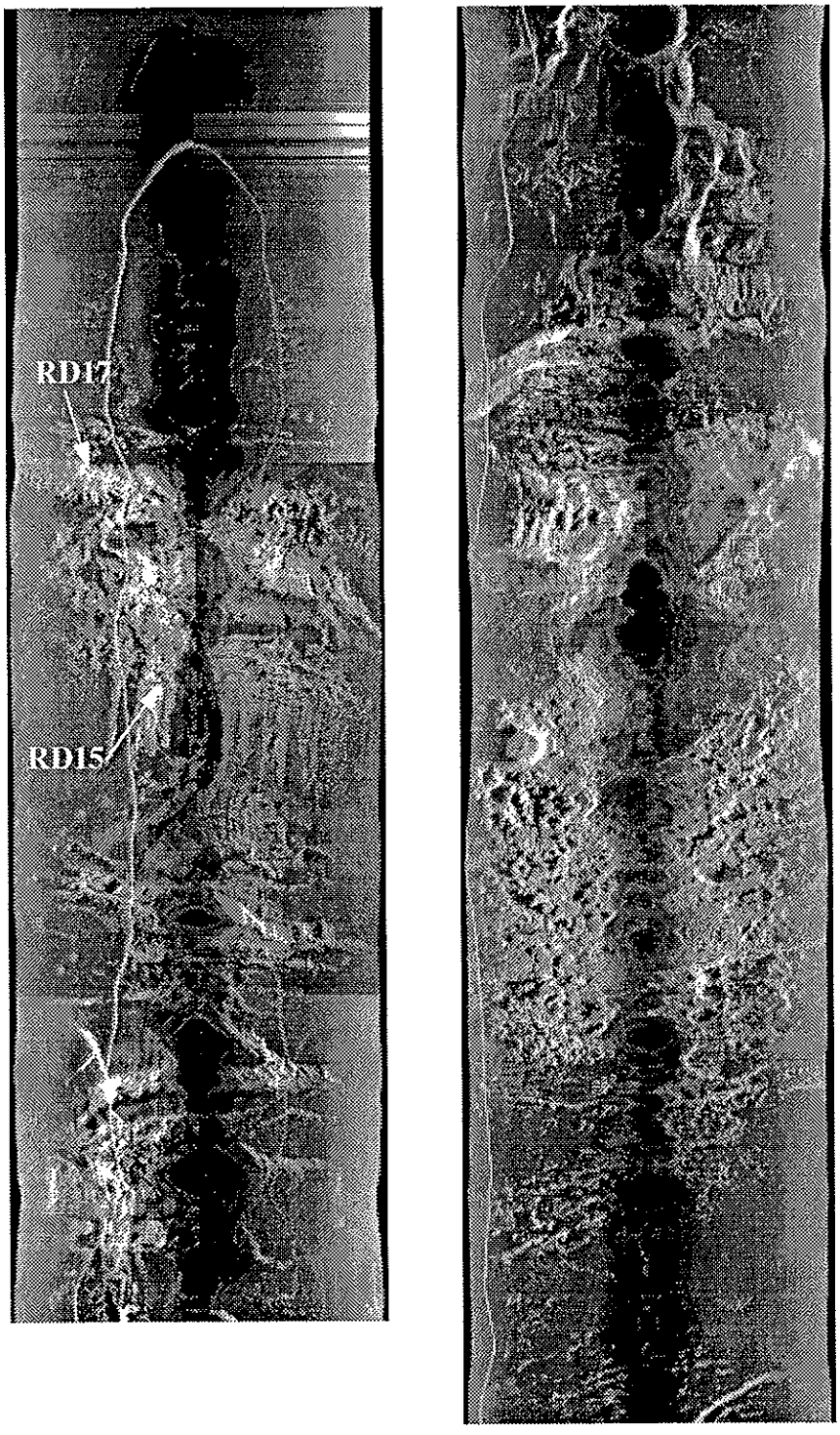

FIGURE 4.12 TOHBI sidescan images from julian day 125.

MO: 446
Start: 29.9991°N -42.9011°W
Time: 126/09:58

End: 29.9473°N -42.3918°W
Time: 127/01:14

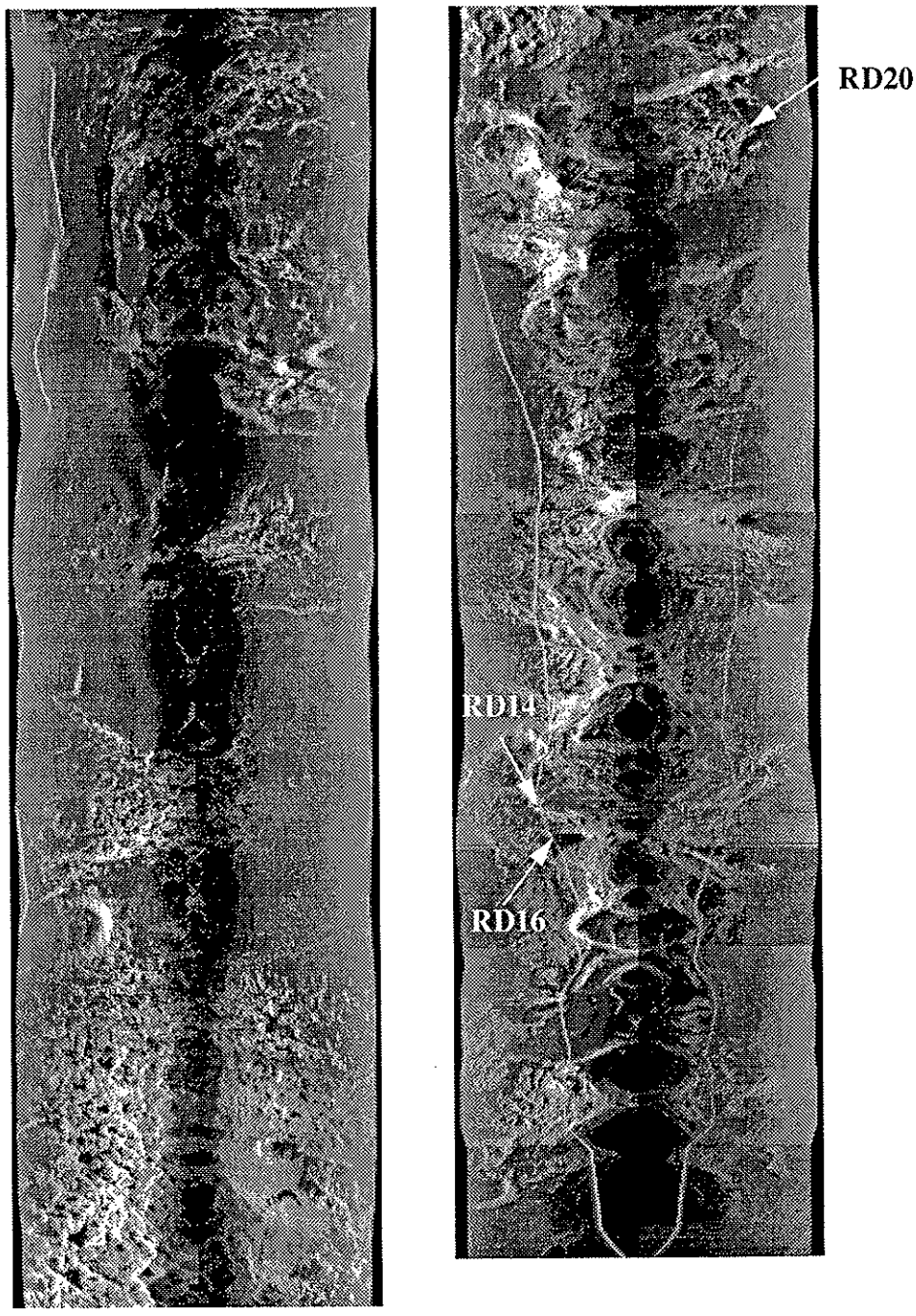

FIGURE 4.12

Tobi sidescan images from julian day 126.Time progresses from left to right and from top to bottom in each tile. The original 8000 pixels across have been subsampled to 200 pixels across. The start and end for time and location have been defined for each magneto-optical disk (and compact disk). Dredge haul locations and detailed images are indicated on the tiles.

MO: 447
Start: 30.0676°N **-30.0676°W**
Time: 127/04:43

End: 30.2144°N –42.0713°W
Time:127/20:46

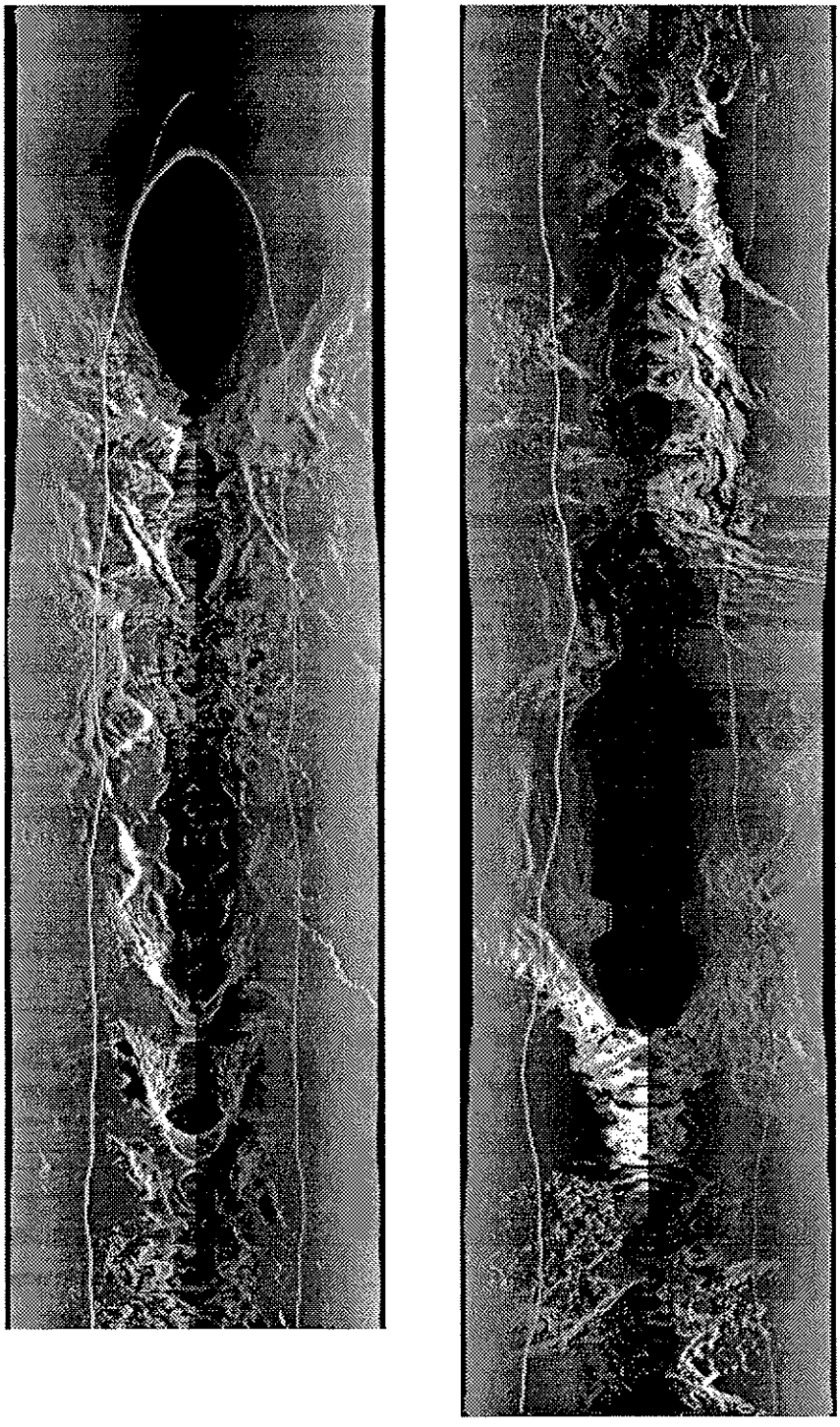

FIGURE 4.13 Tobi sidescan images from julian day 127

MO: 448
Start: 29.9473°N -42.3918°W
Time: 127/20:46

End: 29.9473°N -42.3918°W
Time: 128/12:56

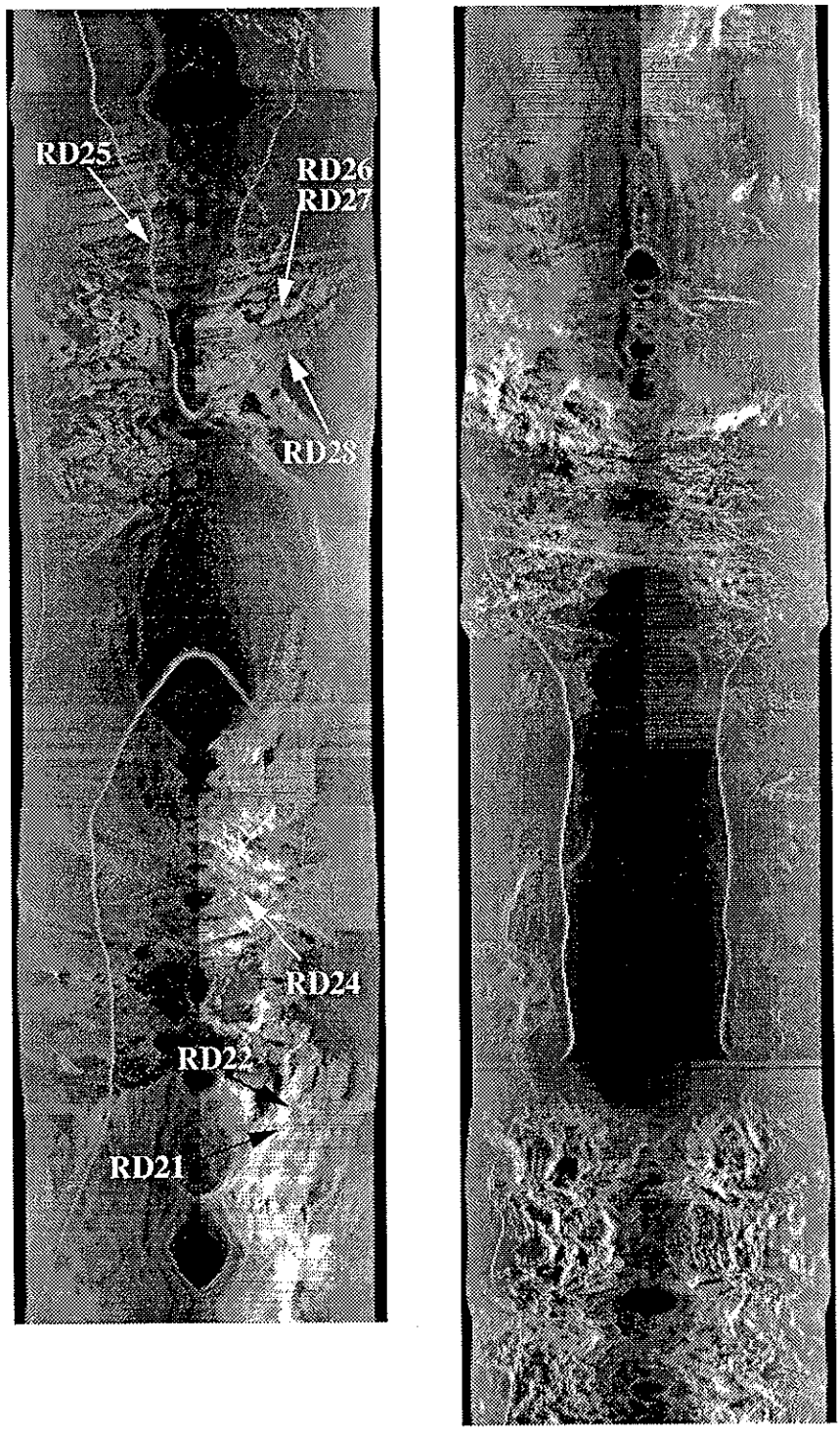

FIGURE 4.14

Tobi sidescan iamges from julian day 127. Time progresses from left to right and from top to bottom in each tile. The original 8000 pixels across have been subsampled to 200 pixels across. The start and end for time and location have been defined for each magneto-optical disk (and compact disk). Dredge haul locations and detailed images are indicated on the tiles.

MO: 449
Start: 30.0322°N -41.9383°W
Time: 128/12:56

End: 30.0853°N -42.1033°W
Time: 129/03:32

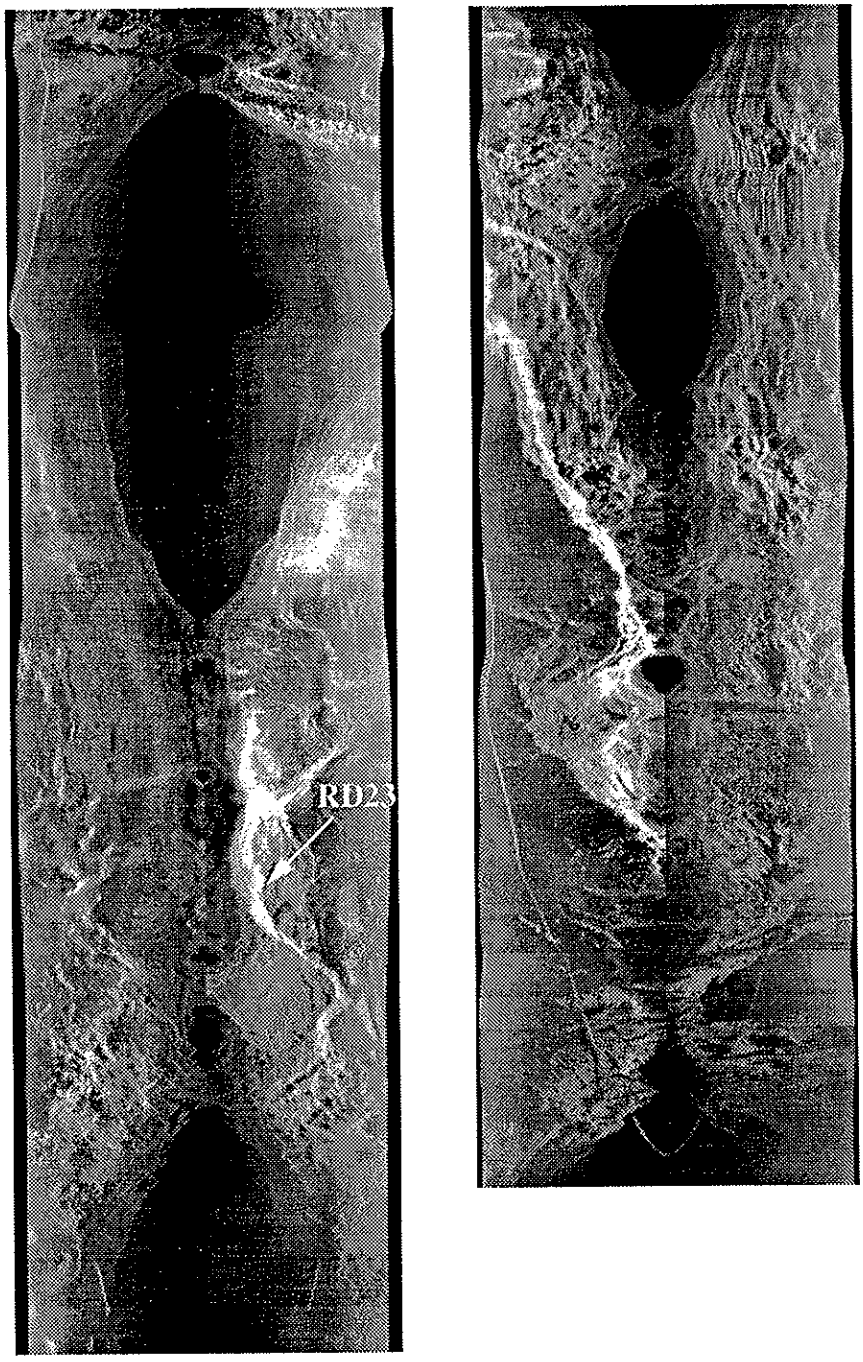

FIGURE 4.15 Tobi sidescan images from julian day 128.

4.4 TOBI Survey Detailed Images

The high resolution of Tobi sidescan enables fine detailed structures to be insonified. The following pages highlights a number of the most memorable and geologically enlightening images gathered by this cruise.

4.4.1 Faults and Faulted Terrain

The destruction by faults of the volcanic carapace is an on going process. **Figure 4.1** shows how faults dissect both single seamounts and the volcanic surface.

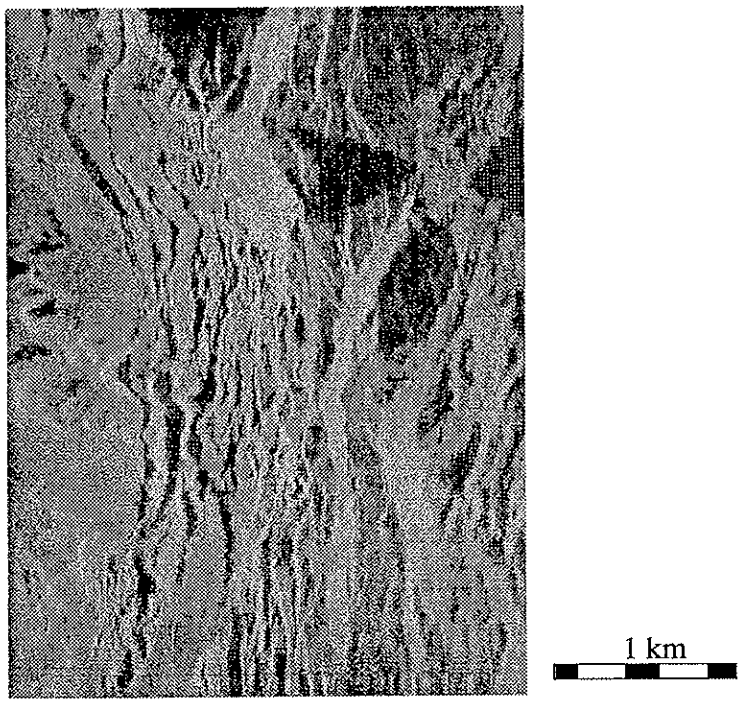

FIGURE 4.1 Detailed tobi sidescan image from the south of the NOBSKA segment. Insonification is from the left of the image.

The tectono-magmatic coupling of spreading ridges is an area of intense speculation. **Figure 4.2a** shows a major fault which terminates into a horse-tail splay less than 1 km to the south of a seamount. The seamount shows no signs of deformation. Is there a link between the location of the seamount and the tipping out of the fault?

As the volcanic carapace moves further from the source of magma supply an increased amount of faulting occurs. **Figure 4.2b** provides an image of small scale faults, all less than the vertical resolution of the SIMRAD bathymetry, dissecting the hummocky terrain and a small fault crossing the flat-top seamount.

At the Atlantis Transform a series of en-echelon splays were imaged peeling of the main transform fault. **Figure 4.3** shows an image of a series of these en-echelon faults which a significant dip-slip offset on them.

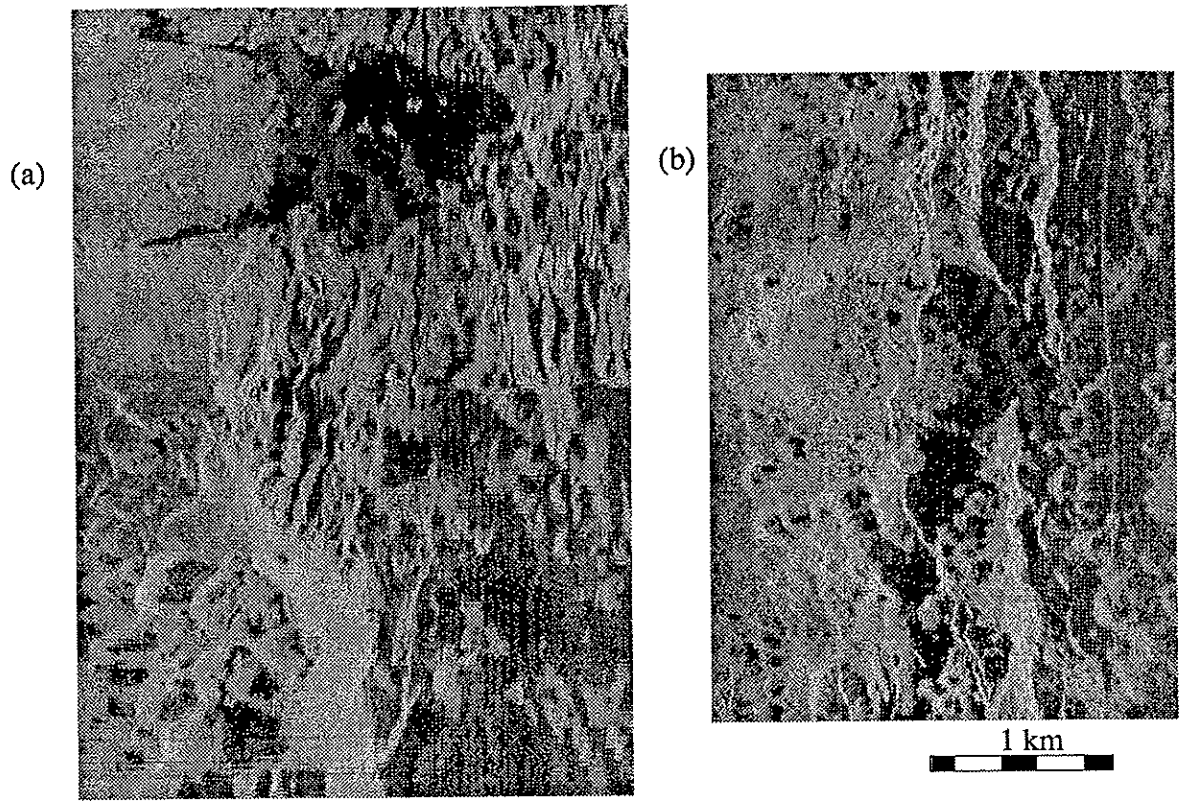

FIGURE 4.2 Sidescan image from the southern end of the NOBSKA segment. Insonification is from the left of the image.

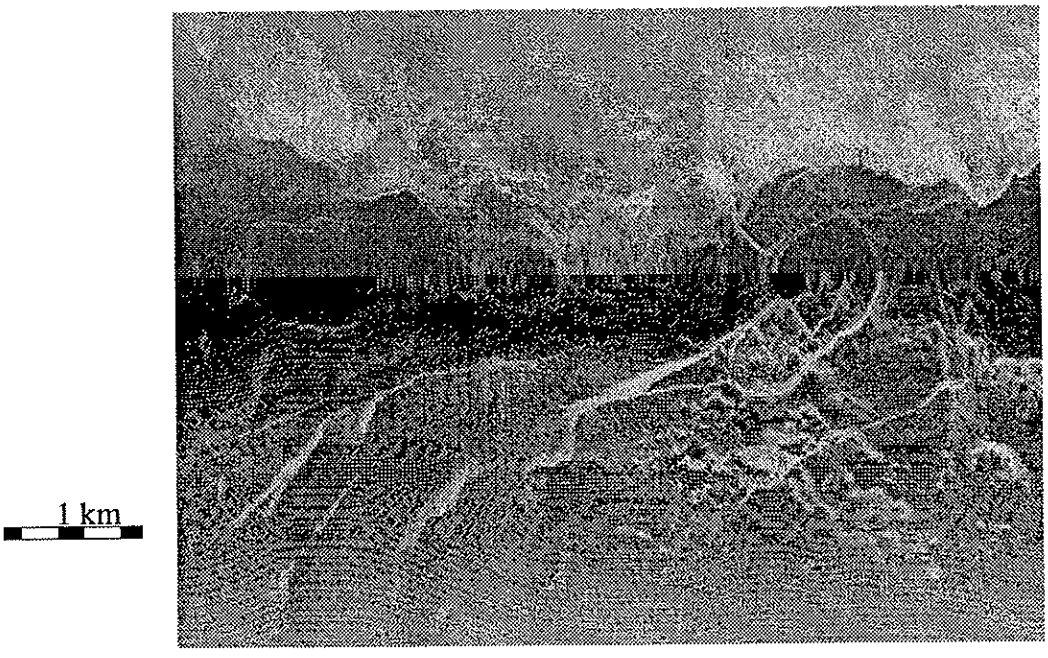

FIGURE 4.3 Fault splays peeling of the western end of the Atlantis Transform fault. Main fault trace lies below the nadir of the sidescan.

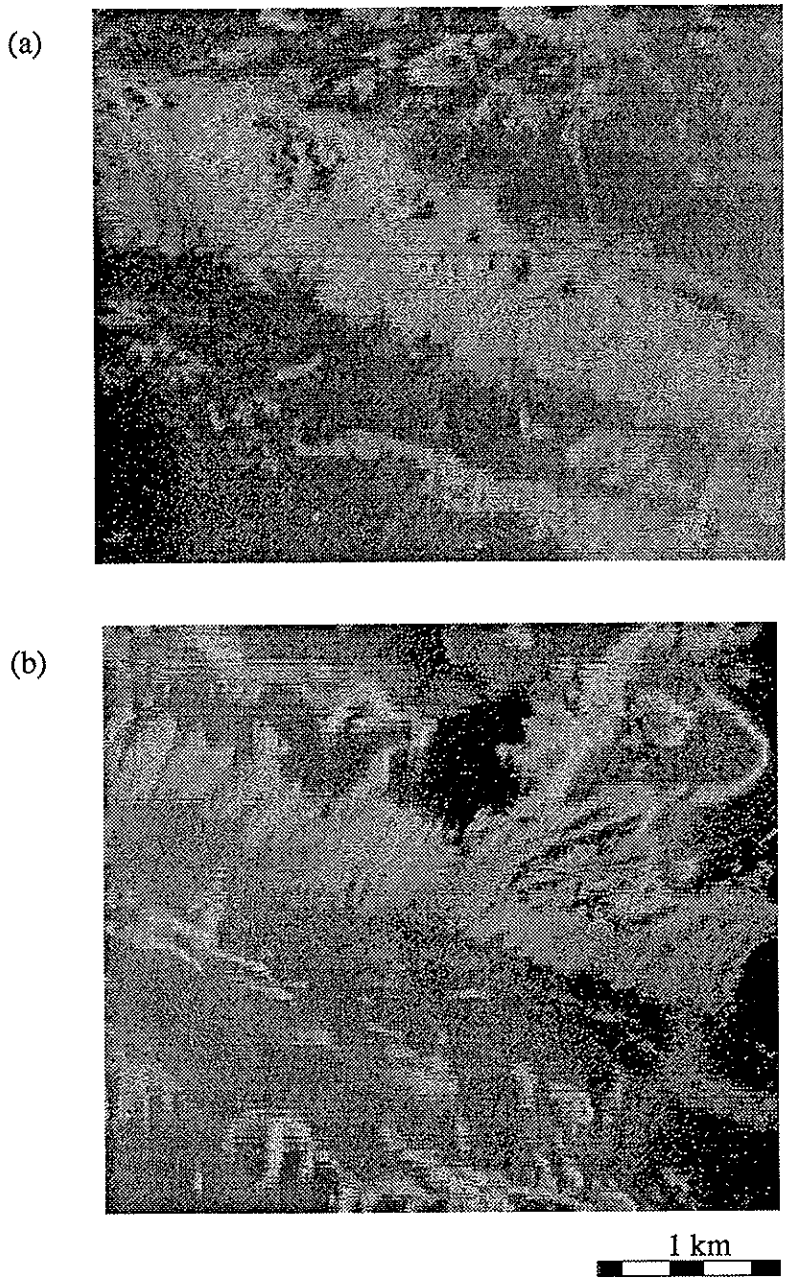

FIGURE 4.4 Old boundary wall faults located 3 - 6 km from the axis, both showing lobate talus fan fronts typical of an active talus slopes prograding across the pelagic covered surface.

As the faults move off-axis so the volcanism stops and pelagic sediments start to cover the surface and the faults. The sidescan images show that the faults remain active for at least the first few kilometres away from the edge of the inner valley. High backscatter from talus fans suggesting that mechanical erosion of the fault scarps, as a result of continued movement, out paces the pelagic sedimentation rate. **Figure 4.4** shows a series of faults located beyond the inner valley where the talus ramps are well imaged and show classic prograding talus fan morphologies.

4.4.2 Volcanic Constructions

Volcanic edifices can take many different forms, from smooth single cone seamounts, hummocky heaps to caterpillar ridges and low amplitude volcanic ridges. A surprising feature about the NOBSKA segment is the abandance of flat top seamounts. A gallery of the flat-top seamount types are displayed in **Figure 4.1.**

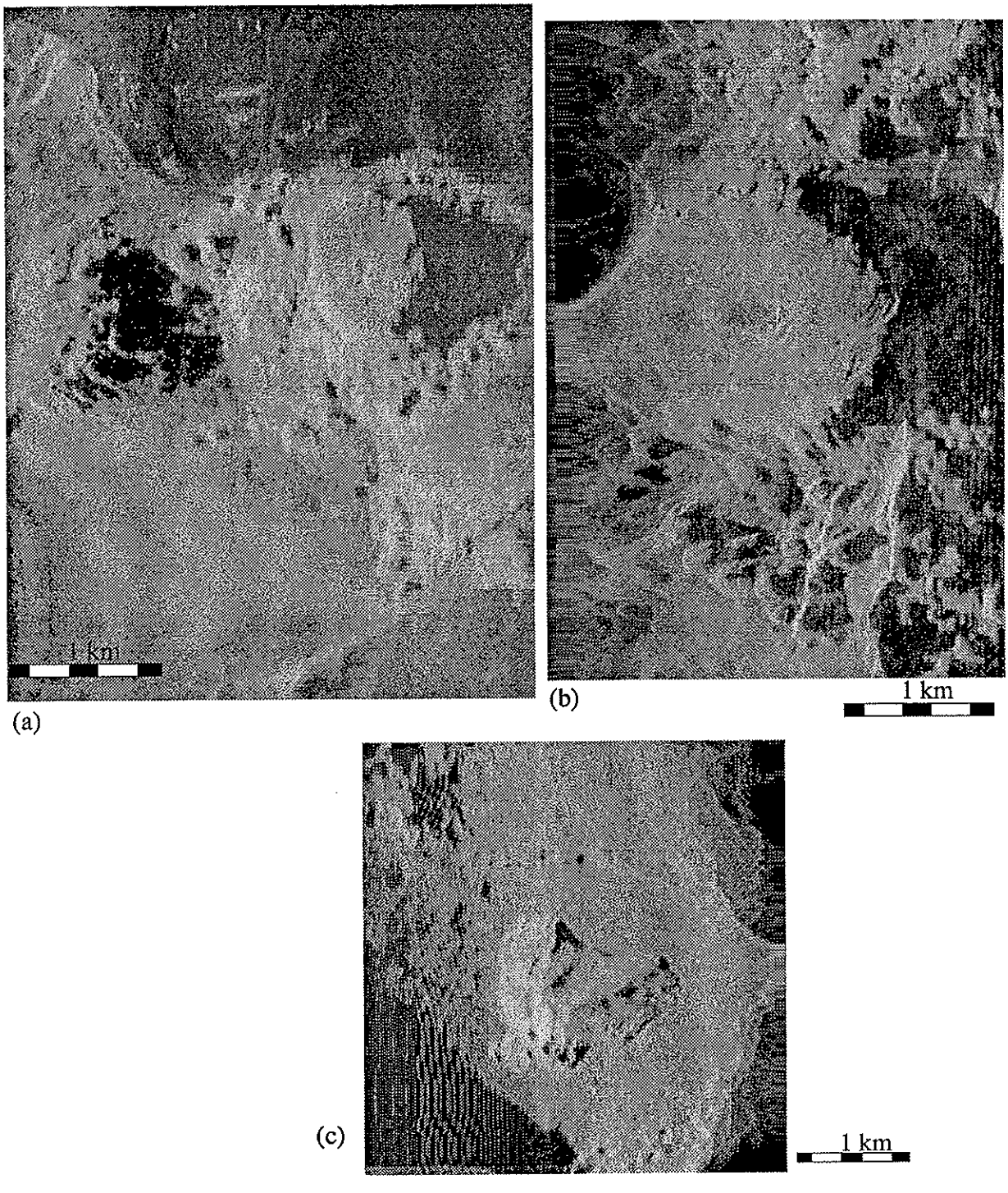

FIGURE 4.1 A selection of seamounts from the NOBSKA segment (a) and (b) are insonified fro the left of the image while (c) is insonified for the right.

The most predominant volcanic construction over the spreading segment are linear "Caterpillar" ridges which have been observed to be cut by and to overly faults. **Figure 4.2** show an example of some well imaged caterpillars from the spreading segment. In all cases the caterpillar ridges are a few hundred metres wide and a few kilometres long with significant elevation to cast a shadow..

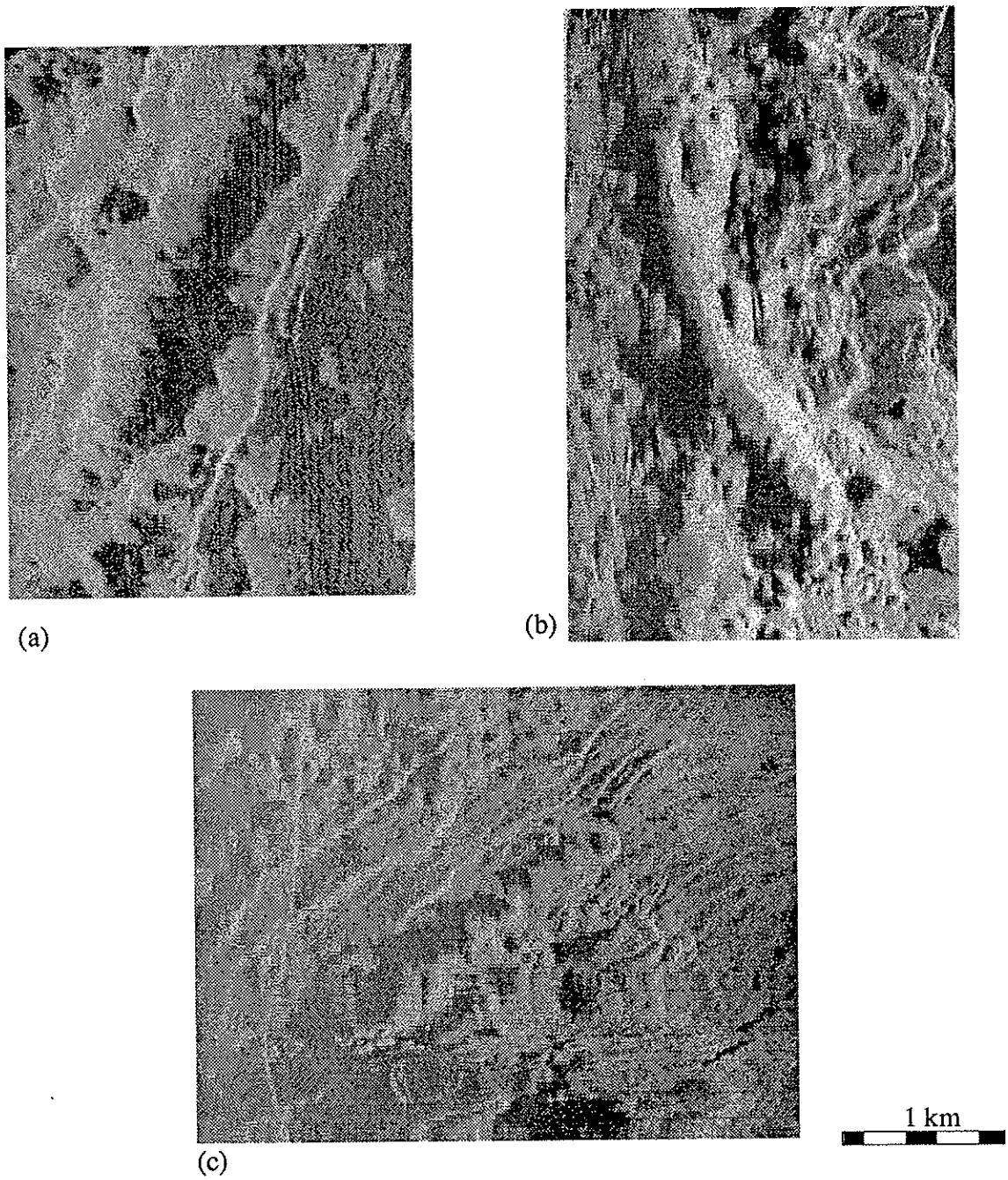

FIGURE 4.2 Caterpillar volcanic ridges. Both (a) and (c) appear to cover faults while (b) curves across the trend of other volcanic features.

4.4.3 Landslide Terrains

Landslipped terrains were recognised on sidescan images of the MAR for the first time by the CD65 cruise in 1992. An objective of this cruise was to establish a link between landslipping, petrology, topography and ridge dynamics. To this objective the inside corner high of the NOBSKA segment and the southern inside corner (IC)high of the segment north of the Atlantis Transform were insonified by TOBI sidescan. A range of morphologies were imaged, from a chaotic and jumbled morphology to regions of where slipped blocks have remained coherent. The lower slope of the northern IC high , where it laps onto the inner vallley in two places is shown in **Figure 4.1**,

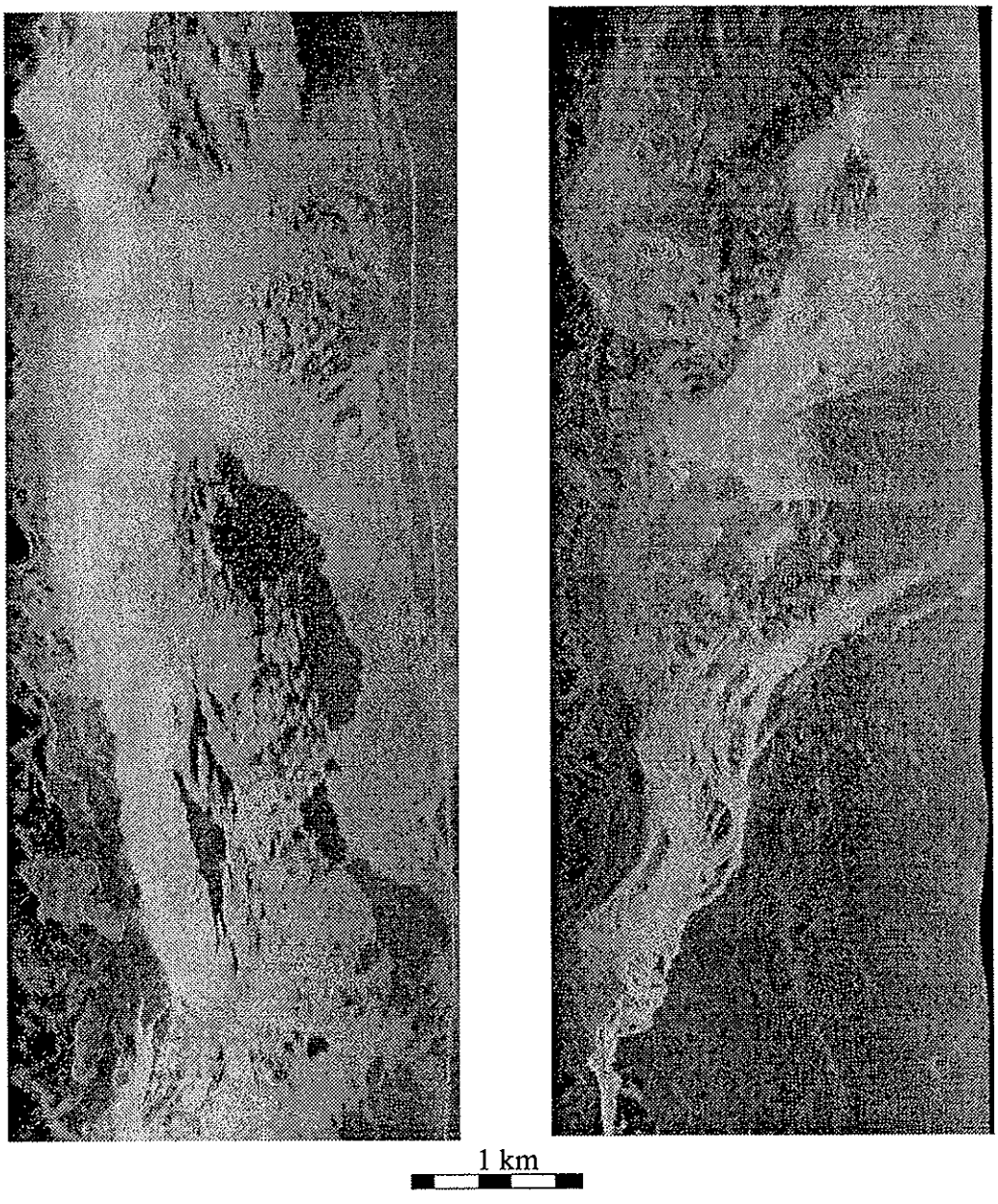

FIGURE 4.1 Toe of the landslide from the northern IC high within the NOBSKA segment. Insonification is from the left of the image. Note the contrast in the backscatter texture which reflects the changes from bare rocks to talus fans. (b) Further south on the same slide, the landslip can be seen onlapping against a small seamount.

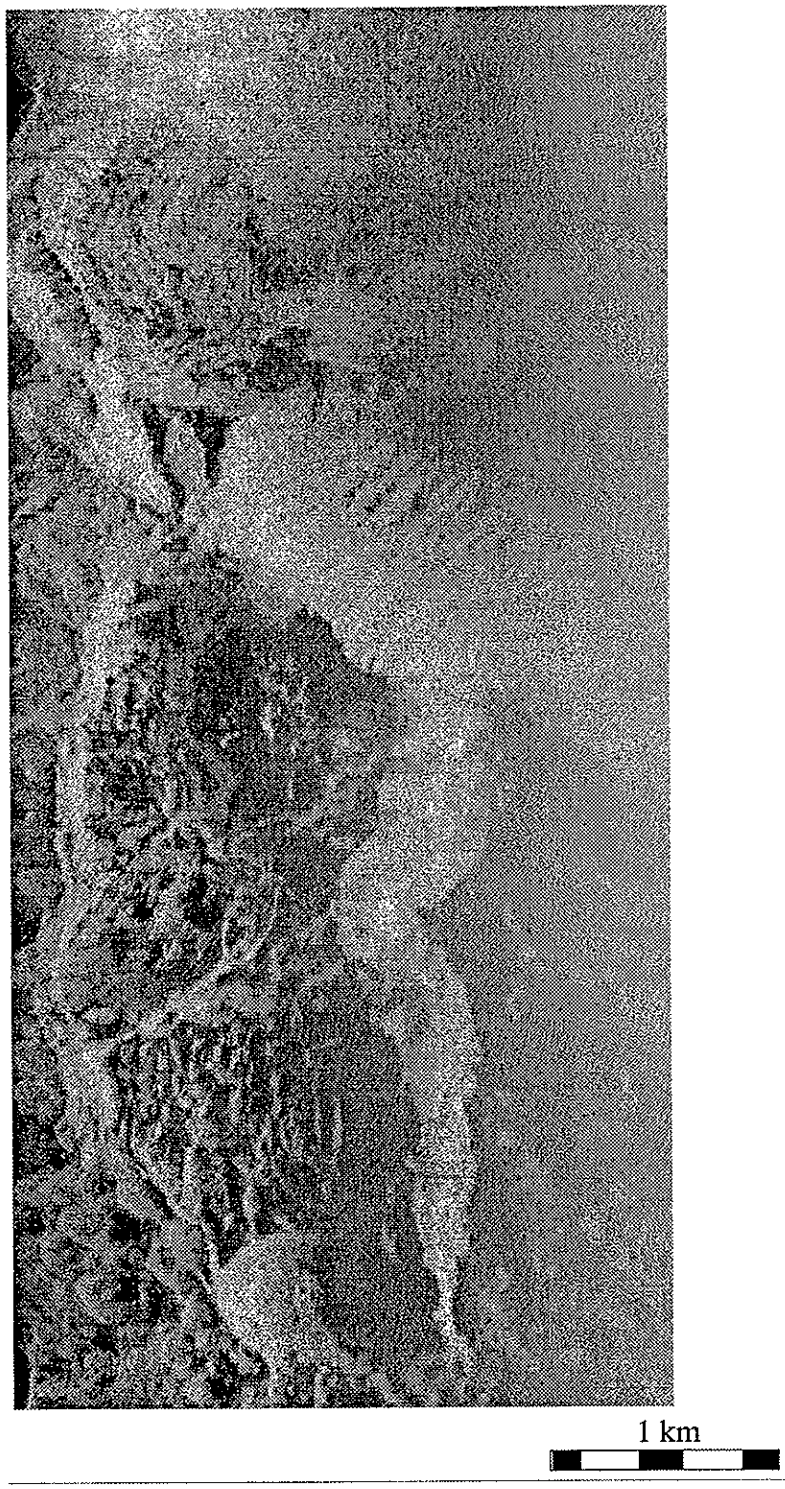

FIGURE 4.2 The landslipped surface from the IC high at the eastern RTI of the Atlantis Transform. Insonification is from the left of the image.

The IC high on the segment north of the Atlantis displays similar landslide morphologies. In this case the slide is imaged covering over a fault, and out into the inner-valley floor (**Figure 4.2**). Note the major talus ramps emanating from the slide toe.

(a)

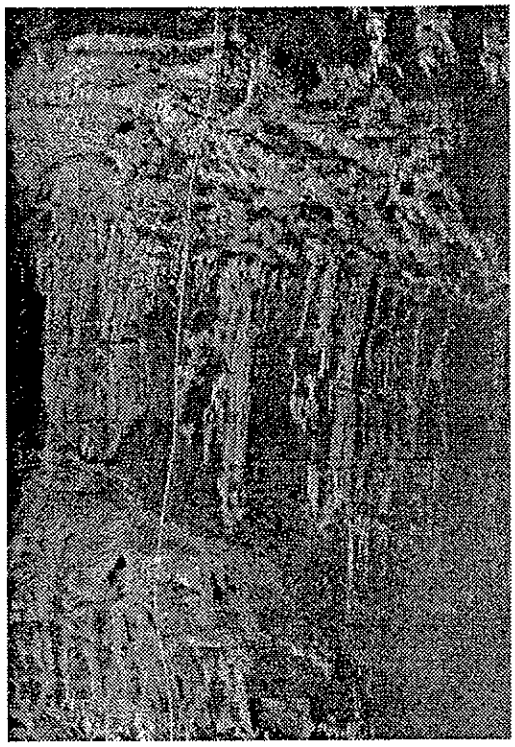

(b)

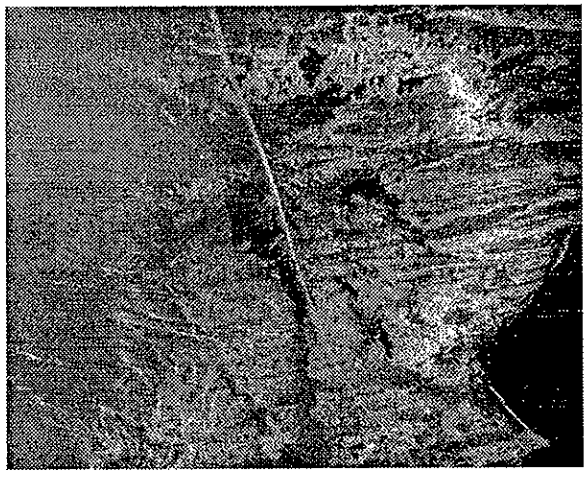

FIGURE 4.3 (a) Striated surface imaged from east of the axis in the NOBSKA segment. (b) Striated surface imaged on "Rose".

The most striking find of this cruise was the discovery of fossil slide planes on which the slides would appear to have slipped across. These were firsted noted on the SIMRAD bathymetry (Section 4.8 on page 78), and targeted with TOBI to investigate their nature. Two zones of "corrugations" have been found, one ~10 km east of the axis, named the "Hinge" after its tilted planar shape, and the second, and larger, is located on the active IC high to the east of the Atlantis. This area has been named "Rose". The corrugated area from the bathymetry shows a higher frequency of striations when imaged by TOBI, with both the striations and the corrugations running parallel to each other and parallel to the interpreted direction of the landslide. **Figure 4.3** shows the two striated areas.

4.5 TOBI Bathymetry

Details of the results of using phase information to construct a bathymetric surface are discussed in Section 5.1.2 on page 97.

4.6 SIMRAD Bathymetry

The increased time allocated to SIMRAD surveys resulted in a broader area of the Atlantis Fracture Zone being surveyed, producing spectacular bathymetric and SIMRAD sidescan data. Since SIMRAD was on constantly through out the cruise we have SIMRAD sidescan and bathymetry to complement the TOBI data, and provide a broader coverage, though poorer resolution. In all a total of 1200 km2 of the NOBSKA segment, the Atlantis Transform and Segment 18 was surveyed. **Figure 4.1** shows a low resolution bathymetry map of the survey, with the white boxes highlighting areas dicussed in more detail later

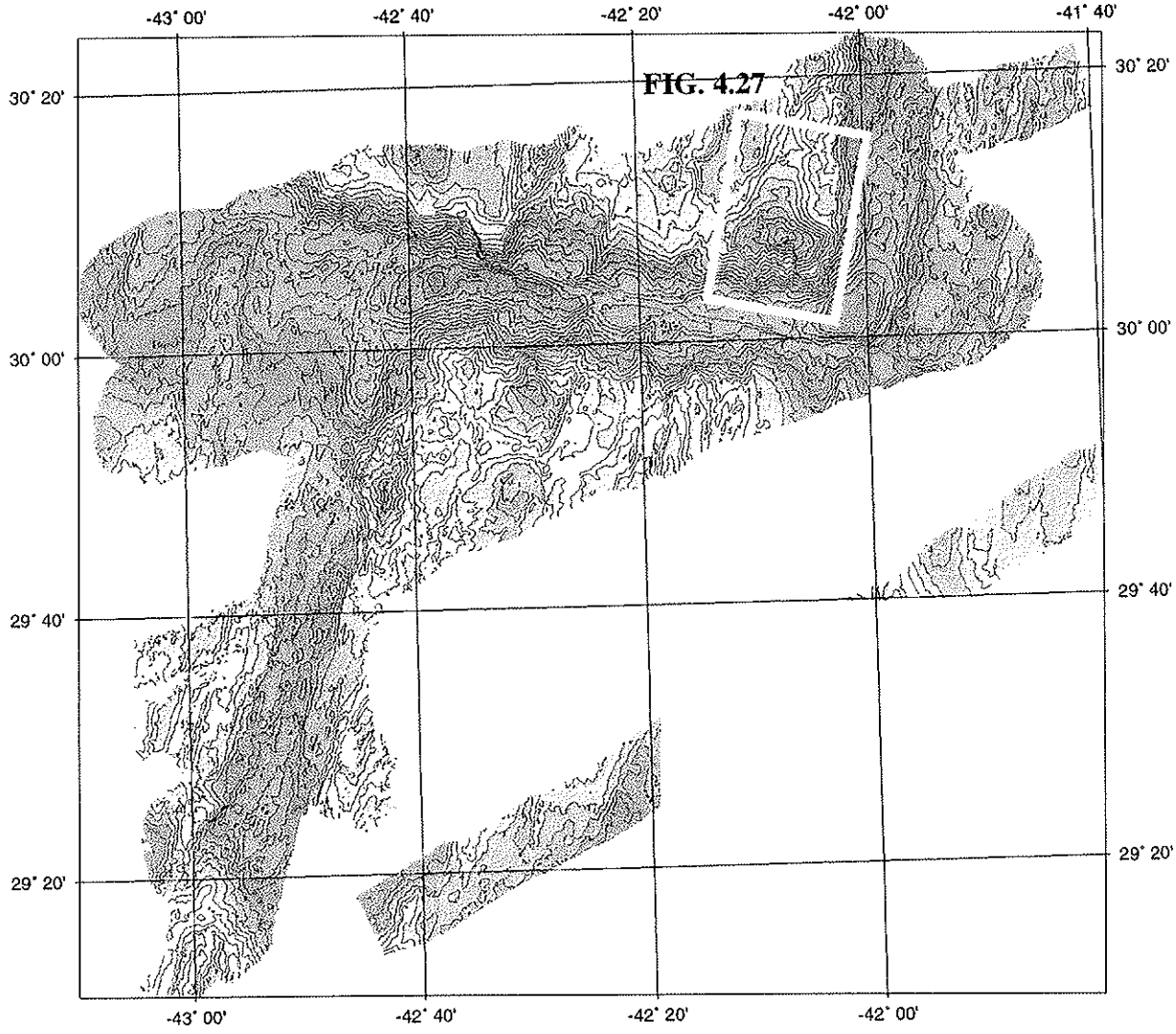

FIGURE 4.1 Bathymetry map of the complete SIMRAD multibeam bathymetry survey.A contour interval of 200 m is used.

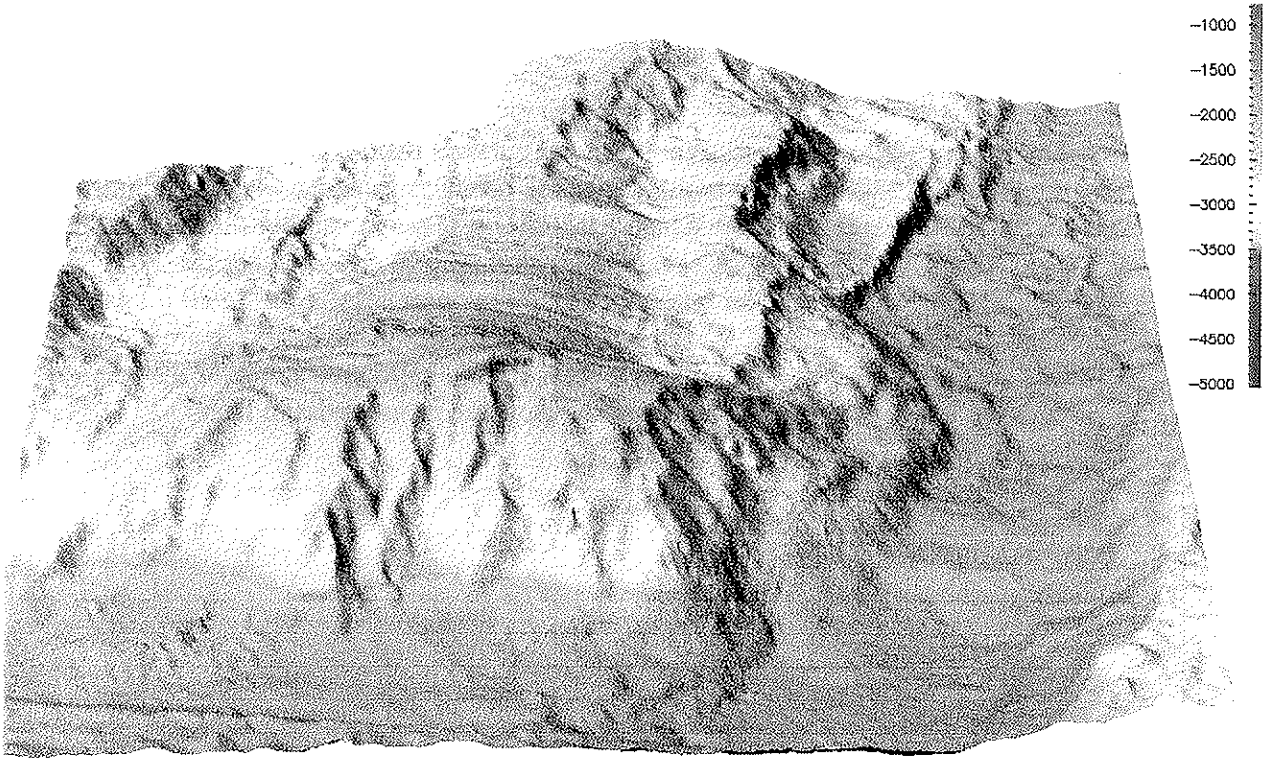

FIGURE 4.2 3-Dimensional view of the IC high to the north-east of the Atlantis Transform.

The increased precision offered by SIMRAD as against other mulitbeam systems can be demonstrated by the increased quality of the images and the increase in the detail that can be observed. The striations discussed in.the previous section were first recognised from the bathymetry data. **Figure 4.2** shows a 3-D image over the IC high known as rose, the corrugations 3are easily recognisable and since they do not run parallel to nor orthogonal to the ship track can be demonstrated not to be an artefact.

Many other similarly striking views have been created, they are stored in the data_explorer_psfiles directory below CD100 (Section 5.6 on page 113)

4.7 SIMRAD Sidescan

SIMRAD sidescan data, gave surprising good results over the whole area. It appears to be insenstive to slopes and concequently provides a ideal texture mapping tool. During the cruise we used the sidescan to identify regions of bare rock (higher amplitude return) to site dredge locations. Figure 4.28 is an example of the type of data the SIMRAD sidescan offers. The processing of this data is discussed in Section 5.2.2 on page 107.

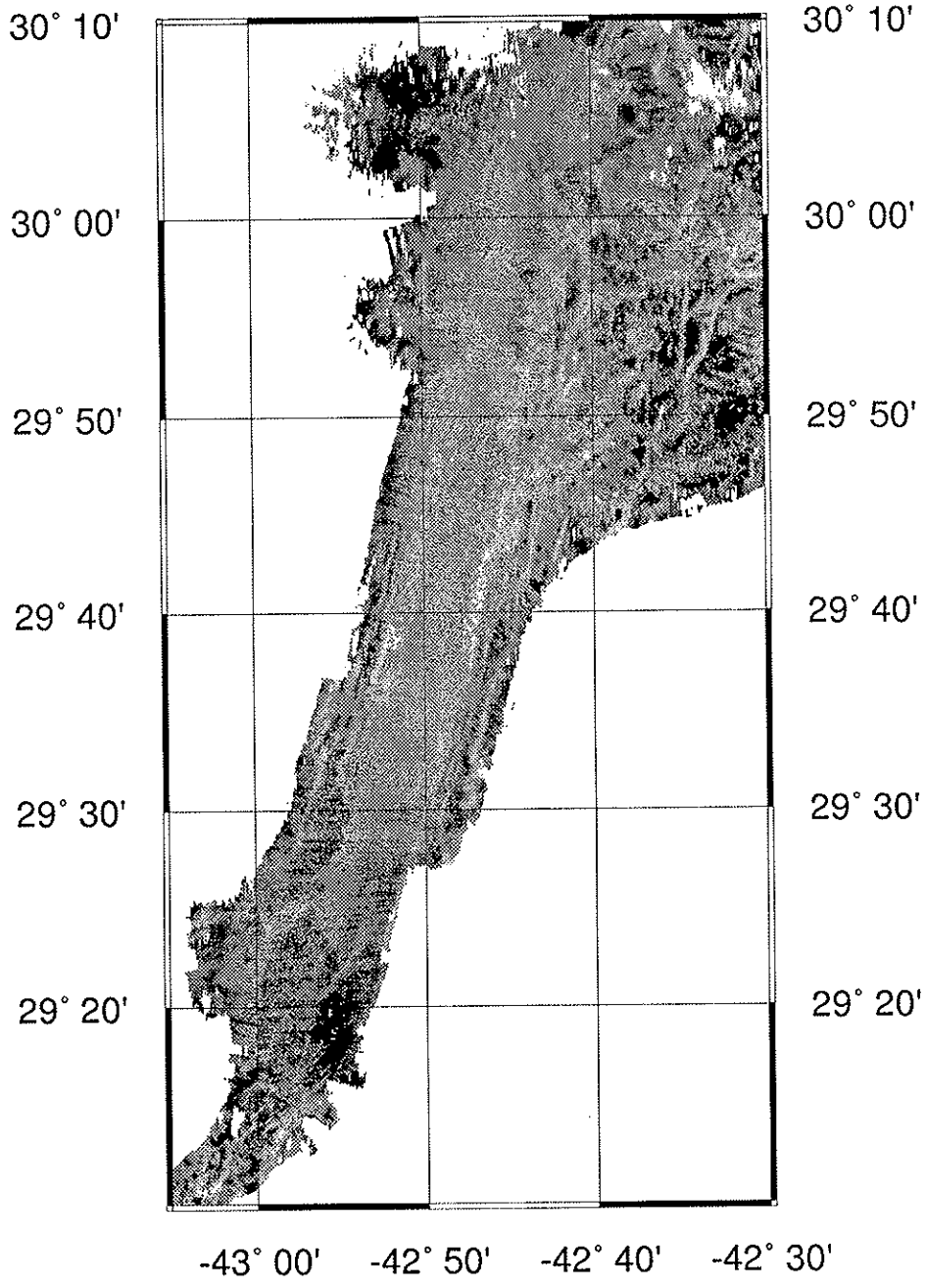

FIGURE 4.1 SIMRAD sidescan sonar coverage over the NOBSKA segment

4.8 Merging datasets *(Debbie Smith*

To produce a composite image of these two data sets I identify the swath of multibeam bathymetry that corresponds to a swath of TOBI side-scan imagery using estimated latitudes and longitudes of the TOBI vehicle. The two data matrices are then resampled to the same physical size (as described below) to ease the process of texture mapping. Each scanline of TOBI side-scan sonar data in its original form contains 8000 pixels of information, 4000 to port and 4000 to starboard. The original data file contains a ping approximately every 4 seconds. We resample each scanline to 200 pixels of information (1/40 the original size), and along track we retain every fifth data point. Even after downsizing the TOBI data, however, the size of the matrix of echo amplitudes is still several times larger than the corresponding size of the matrix of bathymetric depths. To adjust for this difference, the bathymetry data are interpolated and resampled to the same number of points as the TOBI data. If there is a mismatch in the two data sets due to navigational errors, adjustments are made by shifting the TOBI data either along the track or across the track. The images are not warped.

The texture mapped visualization can be accomplished using the "visual programming environment" available in several commercially available 3-D visualization software systems (e.g., IBM's Data Explorer, Advanced Visual System's AVS5). The systems provide easy to use visualization environments that do not require extensive 3-D graphics expertise or traditional programming skills. On the cruise, I used Data Explorer. The visually co-registered gridded bathymetry and TOBI side-scan sonar images are read by the "visual program". The gridded bathymetry data are used in two ways. First to create a 3-D surface, and second to generate a 2-D color image associated with the 3-D surface. The 2-D colorized surface representation of the bathymetry is combined with the TOBI image to produce a composite image that is texture mapped on to the 3-D bathymetric surface to produce the final graphic display. The combination of the TOBI image and the colorized surface enhances the information available from the TOBI image alone.

Figure 1 present examples of TOBI imagery texture mapped on to Sea Beam bathymetry using Data Explorer. Figure 1 (line436b_flattop.ps in data explorer directory) shows an image of the volcanic features constructed on the median valley floor of segment 18.

If commercial 3-D visualization software is not available for use, freely available software exists that can also be used to combine the two data sets. Khoros provides capabilities similar to both AVS and Data Explorer (see <*http://www.khoros.unm.edu*>). In addition, TOBI data and multibeam bathymetry data can be merged using Generic Mapping Tools (GMT). GMT produces similar results but the technique is not that of texture mapping. Instead a less sophisticated technique of pixel lookup is used that requires two data sets of identical physical dimension. In this case using the program "*grdview*", artificial illumination of the contoured, colored 3-D surface is based on the values of the TOBI echo amplitudes.

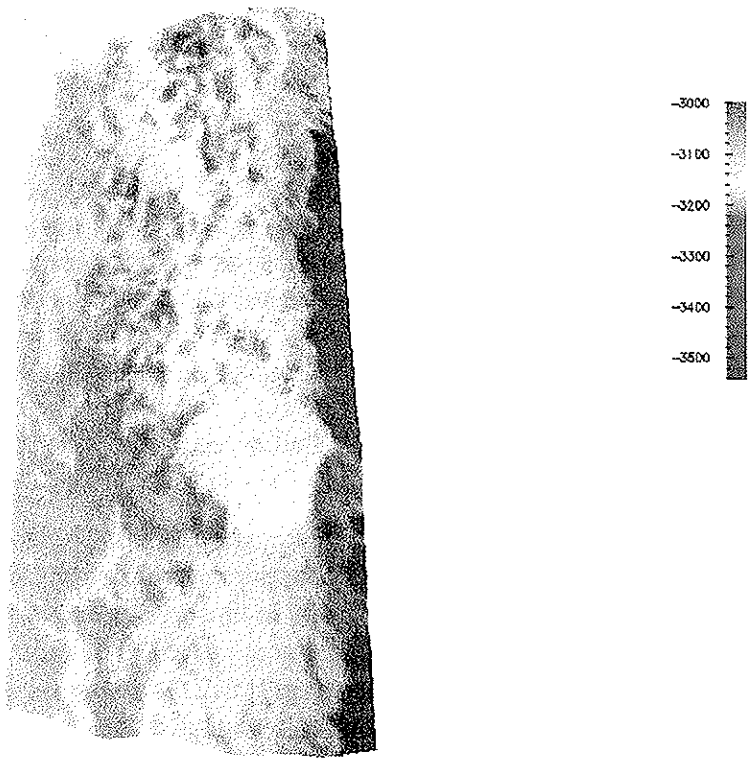

FIGURE 4.1 Texture map of TOBI sidescan combined with Seabeam bathymetry.

4.9 Magnetic Survey

4.10 Gravity Acquisition and Mantle Bouguer Anomaly Calculation (*Sidney Mello & Donna Blackman*)

Gravity was measured with a shipboard La Coste & Romberg meter and values of spring tension, cross coupling and digital gravity were monitored on a screen. The values sampled every 10 seconds come from a running 5 minute average of the gravity which, along with spring tension and cross coupling readings, are logged by RVS. Ships navigation is determined mainly from GPS data. RVS removes jumps in position or faulty position trends due to changes in the satellite constellation (or whatever else) and applies a 10 minute smoothing. From this smoothed navigation, the Eotvos correction is computed and an initial Free Air Anomaly is determined.

A gravity tie was made in Ponta Delgada by Chris Paulson of RVS and it is his intent to do another in Cadiz. The apparent drift determined between the past set of ties (Lisbon-Ponta Delgada) was in line with previous drift values but on the high side. The behavior of the meter appeared to be quite stable for CD100, the only noisy period was during a storm (jd 121) and the subsequent few days when seas were high. This noise was in an expected form as small, high frequency oscillation about the steady trend of a signal. A continuous paper record of the spring constant, cross-coupling and gravity values was kept running throughout the cruise.

Martin Beney of RVS was responsible for the navigation and free air gravity processing. Bad or suspect records were down graded to a 'data quality' value of 30 in the record (data quality of 50 is good). A plot of along-track FAA values for the area near the eastern ridge-transform intersection indicated that cross over errors were less than 2 mGals and in many places they were 0-1 mGal. This check included full-speed Simrad lines, slower, somewhat variable TOBI lines and some approaches to dredge sites. Therefore, the gravity data are clearly of high quality. The close line spacing in some regions of the study area and the fact that several tie lines were incorporated in the track plan provide for a reasonably high resolution data set.

The mantle Bouguer anomaly for the RTIs and transform area was computed following the methodology of Forsyth and coworkers. Since the Atlantis transform strikes at about 068 , a rectangular box with that orientation was chosen for the calculations. This rotation added a couple steps to the process but it provided better bathymetric coverage for consideration in the Parker algorithm which assumes the surface is spatially periodic.

The following steps were used to obtain the mantle Bouguer anomaly map and the relevant programs are in /home/vartfar/donna/ or are GMT:

RVS provided FAA as lat, lon, initial free air anomaly (mgals) --> *.xyz

blockmean (*.xyz) --> *.bxyz

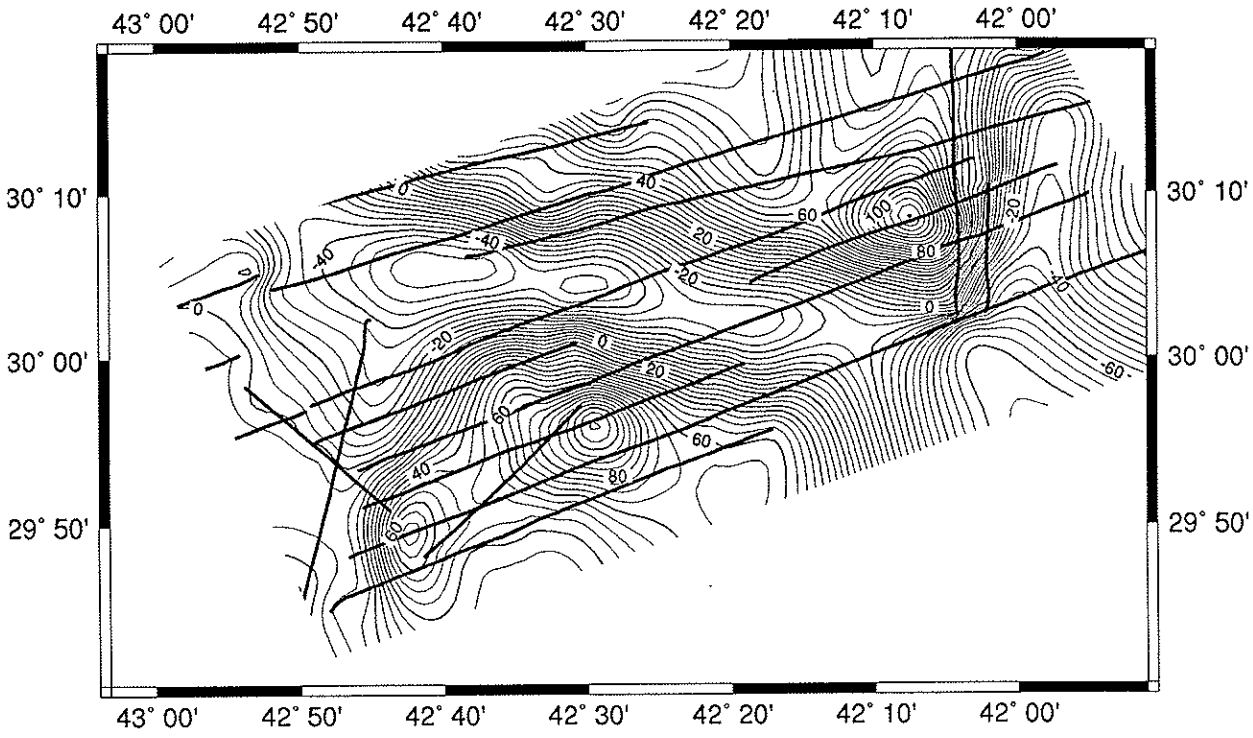

FIGURE 4.1 Free-air gravity map over the Atlantis Transform, with the track lines of the survey..

surface (*.bxyz) -T0.75i -T0b --> *.Ggrda lat, lon based grid of FAA (**Figure 4.1**)

llrot2xy (*.xyz) --> *.uvz rotate xy to transform parallel coordinates

blockmean (*.uvz) --> *.buvz

surface (*.buvz) --> *.Bgrd bathymetry in uv-space at 500 m grid space

predicted attraction of interfaces

tparker (*.Bgrd) --> sf.uvz & cm.uvz

average depth to interfaces (-3000m, -6000m)

density contrasts at interface (1.77 g/cc, 0.5 g/cc)

power series expansion to order (3)

blockmean (sf.uvz & cm.uvz) --> sf.buvz & cm.buvz

surface (sf.buvz & cm.buvz) --> sf.grd & cm.grd uv grids of predicted interface attraction

grdmath sf.grd + cm.grd --> pred.grd500 m grid spacing

llrot2xy (FAA track segments) --> trak.uvobserved FAA along track in uv-space

grdtrack (trak.uv pred.grd) --> pred.uvzpredicted values along track

Dredge Numbr	Latitude	Longitude	Depth Range	Contents[a]				Detailed Description
				B	G	S	O	
26	30 08.4'N	42 06.7' W	1200	Empty				page 93
27	30 08.4'N	42 06.7' W	1200				✓	page 93
28	30 07.8'N	42 07.3' W	900	✓			✓	page 93

TABLE 1. Dredge sites, location and summary of contents

a. B= Basalt/pillpow basalt,; G = gabbro; S = serpentinite (or serperntinised rock); O = other rock type (peridotite, pyroxeneite)

Dredge 1, starts at 29 46.0'N 42 44.5' W, heading east, 2400 - 2000 m.

The dredge was sited on the large debris flow that is very bright in the image from Tobi line 1, and has flowed down to cover up a large fault scarp (or possible earlier debris flow) on the southern end of Yellow Mountain. The site is close to the 1985 earthquake swarm, and may have moved at that time. This is a large haul of basalt fragments in size up to 50 cm and down to basalt glass sand. There are three types of basalt in the haul, aphyric, moderately phyric and highly phyric. Aphyric fragments are the most abundant. The phyric basalts contain large megacrysts of plagioclase and olivine, with the plagioclase much more abundant than the olivine. The basalts are apparently little weathered: there is much fresh glass in the haul and relatively little palagonite. The fragments are not coated with manganese oxide. Also in the haul are lumps of basalt glass, reddened pieces of phyric lava and fragments of indurated ooze. The dredge brought up two very small red shrimp, placed in a polythene bag in the scientific deep freeze. There was also a small gastropod and a branch of ?bryozoan?, preserved in alcohol. A representative selection of the basalts was labelled and bagged. The remainder was disposed of over the side, since the usefulness of basalts collected from a debris flow unit is limited.

Dredge 2, starts at 29 47.0'N 42 43.3' W, heading east, 2150 - 2000m.

The dredge is sited on the fault scarp or debris flow underlying the fresh debris flow sampled in dredge 1, is over the side at 1005, the pinger on at 1016, there are bites from 1118 - 1145, and the dredge is back on board at 1235. There is a large haul of basalt fragments ranging from 50cm diameter down to gravel, with some deep water coral pieces, a whole gastropod shell and one glacial erratic. The basalts include both phyric and aphyric types. The phyric basalts contain large megacrysts of plagioclase and olivine, with more plagioclase than olivine, which in some samples make up more than half of the rock. Most basalts are fragments of pillows (the largest is one whole pillow), but some are not so easily assigned to parts of pillows. There are some fragments of indurated sediment, some fragments of pale grey basalt glass breccia, and some of red-weathering basalt. The coral pieces include a fine whole manganese-stained calyx. The glacial erratic is of gneiss, rounded at the edges, and weathered red. The remainder was disposed of over the side, since the usefulness of basalts collected from a debris flow unit is limited.

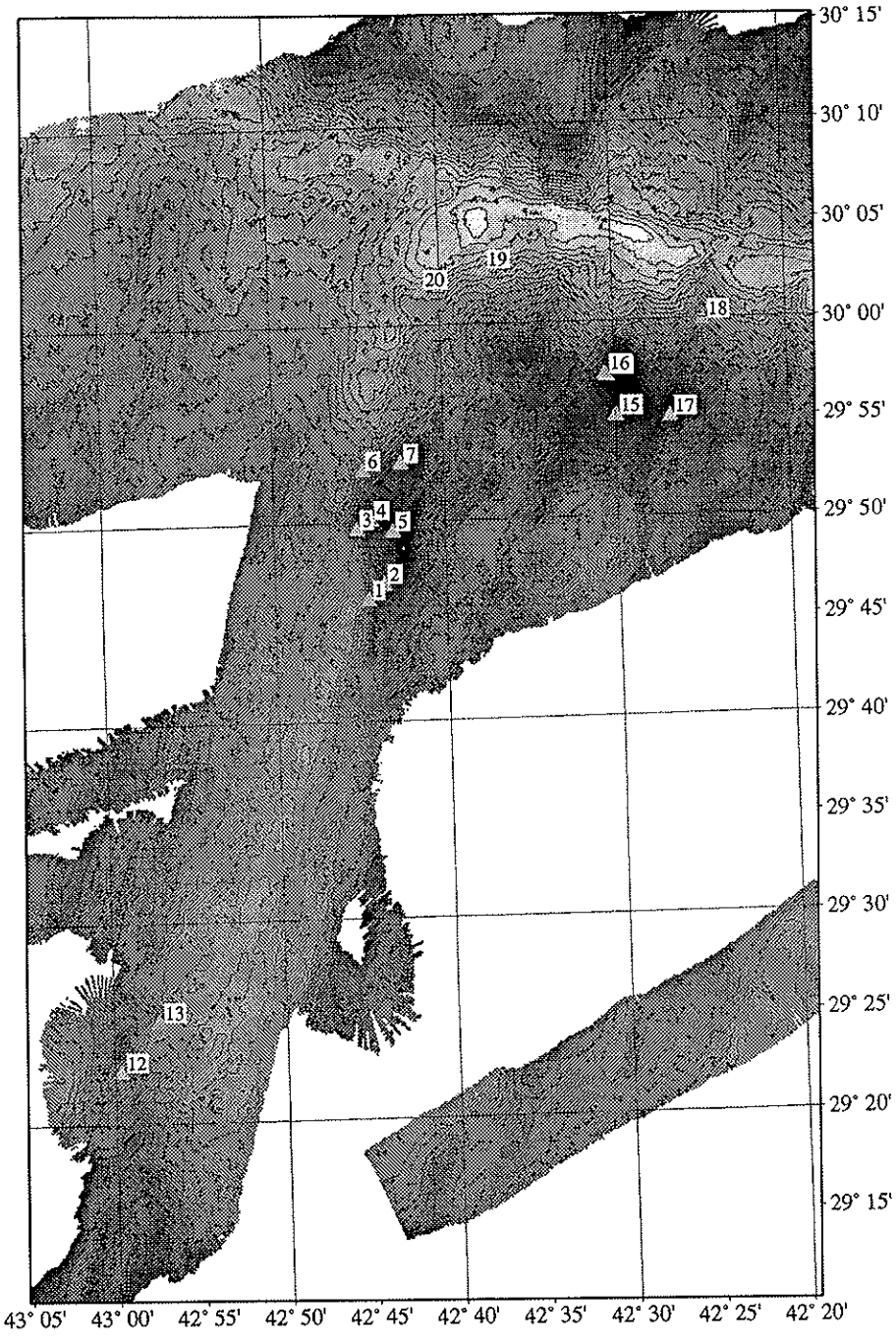

FIGURE 4.1 Location map for all dredges within the NOBSKA spreading segment. A black triangle represents the location of the ship at the dredge haul site.

Dredge 3 starts at 29 49.8'N 42 4.9' W, heading east, 2190 - 2000m.

It was sited on the cliffs on the W side of Yellow Mountain overlooking the median valley, is over the side at 1320, the pinger is on at 1330, and is back on board at 1615. This haul contains several hundred blocks of basalt, ranging in size from 40cm down to gravel, mostly highly porphyritic, with phenocrysts of plagioclase (major) and olivine (minor). A minority of the blocks are aphyric or sparsely phyric. The basalts are moderately weathered. There were some small pieces of indurated ooze and small fragments of basalt glass breccia. Some of the smaller fragments may be of somewhat altered basalt. All of these were

bagged separately in small polythene bags. A representative selection of the basalts was labelled and bagged. The remainder was disposed of over the side, since the usefulness of basalts collected from a debris flow unit is limited.

Dredge 4 starts at 29 49.9'N 42 43.9' W, heading eastwards, 1600 - 1500m.

It is targeted at a bright patch in the Tobi image with a flow texture near to the top of Yellow Mountain, that may represent material from the top that has slid down a short distance only. The dredge went over at 1650, and was back on board at 1925. It contained 42 pieces of basalt, and a number of chunks of indurated ooze. The basalts fall into two kinds. Most are slightly weathered pillow fragments, including one fine chunk of pillow of display quality. Some of the smaller fragments appear to be of metabasalt. They are distinctly green, probably more a smectitic green than a chloritic green, and one is largely made up of a milky quartz vein. Two of the other samples seem to be a network of quartz veins cutting altered basalt glass breccia. These clearly form part of a metamorphic/hydrothermally altered suite. All of the samples from this haul were labelled and bagged.

Dredge 5, start at 29 49.6'N 42 42.9' W, heading eastward, 1350 - 1200m

This dredge is intended to sample the summit of Yellow Mountain, in the hope that any serpentinite may be outcropping there. The dredge is over at 0410, the pinger at 0428, and the dredge back on board at 0630. It contains 16 fragments of aphyric to porphyritic basalt pillows, all rather weathered with palagonitic rinds, and manganese oxide coatings. The largest is a substantial piece of pillow 75cm across. Three of the fragments are attached to indurated creamy brown pelagic ooze. One fragment is of palagonite-cemented basalt glass breccia. There are fragments of coral and pieces of sponge, including a strange warty, pliable outer covering.

Dredge 6, start at 29 52.5'N 42 44.3' W, heading eastward, 2650 - 2500m

This is sited on a fissured bulge imaged by Tobi on the W flanks of Yellow Mountain above the median valley. It goes overboard at 0714, the pinger at 0721, and is back on board at 1016. The bag contains a large haul of basalt pillow fragments, moderately weathered, but wih much fresh glass. the fragments are many part of pillows, ranging in size from 50cm diameter down to gravel. The basalts divide into three groups: (a) aphyric to sparsely phyric basalts with plagioclase and olivine phenocrysts and very few vesicles (as has been the case with aphyric lavas in other dredge hauls), (b) similarly aphyric to sparsely phyric basalts, but with abundant vesicles, (c) highly phyric rocks, with abundant olivine and plagioclase megacrysts, and sometimes containing more olivine thyan plagioclase phenocrysts. Some of the pheocrysts in class (c) are very large indeed, up to 1cm across. There was no biological material in this dredge. A representative selection of the basalts was labelled and bagged. The remainder was disposed of over the side, since the usefulness of basalts collected from a debris flow unit is limited.

Dredge 7, starts at 29 53.2'N 42 42.4' W, heading eastwards, 2200 - 2100m

This dredge is on the closest of the finger ridges that run N from Yellow Mountain to the Tobi line, and imaged on Tobi line 1. It is over the side at 1044, the pinger is in at 1056, and the dredge is on board again at 1300. It contains a

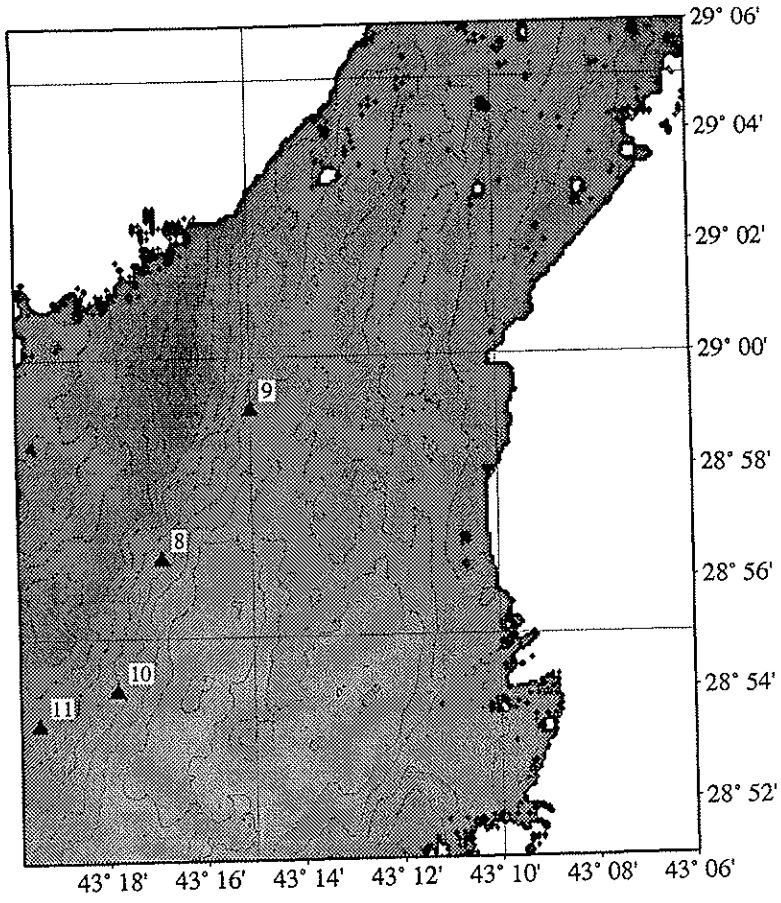

FIGURE 4.2 Location map for all dredge hauls with the Broken-Spur segment. Black triangles represent the location of the ship at dredge deployment site.

good haul of basalt fragments, moderately weathered with palagonite in the pillow rinds and marked coating by manganese oxide. The basalts could be divided as follows: (a) In the main dredge bag: (i) fragments of basalt from 60cm to gravel in size, aphyric and sparsely vesicular. (ii) blocks of aphyric moderately vesicular basalt from 20cm down to gravel in size. (b) In the pipe dredge: blocks of aphyric, sparsely vesicular basalt from 40cm to gravel in size, somewhat more weathered than those in the main dredge, and with a markedly greater thickness of manganese oxide than those in the main dredge. A representative selection of the basalts was labelled and bagged. The remainder was disposed of over the side, since the usefulness of basalts collected from a debris flow unit is limited.

Dredge 8 starts at 28 56.4'N 43 16.6W, 3400 - 3100m, heading westwards.

This dredge is on a domal feature in the slide zone at the Segment 17 SW inner corner high, N of CD 65 Dredge 34. The dredge went over at 2313/112, the pinger at 2325/112 and the dredge was on board again at 0235/113. The dredge contained hundreds of rocks, ranging from 40cm in diameter downwards, and gravel, sand and tan-coloured pelagic mud. All of the rocks were free from manganese oxide coating. They were divided into four main groups: (a)

fragments of aphyric basaltic pillows with glassy margins, partly replaced by palagonite, showing radiaring crudely columnar jointing, (b) fragments of aphyric basalt, both moderately vesicular and sparsely vesicular, without clear glasy margins, (c) fragments of dolerite, often looking very fresh, conatining large acicular crystals of plagioclase, (d) about 12 specimens of gabbro, uniform in texture, conatining orange weathered olivine crystals, perhaps pieces of high level gabbro. Both groups (b) and (c) may contain metabasalt, since their colour is appropriate for greenschist facies alteration, a bluish-grey, and some of the acicular grains may be actinolite. Also in this dredge haul were 4 or 5 fragments of indurated ooze. A representative selection of the basalts was labelled and bagged. The remainder was disposed of over the side, since the usefulness of basalts collected from a debris flow unit is limited.

Dredge 9 starts at 28 59.2'N 43 15.1' W, 3400 - 3200m, dredging northwestwards.

The site for this dredge is on a steep part of the Segment 17 flow zone near its N end and just to the W of W Seamount. The flow unit on which this dredge was made is shown in a Tobi image in the CD 65 cruise report. The dredge went over at 0322, the pinger on at 0322, and the dredge on board again at 0645. It contained about 100 fragments of rock ranging in size from 40cm to sand size, and some tan-coloured pelagic mud. The rocks are of three types: (a) greenish knobbly serpentinite, with a dull grey matrix of serpentinised olivine with scattered pseudomorphs of enstatite, apparently replacing harzburgite (in one specimen the enstatite may be fresh, since it appears to be represented by shining honey-coloured crystals), (b) one or two pieces with a more uniform texture, and no enstatite pseudomorphs, that may be serpentinised dunite, (c) One or two pieces of dolerite, dark grey in colour, with laths of plagioclase. The pieces of serpentinite are cut by carbonate veins.

Dredge 10 starts at 28 54.3'N, 44 18.0' W, 3150 - 3000m, dredging westwards.

This dredge was placed on a bright domal feature on the slide zone SW of CD 65 Dredge 34. The dredge went over the side at 1625, and the pinger at 1635. It was back onboard again at 1952. The dredge brought up an enormous haul of rock fragments ranging in size from 40cm diameter down to sand. The fragments are of four types: (a) fragments of pillow basalt, with glassy rinds partly altered to palagonite, and with a well-developed spherulitic texture in the chill zone beneath the glass (perhaps 70% of the dredge haul), (b) pieces of serpentinised harzburgite, entirely serpentinised, and containing chrysotile veins, (c) fragments of pyroxene-rich peridotite / wehrlite / pyroxenite, which are dense and hard and show a high proportion of pyroxene crystals when broken open, (d) pieces of grey serpentinitic muddy sand (as in CD65 dredge 34) A representative selection of the basalts was labelled and bagged. The remainder was disposed of over the side, since the usefulness of basalts collected from a debris flow unit is limited. Most of the serpentinites were preserved, as were all of the fragments of serpentinite sand.

Dredge 11 starts at 28 53.3'N 43 19.6' W, 2840m, dredging north-northeastwards

The dredge runs along the horizontal bench that forms the top of the slide zone at the south end of the slide zone, as imaged on CD 65 Tobi. It is over the side at 2022, and the pinger is on at 2030. The dredge is back onboard again at 2310. The dredge contains about 50 clasts of pillow fragments and other pieces of

basalt. The fragments range in size from 50cm down to gravel. Most pieces have glassy rinds partly altered to palagonite. There is a variable thickness of manganese crust. Some of the fragments are lava shelves from inside one or more lava tubes, with a very flat surface above, and a knobbly stalactitic surface below. Other fragments are of more massive basalt. Many of the pillow fragments show spectacular spherulitic devitrification textures beneath the glassy margins, usually not directly beneath them, but a centimere or so into the pillow, with black spherules up to 5mm in diameter. A representative selection of the basalts was labelled and bagged. The remainder was disposed of over the side, since the usefulness of basalts collected from a debris flow unit is limited.

Dredge 12 started at 29 22.7'N 42 59.7' W, 3000-2700m, dredging northwards.

This site is at the southwest edge of the major steep scarp that sits near the SW end of Segment 18. We heave to to move Tobi at 1310, and put the dredge over the side at 1400, with the pinger on at 1405. The dredge is back on board at 1628. It contains one huge block of rock, about 50 ten-cm sized fragments, and smaller cobbles. There are two principal rock types: (a) Pillow fragments (?metamorphosed to low greenschist facies with blue coating of ?celadonite on joint faces), with clear pillow margins on some fragments, and otherwise fine-grained and sometimes vesicular basalt, (b) coarse doleritic - gabbroic rock fragments, very uniform in grain size (with no visible chilled margins). Some of the coarse blocks, including the very large block, have large phenocrysts in a very coarse groundmass, suggesting that these are pieces of very thick sills or very wide dykes. There are a number of small pieces of rock, gathered together in one small bag labelled oddities, that represent fragments of porphyritic basalt, etc., etc. A representative selection of the rocks was labelled and bagged. The remainder was disposed of over the side, since the rock types as seen on deck were very uniform.

Dredge 13 started at 29 25.0'N 42 57.4' W 3300-2700m, dredging to the NNW

This dredge was near the foot of the major scarp at the SW end of Segment 18, about one third of its length from its E end. The dredge was overboard at 1820, the pinger on at 1830, and the dredge back on board at 2130. It contained about 3 kg of cobbles and pebbles of metabasalt, a modest and retiring haul that brought cheers from the assembled scientists watching it come on deck; it was the smallest yet, but entirely satisfactory for petrology. The fragments fall into 3 groups: (a) angular fragments of coarse metabasalt, blue-grey in colour and probably pieces of dyke rock, (b) irregular fragments of breccia composed of angular clasts of metabasalt in a khaki-colured matrix of crushed basalt, cut by veins of ?calcite and ?quartz, which are probably pieces of fault breccia, since the dredge is on a steep scarp, (c) small clasts of fine-grained basalt including pieces with spherulitic texture and some fragments of glass, probably representing pieces of pillows. The khaki colour of the fault matrix suggests smectite or smectite/chlorite clays are present, while the colour of the clasts suggests greenschist facies. Every fragment of this dredge haul was lovingly preserved.

Dredge 14 started at 29 57.3'N 42 30.4' W, 1800m, dredging S.

This site is in the cirque at the NW corner of Hinge Mountain, at its S side, designed to find out the composition of this large slab of rock. The dredge goes over the side at 0101/124, the pinger is out at 0109, the dredge is on the bottom at 0154, and the remains back on board at 0258. After 15 minutes on the bottom there is a sudden and enormous bite, up to 7 tonnes. When the wire is reecovered, the dredge chain comes on board, but the dredge is not there. It is clearly a hungry mountain.

Dredge 15, started at 29 55.1'N 42 30.0' W, 1550m, dredging NW.

This site is in the middle of the flat block of Hinge Mountain, where we later see strong lineations, partly covered by sediment, from Tobi. The dredge goes over the side at 0358/124 and the pinger is on at 0408. There is a problem with the swivel on the pendant, and the dredge has to be brought back on board for the wire to be sorted out. The dredge is over the side again at 0530, the pinger is on at 0540, and the dredge on the bottom at 0655. There are large bites, and the dredge is brought in slowly , then off the bottom at 0722, and back on board at 0819. The dredge haul is small, about 1.5kg of rock, and contains about 20 fragments, the largest 15cm in size. There are 5 types of rock: (a) Most abundant are pieces of creamy limestone/indurated ooze, which are intensely bored, with occasional fragments of bivalve shells in the holes. Worm tubes line the holes, and the pieces have a thin coating of manganese oxide. (b) One angular fragment, 5cm in size, is of basalt. (c) Two very small rough pebbles, 3cm in size, are of serpentinised harzburgite. The areas of olivine are orange-red, suggesting that the last olivine was destroyed by weathering and not by serpentinisation. (d) There is one piece of pumice. (e) And there are several fragments of coral coated thinly with manganese oxide.

Dredge 16 started at 29 57.6'N 42 30.3' W 1850m, dredging E.

This site is again in the cirque at the NW corner of Hinge Mountain, this time on its E side. The dredge is over the side at 0859/124, and is on the bottom at 0948. By 1000 the dredge is firmly stuck on the bottom, and the ship, dredging downwind, cannot get back fast enough over the dredge. Tension stays high until there is a 7 tonne bite, and the chain comes free. The chain is back on board at 1108, with no dredge, another victim of the hungry Hinge Mountain.

Dredge 17 started at 29 55.0'N 42 26.9' W 2000m, dredging W.

The station is on the large fault bounding Hinge Mountain to the east, targeted about half way up the fault to collect some talus. The dredge is over the side at 1255/124, and on the bottom at 1335. There are one or two bites including one very large twitch, and we start to haul in at 1405, bringing the dredge back at 1450. The pipe dredge has been torn from the dredge bag, ripping two holes in the corner of the bag. The dredge contains two angular fragments of weathered aphyric basalt. The larger one, 20cm in size, is part of a pillow margin with a chilled rind at one end, and a skin of limestone/indurated ooze on two surfaces. The smaller fragment is uniform in texture. Both have a thin coating of manganese oxide.

Dredge 18 started at 30 00.0'N 42 25.0' W 3200m, dredging SW

The dredge is on the finger ridge that runs down into the transform valley from the NE corner of Hinge Mountain. The dredge is over at 1552/124, and the pinger is on at 1600. The dredge is back on board at 1856, containing two fragments of weathered pillow basalt with orange palagonite rims replacing glass, and coated with several millimetres of cauliflower-textured manganese oxide.

Dredge 19 started at 30 02.6'N 42 37.6' W 4250m dredging SW.

This is on a rounded bulge of the topography close to the western RTI of the Atlantis Transform, showing bright on Tobi. The dredge is over the side at 2016/124, the pinger is on at 2020, and the dredge is back on board at 2350. This virgin dredge frame is seriously bent by the time it arrives back, and it and the pipe dredge contain a small haul of mafic and ultramafic plutonics, together with a good amount of tan-coloured ooze containing a sand fraction of mineral grains. Rock types include: (a) Pieces of harzburgite weathering a dun colour, and thus probably containing fresh olivine (some of these are clearly clasts in breccia because they have pieces of breccia matrix adhering to them). The largest fragment has a wide chrysotile vein attached to one side. (b) Angular clasts of dark pyroxenite or wehrlite, made up of large crystals of pyroxene up to 2cm in diameter. (c) One large piece of gabbro, with chalky-white euhedral palgioclase crystals and ophitic clinopyroxene. The plagioclase may be altered to prehnite, and the rock may have been transformed to rodingite. (d) Some small clasts of fine-grained breccia, containing mm to cm sized angular fragments of rock (?peridotite?) in a fine-grained greenish matrix.

Dredge 20 started at 30 01.7'N 42 41.2' W 4100m, dredging SW.

This dredge is on a fissured slope imaged by Tobi close to the western RTI. The dredge is over at 0107/125, the pinger is on at 0117, and the dredge back on board at 0435. The dredge contains about 20 chunks of aphyric pillow basalt, up to 40cm in size. The chunks have chilled margins (now largely replaced by palagonite), columnar joints and large internal vesicles. The basalts are moderately weathered and have a thin coating of manganese oxide.

Dredge 21 started at 30 05.8'N 42 03.3' W 2900m, dredging W.

This dredge was sited on the very bright debris flow material on the eastern slopes of Rose, just above an outcropping scarp, imaged on Tobi Line 16. The dredge was over the side at 0500/129, the pinger was on at 0508, and the dredge was on the bottom at 0608. It became stuck at 0651, and the ship came round to pull from the other direction. At 0729 the dredge was off the bottom and was on board, empty at 0833, with the pipe dredge lost on the bottom.

Dredge 22 started at 30 06.0'N 42 03.6' W 2550m dredging W.

This site was just up the slope from Dredge 21, on the same bright sheet of debris. The dredge was over the side at 0909/129, the pinger on at 0912, and the dredge on bottom at 0957. The dredge was stuck at 1015, and the ship came around again to pull the dredge free, which it did at 1055. The dredge was back on board at 1130 with a large haul of gabbroic and ultramafic rocks (in the broad sense) with a variety of grain sizes and textures. The fragments are angular, up

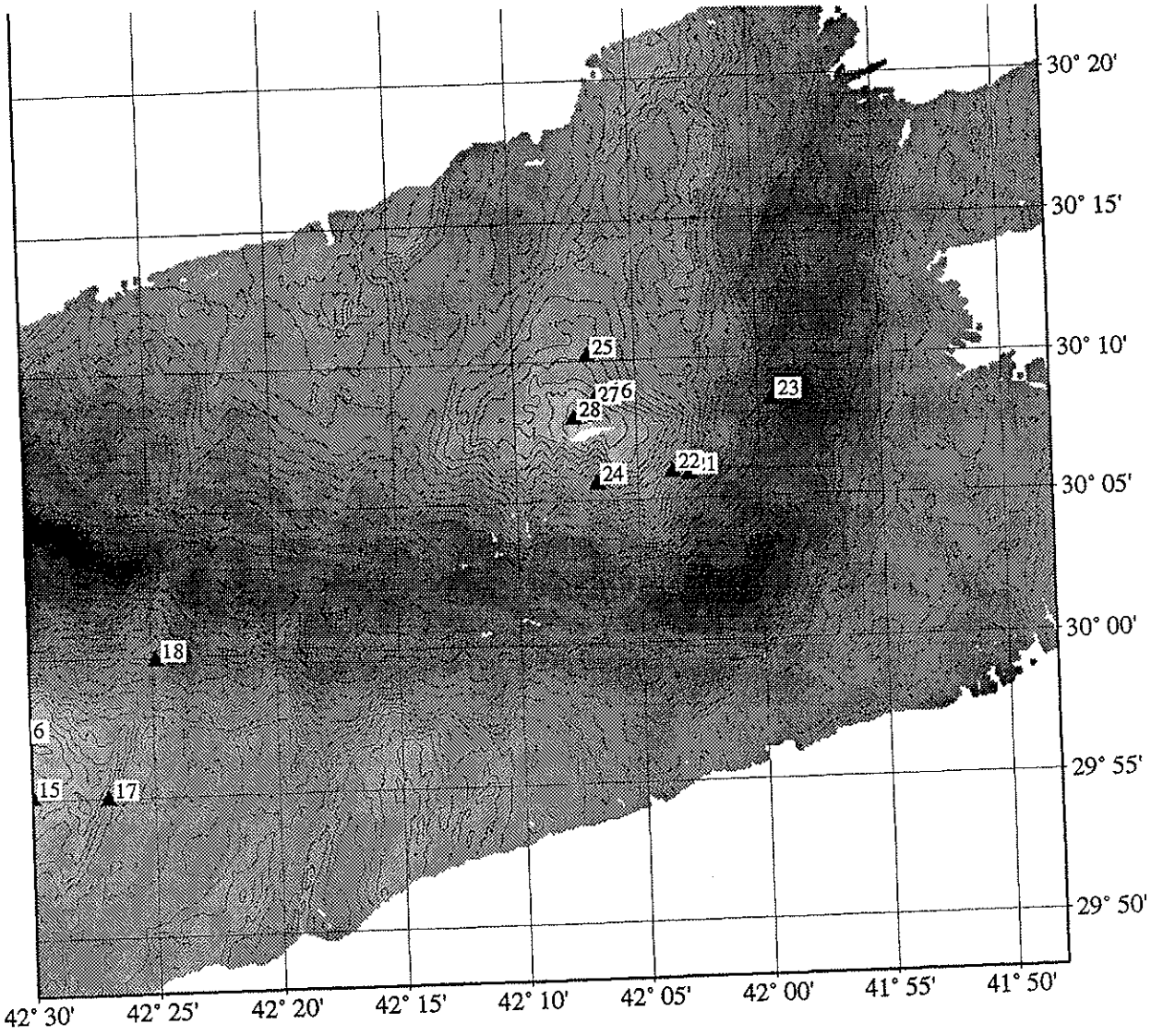

FIGURE 4.3 Location map for all dredge station conducted on the western RTI within segment 1 north of the Atlantis Transform.

to 40cm in size. There appear to be no deformed gneissic rocks in the dredge haul, and no harzburgites. Some of the rocks are cut by high-temperature amphibole veins. The rocks have a thin coating of manganese oxide, and are also coated with orange iron oxyhydroxide from weathered sulphides, perhaps from the rocks themselves, or from sulphides originally between the fragments.

Dredge 23 started at 30 08.5'N 41 59.6' W 4200m dredging W

This dredge was on the debris flow coming down from the down-slipped block, near to the median valley floor, and imaged on Tobi Line18. Some of the debiris may have come from the top of Rose, to judge from the contours. The dredge was over the side at 1236/129, the pinger was on at 1245, the dredge was on the bottom at 1409, and back on board at 1620. This dredge brought up: (a) a large number of aphyric pillow fragments, (b) many fragments of coarser rock that may be fragments of dykes, including one with a chilled margin similar to a dyke margin, (c) one piece of serpentinite, coated with white soapy talc, (d) one

piece of gabbro with a strong gneissic fabric, and (e) two pieces of breccia composed apparently of angular fragments of basalt set in a fine matrix.

Dredge 24 started at 30 05.7'N 42 06.6' W 2250m, dredging N.

This dredge was targeted at a stone chute in one of the gullies running down from the top of Rose, imaged by Tobi on Line 16. The site is about 2km east of the site where Atlantis dredged serpentinite in 1947. The dredge was over the side at 1745/129, the pinger was on at 1755 and the dredge was back on board at 2021. The dredge contained 7 rock fragments weighing about 4 kg: one angular fragment of gabbro and six pieces of wholly or partly serpentinised harzburgite. There is no manganese oxide coating to the fragments. One of the harzburgites has a dun-coloured weathering rind, and probably has fresh olivine in it.

Dredge 25 started at 30 10.1'N 42 07.2' W 1650m, dredging SW

This dredge was targeted at the striations running across the smooth surface at the N of Rose. It was over the side at 2100/129, the pinger was on at 2104, the dredge was on the bottom at 2132, and was back on board at 2238. It was a difficult dredge across bare rock, and only brought back two small pieces of rock, both serpentinised harzburgite. This does demonstrate that harzburgite is involved in the faulting that formed the striations.

Dredge 26 started at 30 08.4'N 42 06.7' W 1200m dredging SW

This site is in a small corrie near the top of Rose. The dredge was over the side at 2302/129, the pinger was on at 2307 and the dredge was back on board at 0010/130. There was a large bite shortly after the dredge reached the bottom, which suggested that the dredge was strangled, but when it was brought back it had not strangled, and also had nothing in it.

Dredge 27 started at 30 08.4'N 42 06.7' W 1200m dredging SW

This is the same site as Dredge 26, and again in the small corrie near the top of Rose. The dredge was over the side at 0042/130, the pinger was on at 0049, the dredge was on the bottom at 0114 and back on board at 0206. The only product of this dredge was a delicate, pink, branching coral. At this stage, we gave up the corrie and tried to sample the top of Rose.

Dredge 28 started at 30 07.8'N 42 07.3' W 900m dredging S

This site is on the summit plateau of Rose. The dredge was over the side at 0233/130, the pinger was on at 0241, the dredge was on the bottom at 0258, and back on board at 0400. It brought back a small piece of limestone and a small angular clast of basalt.

4.12 Shrimp

Overview of results

Camera run 1 starts at 28 58.8'N, 43 13.3' W in 3500m and finishes at 28 59.5'N, 43 15.7' W.

It is targeted to run across the hummocky volcanics just to the W of W Seamount, and then go up the slide slope and through the site of Dredge 9 to the top of the slope. The site for this station is on a steep part of the Segment 17 flow zone near its N end. The flow unit on which this camera station was made is shown in a Tobi image in the CD 65 cruise report. Shrimp is set up with black and white film to check exposures with the camera, but there is a wind-on problem. Only the first 30 or so frames come out, showing talus breccia, and then there is no more winding-on. The camera frame brought back two fragments of porphyritic basalt with manganese oxide encrustations.

Camera run2 starts at 29 00.0'N, 43 12.3' W and finishes at 28 59.8'N, 43 13.3' W

Camera run 2 is designed to look at the volcanics around and at the top of W Seamount, and to peer into its crater. The run is in two lines, one from 29 00.0'N, 43 12.3'W to 29 00.2'N, 43 13.3'W, and the second from 28 59.6'N, 43 12.3'W to 28 59.8'N, 43 13.3'W. Both lines run into the now strong wind, and the ship drifts back from the end of one line to the start of the next with the camera above the seafloor. In the middle of the first line the camera passes over the centre of the crater of W Seamount, and the altitude pinger measures its depth as 125m. The camera is overboard at 2022, and the first photograph is at 2158. The first line ends at 2325, the second line starts at 0056/115, and the end of the line is at 0200/115. The camera is back on deck at 0316/115. Because of a broken connector, the flash is not synchronised with the shutter, and no photographs result. Three pieces of volcanic glass come up on the camera frame.

Camera run3 starts at 29 49.1'N 42 41.4' W, at 1650m

Camera station 3 is planned for the top of Yellow Mountain, to see if it is a large volcano, and to test the camera system to se if it is working. Just before launching, Dave Edge reports that the wind-on problems have been caused by friction between the film spools and the camera cover. Camera station 3 starts at 29 49.1'N 42 41.4'W, at 1650m and is planned to finish on the summit plateau of Yellow Mountain. The camera goes over at 1957/123, and is at the bottom by 2056. Once the camera reaches the bottom it becomes clear that control of its height is very difficult, since it has to be 3-7m above the bottom, and the swells are as high as that, to say nothing of the irregularities of the bottom. The camera takes pictures, but continually collides with the bottom. We decide to abandon the station in view of these difficulties at 2152. When the camera is back on board at 2240, its battery packs have become dislodged, and have fallen out of the frame. There are no spare battery packs on board, so we are now without a camera. The station produces about 70 images of sediment and rocks that need to be printed for further investigation.

CD 100
NOBSKA

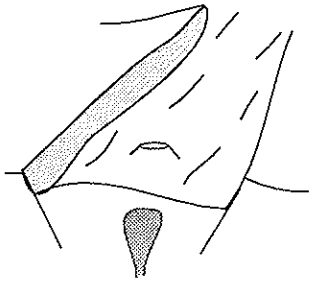

Section 5 Data Processing & Storage.

The Honey Pot

5.1 TOBI Processing

5.1.1 Sidescan (*Eddie McAllister*)

Processing of TOBI sidescan was carried out using the WHIPS (Woods Hole Image Processing System). The software was supplied by SOC, and contained a number of programs (written by Tim Le Bas) developed explicity for processing TOBI sidescan data.

The approach to processing taken on CD100 was influenced by the experience gained in TOBI processing by Peter Slootweg and Roger Searle on CD99. Their experience showed that many of the WHIPS scripts were developed to produce large mosaics based on a complete survey of sidescan data, and that the scripts were not useful on a daily basis. Accordingly we developed a number of small scripts which were used to process a single days TOBI data.

A number of changes were made to the main programs within WHIPS:

- change the sidescan sampling frequency within the *raw2whips_tobi2* program from a 8000 pixels to 1000 pixels across track to 2000 pixels across track. The new program was renamed *raw2whips_tobi2.1*.
- altitude smoothing in *tobtvg2* was ammended to remove a step that smoothed the altitude based on the pressure data. This assumes TOBI is a terrain following vehicle. The altitude was smoothed simple using a median and low-pass filter. The new program was called *tobtvg_smooth*.

The script which controlled all the calls to the main WHIPS programs is called make_tobi_processCD100, and is located in the directory ss_cdf/scripts which lies immediately below the CD100 directory. The script reads directly from the TOBI data compact disc and produces as its end product a slant range corrected

image. An option within the script is to accept or reject the smoothed altitude carried ou by tobtvg_smooth. At the moment the script simply exits of the altitude is not acceptable. This will be updated in Leeds to calculate the altitde directly from the profiler data. The script:

```
# Simple script to run and test some of the whips routines.
# make_tobi_processCD100 $1 $2
# $1 = cdrom directory number
# $2 = output file name
# $3 = tobi nav & wireout
#Convert from raw data stripping out the sidescan data.
# Creates a netcdf sidescan file of width 2000 pixels (1 averaged from every 4)
echo "Running : raw2whips_tobi2"
raw2whips_tobi2.1 -i /cdrom/$1/tobi.dat -o raw2cdf/$1.cdf

#Strip out the magnetics from the raw data
echo "Running raw2mag"
raw2mag_tobi2 -i /cdrom/$1/tobi.dat -o ../mag/tobi/raw/cd100_$2_tobi.mag -r

# Pad out sidescan file to ensure that each starts on an even minute

echo "Running alline"
alline -i raw2cdf/$1.cdf -o alline/$1.cdf

#Smooth the altitude reading
echo "Running tobtvg2 on altitude"
tobtvg_smooth -i alline/$1.cdf -o alt_sm/$1_alt.cdf -a

# Check the smoothed altitude against the raw altitude.
listhdr_tobi -i raw2cdf/$1.cdf | awk '{if (NR > 1) print NR, $11}' | psxy -R1/
15000/1/1200 -P -JX15/10 -Ba1000f100:"Time (4sec intervals)" :/
a400f100:"Altitude" :WSen -K -X2 -Y2 >! alt_test2.ps

listhdr_tobi -i alt_sm/$1_alt.cdf | awk '{if (NR > 1)  print NR, $11}' | psxy -R1/
15000/1/1200 -P -JX15/10 -W1/255/0/0  -O >> alt_test2.ps
pageview alt_test2.ps &
echo -n "Do you wish to accept the smoothed altitude? [y/n] "
set ans = ($<)
if ($ans == "n") exit;

#Merge with the ship navigation data
echo "Merging ship navigation with sidescan"
mrgnav_tobi2 -i alt_sm/$1_alt.cdf -n ../nav/ship/ship_navigation -o nav/
$1_ship.cdf -s

#Merge with TOBI NAV file.
echo "Merging the calculated tobi location with sidescan"
mrgnav_tobi2 -i  alt_sm/$1_alt.cdf -n ../nav/tobi/tobi$2_whp.dat -o nav/
$1_tnav.cdf -t -w

#Apply slant-range correction
echo "Apply slant range correction"
tobslr2 -i nav/$1_tnav.cdf -o slrc/$1_slr.cdf -r 3.0,3.0
```

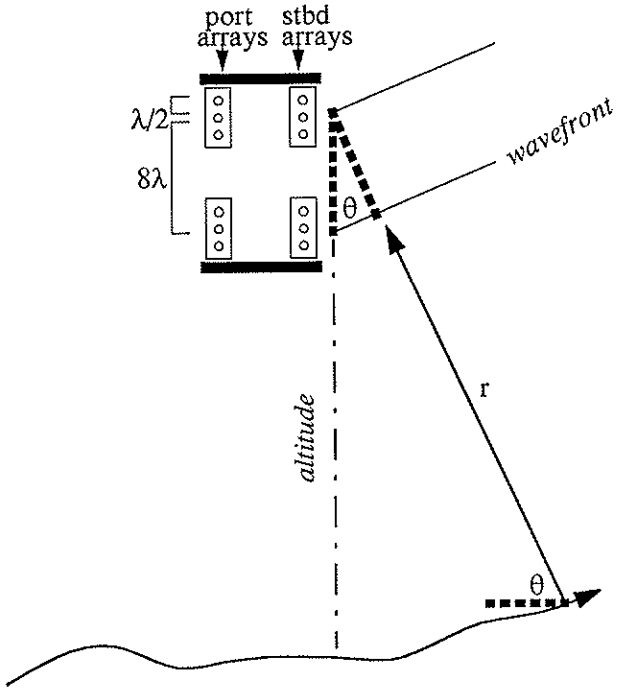

Figure 5.1 Diagram showing TOBI hydrophone arrays and the geometry of arriving wavefronts that are offset between the arrays.

5.1.2 Bathymetry (*Donna Blackman*)

Swath bathymetry obtained from TOBI uses two vertically offset hydrophone arrays, each with three individual rows of sensors. The fundamental data for the depth calculation is the phase seperation (time offset) of the waveforms received by the two arrays (or two rows for unambiguous phase). This phase seperation is a function of the angle between the arriving wavefront and the approximately vertical plane in which the receiver arrays lie. The approximate location on the seafloor at which the outgoing pulse was reflected can be computed trigonometrically (**Figure 5.1**).

The frequency of the port transducer is 30370 Hz and the starboard signal is 32150 Hz, giving wavelengths of 50 mm and 47.3 mm, respectively. The outer rows within each array are seperated by 25 mm (~λ/2) and the two arrays are seperated by 0.398 m (~8λ). The depth of TOBI can be determined from it's pressure sensor or through a combination of the vehicle's altitude (derived from two-way travel-time of first break in the sidescan record or the 7.5 KHz profiler trace) and seafloor depth determined otherwise (e.g. Simrad) for a known position.

The 'swath record' for each of the port and starboard sides was split into two portions for CD100: 0-4 seconds of ambiguous phase; 0-4 seconds of unambiguous phase. Only every other value of the continous 4 second data stream (1000 samples per second) was retained in order to fit both ambiguous and unambiguous values into the 4000-sample record. No averaging was done

before this subsampling. The first 100 ambiguous values contain a calibration pulse, the first half of which is 0 and the second of which has value 1500. The last 50 samples of the unambigous record are 0.

The unambiguous phase values should vary from 4π-0 since the effective receiver seperation is 2λ. Phase differences between each of the 2 sets of rows in the upper array are added together and to the sum of the differences between the two sets of rows in the lower array to obtain the recorded value. An unambiguous 2π wrap is represented by a value range of 3216 starting at an apparent offset value of 201. For the ambigous phase determination, readings from the sensors are weighted by a ratio of 1:2:1 for the outer:middle:outer row in each array. The ambiguous phase values should vary from 2π-0 up to 8 times. This 2π wrap is represented by a value range of 2412 and there is an apparent offset of 804 (~256π) in the ambiguous records. Near-vertical arrivals (θ near π/2) have very low signal since they fall in the null of the beam so only the end of the first unambigous 2π-0 wrap and the 3rd or 4th ambiguous wrap can be recognized in the early part of the phase records. Signal-to-noise ratios in the outer part of the swath are also low so it is typical to detect only up through the 5th or 6th ambiguous wrap. This corresponsds to a (half) swath width of about 1500 m for a TOBI altitude of about 600 m.

The unfiltered phase data is quite noisy with spikes throughout the record, although their amplitude is reduced when strong phase signal is present. The port side record tends to be somewhat noisier and recognizing unambigous and ambiguous wraps visually is generally more difficult than for stbd. Passing the phase data through a simple median or box-car filter is sufficient to bring the signal above a background noise level (**Figure 5.2**) Filter half-widths of 5-7 (10-15 millisecond full width) produce a fairly clean signal while still retaining most of the amplitude near the wrap points. The median filter (*smshint_med.c*) does a better job of passing extrema just at the wrap than does the box-car averaging scheme (*smshint_lpf.c*).

The ambiguous phase data are slightly clipped, although this should not matter for phase interpretation since it is the noise that is cut off. The clipping of the sidescan amplitudes, which occurs rather often, is more of a problem in terms of limiting our ability to post process the data using the full range of reflectivity values that would have been received.

SSwath data from the first two lines (CD431 & 432) have garbage in every other ambiguous sample due to an indexing problem in the recording software. This was corrected for the start of line 4. When not accounted for, the data appear to contain 'beats'. The first part of line 4 (CD8) is rather noisy but there are good stbd records to be found. Successive swath data (CD RUN8_2 onwards) appear to be useful. Both port and stbd swath signals disappeared between lines 12 & 14. The stbd signal came back and looked fine before line 15 and the remainder of the run but port did not recover. The hydrophone tube on the lower port array had been cracked, likely during recovery after line 10, and the loss may have been related to leakage since the crack was simply taped as no extra tube was available, although the tape appeared to have held upon visual inspection after recovery.The program *raw2list.c* extracts up to 5 records from a specified time, writes ascii files (*uamb.lst, amb.lst, ss.lst*) and has an option for either median

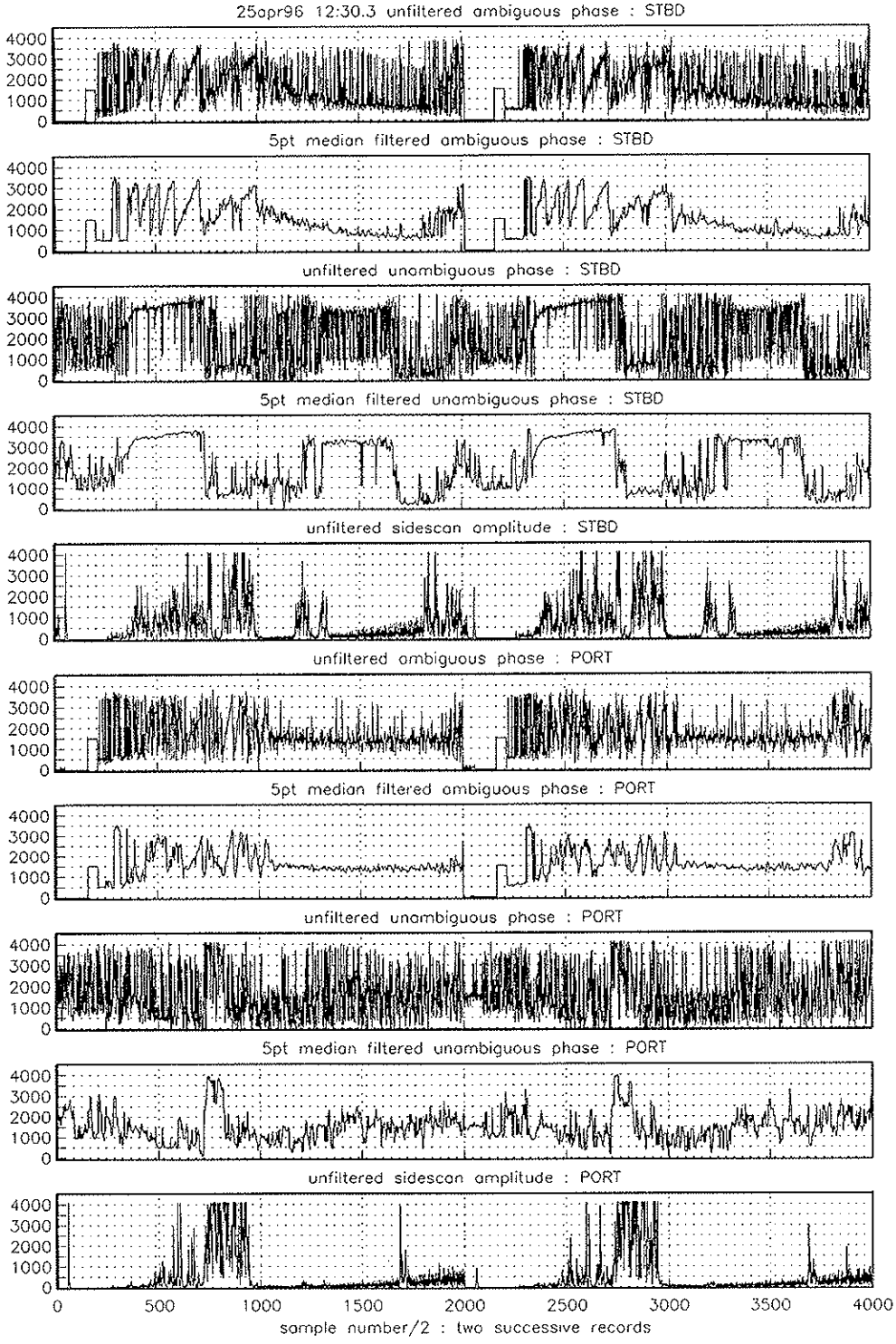

Figure 5.2 Comparison of unfiltered and filtered pahse data. See text for full discussion.

box-car filtering of the data (*-m or -b*) Successive data values are written in column format to the files so time step is constant (0.002 seconds) and not included. The program *raw2list_bat2.c* attempts to process a few swath records and to convert phase to depth values. The SNR of the SS record is checked but currently only the record section before the first SS break is set to a *NODATA* value in the swath record. The stbd phase is inverted so that it wraps 2π-0 rather than its initial 0-2π. The position of the unambiguous and ambiguous wraps is determined in the subroutine *wrapnz*. The code checks the phase difference between points seperated by *ofac*filtlen* where *ofac* is an input option (default value is 3) and *filtlen* is the length of the filter chosen with option *-b* or *-m*. If a difference greater than *jscl* times the 0-2π scale range is found, then narrower sections (+/- *filtlen*) within this window are searched to locate a more precise wrap position. *jscl* can be set with the *-w* option but it defaults to 0.75. The agreement, or lack thereof, between θ determined using the unambigous vs ambiguous phase data is checked and a misfit greater than *adeg* (hardwired to 5 degrees currently) is printed to the screen. The modified phase angles (inverted, set to *NODATA*) and the computed depths are output to ascii files (*uang.lst, ang.lst, zuamb.lst, zamb.lst).*

The programs *raw2whips_bat2.c* and *tobbat.c* were written by Peter Slootweg (and Tim Le Bas in places) with the intent of batch processing TOBI swath data. *raw2whips_bat2* reads the raw image file (from CD), allows for screening of swath data based on the SNR of the SS data (*-f -s* options), provides filtering if requested (*-z -j* options), attempts to unrwrap the ambiguous phase wraps (*-w* option with 5 different choices). A subsection of the raw file can be processed (*-t -n* options) and the output can be either incidence angle (θ) or approximate depth.across the swath. A couple minor indexing problems for CD100 format data were found in *raw2whips_bat2*- these are corrected in *raw2whips_bat3* . The whips output can be viewed with *viewwhips* but it is difficult to discern whether the unwrapping has worked or not (for a range of *-w* choices). The default of having depth as the output (rather than incidence angle which is specified by option *-u*) does not appear to give reasonable results and this must be due to differences in the programs wrap scale parameters (at least) and those in place during CD100. The method of extracting pressure in *raw2whips_bat2* is outdated and the phase offsets appear to have changed since the program was initially written. *tobbat.c* appears to be set up for input of incidence angle image data, correction of roll bias and ray tracing through a water velocity profile with results interpolated to a new corrected-depth image file. Attempts to run it on the output of *raw2whips_bat2/3* were not successful; some of the problem must be the incorrect parameters for the incidence angle calculation.

In summary, the acquisition of phase bathymetry data on cruise CD100 has been successful in a first-stage manner for pehaps half the initially expected swath width and for most, but not all, of the TOBI lines. There is a fair amount of work required before the phase data recorded can be reliably mapped into bathymetry in its appropriate place on the seafloor. Further software development will be necessary so that automatic recognition of phase wraps is possible amongst the noise but, given some effort, this can be accomplished.

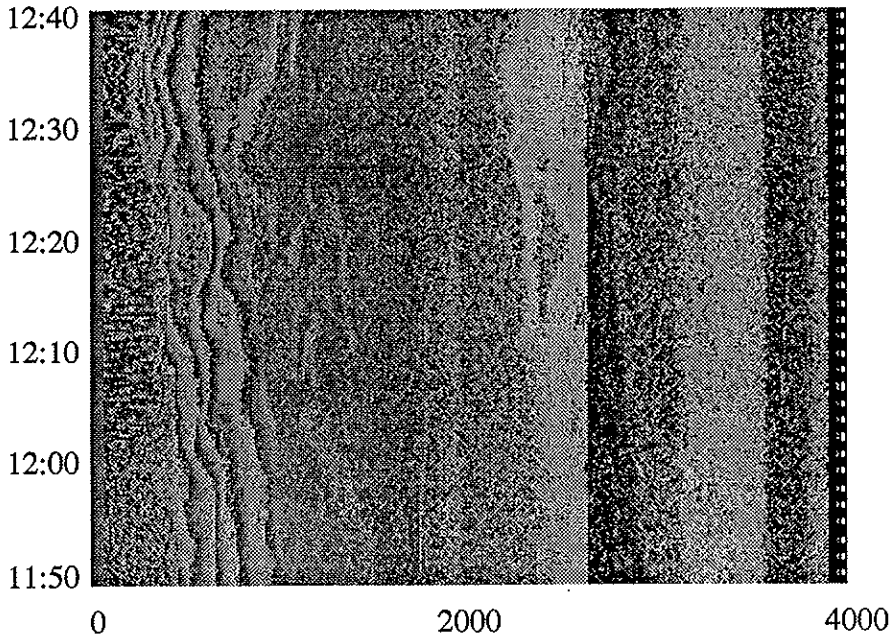

Figure 5.3 Example of STBD ambignous and unambiguous phase covering a 50 minute period. See text for full discussion.

Calculating Bathymetry Profiles

We attempted to extract bathymetric information from the ambiguous phase of the starboard (STBD), which seemed less noisy and more consistent with the unambiguous phase. To revise, the phase differences for the TOBI transducers separated by 2λ (unambiguous phase) and 8λ (ambiguous phase) are both recorded at the end of the TOBI raw files subsampling the original 4 s record with 1000 samples per second for each phase to half a sampling rate. In this way both ambiguous and unambiguous phase are fitted in a 4000 sample points record. In **Figure 5.3** the STBD record of April, 25 (julian day 116) between 11:50 and 12:40 is presented in grey scale. The first 2000 sampling points correspond to 4 s recording of the ambiguous phase, the last 2000 points to a 4 s recording of the unambiguous. Note the phase wraps (sharp white to black transitions, black corresponds to lows, white to highs), especially the phase wrap in the unambiguous phase (cycle 1). This wrap appears quite prominent and in the same time throughout the record. It should, in fact, follow one of the ambiguous wraps closely, so it cannot, at present, be trusted to identify cycles in the ambiguous phase. The ambiguous phase in this record is more complex, and appears to repeat bathymetry. In places in **Figure 5.3** as many as 4 wraps of ambiguous phase can be seen after the water column is passed (only three are detected at around 12:20) and before noise starts to dominate at far range. Within the wraps are areas of speckle, representing shadow on the sidescan image (compare with figures 5.4 and 5.5). In order to extract bathymetry, the

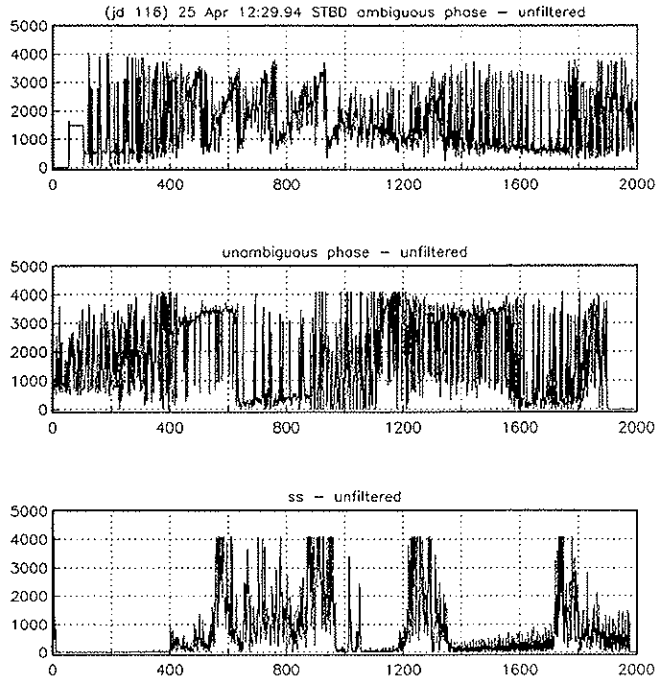

Figure 5.4 Unfiltered example of the ambiguous amd unambiguous phase, plus the sidescan on the STBD side.

ambiguous phase wraps must be identified and, without unambiguous phase, we must rely on the observed bathymetry.

The raw record of April, 25, 12:29.94 for the STBD ambiguous and the unambiguous phase and the sidescan (ss) in **Figure 5.4** appears very noisy. The signal is harmed by spikes with amplitudes of the signal level. An initial try of despiking using a simple 5 point median filter (**Figure 5.5**) allows easier detection and identification of the phase wraps. Identification of the cycles scales the vertical axis of **Figure 5.5** (scaled sine of the angle of incidence of the backscattered signal). The sine of this angle of incidence allows the computation of the distance travelled by the backscattering echo, which in turn facilitates derivation of bathymetry.

To illustrate how important it is to correctly identify the ambiguous phase wraps, the wraps of the ambiguous phase record in **Figure 5.5** were interpreted by correlation with cycle 1 of the unambiguous phase as cycles 5,4,3 and 2 (between 450 and 950 sampling points), and then as cycles 6,5,4 and 3. The derived bathymetric profiles are shown in figures 5.6 and 5.7 respectively. In figure 5.7 it is not only the depth of the seafloor that increases with different identification of the cycles, it is also the slope that changes quite abruptly, giving significantly different topography. The profile in figure 5.7 corresponds more closely to the observed overall profile than does that of figure 5.6. Disregarding the noise that was inherently passed to the bathymetric profiles of figures 5.6 and 5.7, the resolution of the topographic features that can be achieved by proper usage of this information is promising.

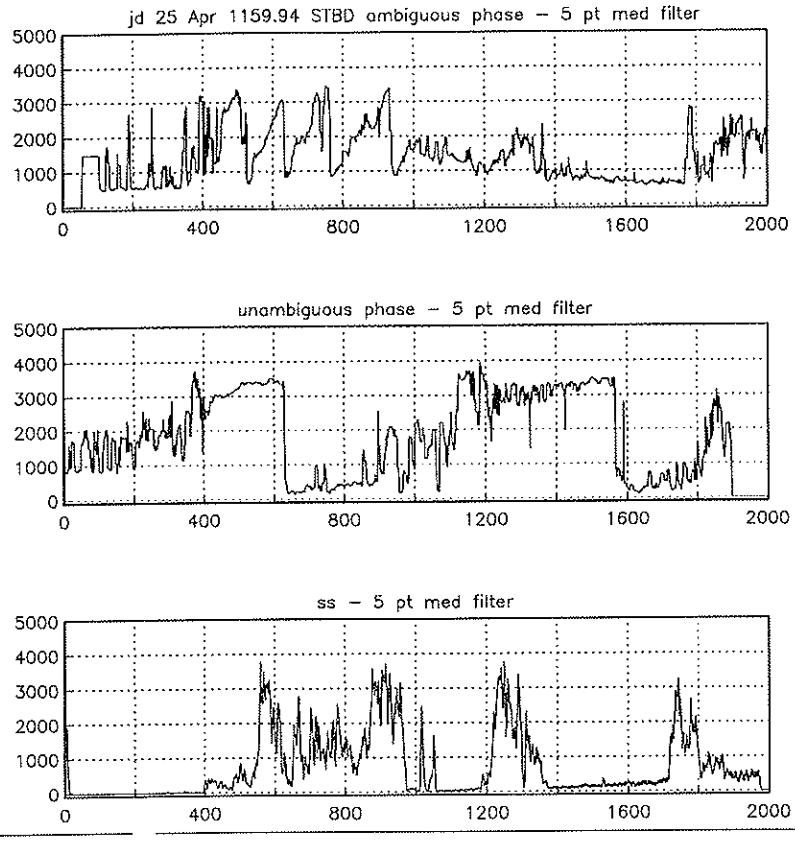

Figure 5.5 Filtered example of the ambiguous amd unambiguous phase, plus the sidescan on the STBD side.

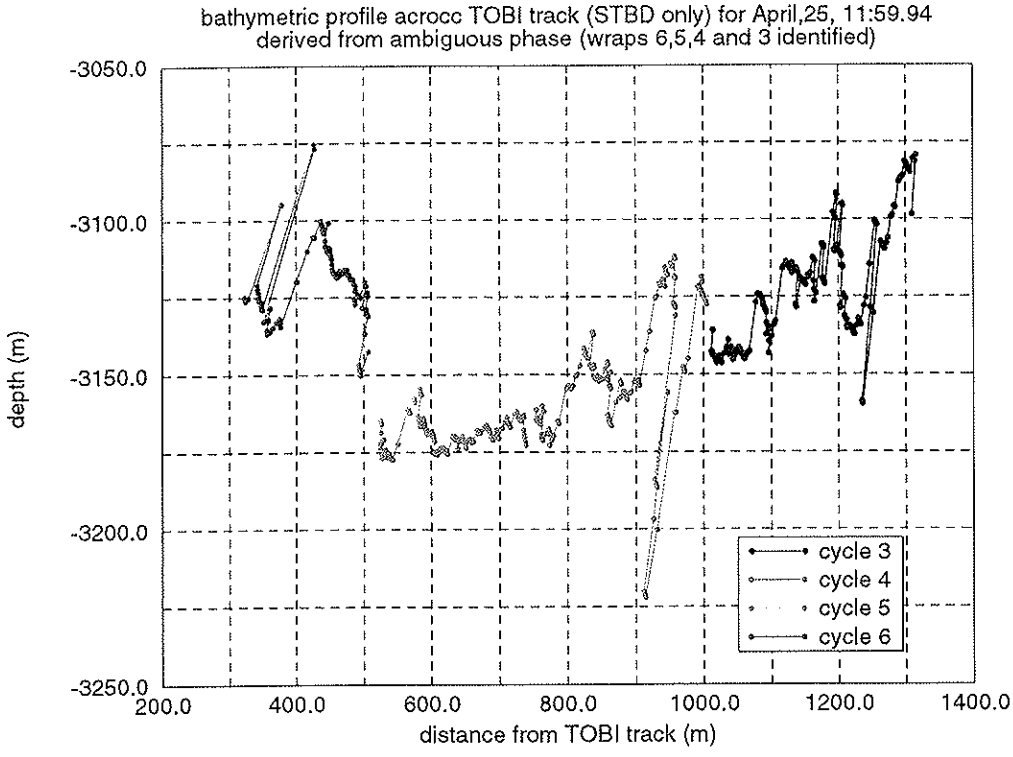

Figure 5.6 Bathymetric profile derived from ambiguous phase, using wraps 6,5,4 and 3.

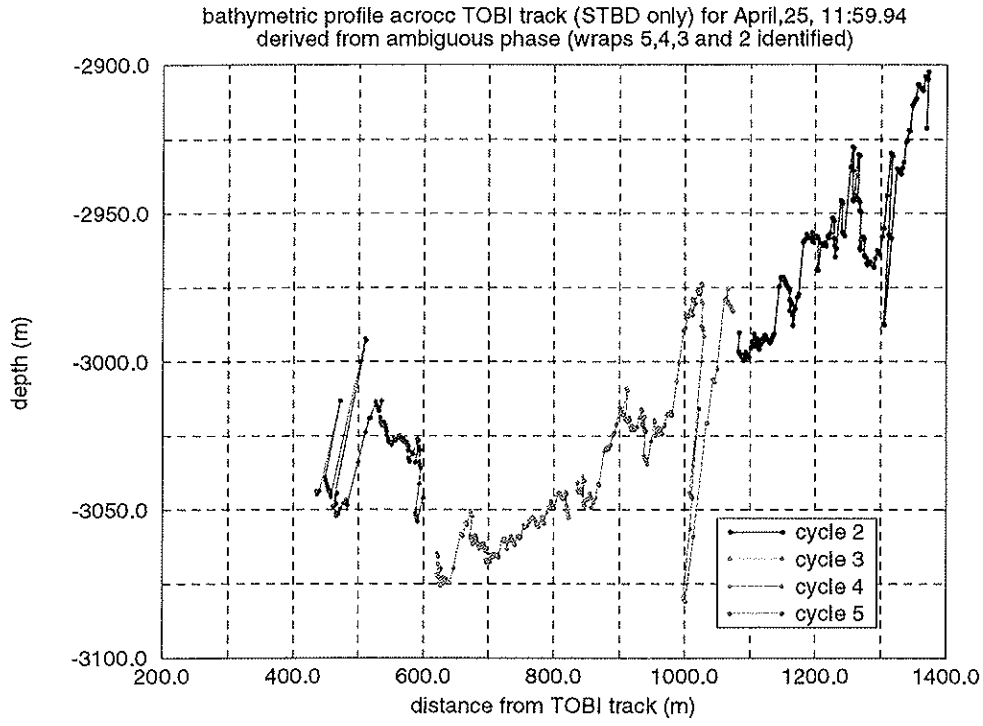

Figure 5.7 Bathymetric profile derived from the ambiguous phase

5.1.3 Magnetometer (*Rachel Pascoe*)

The magnetics data processing starts with the *.mag file in /local/disk3/CD100/mag/raw. The format of this file is typically Header information yymmdd hhmm sss alt wire vehicle_depth Vx Vy Vz roll pitch gyro where Vx, Vy and Vz are the 3 components measured by the TOBI magnetometer, before any corrections and are in volts. The seconds column is actually seconds*10. Sometimes the total field is calculated and included in this file.

STEP 1 - remove header information so file can be read into MATLAB

This is achieved using the awk command file striphead.awk - awk -f striphead.awk cd100_*_tobi.mag > cd100_*_nohead.dat

where the * refers to the cd number. It is worth checking that all the columns are included in the new file after running this command as this varies from file to file.

STEP 2 - remove time glitches from the data

Typically there are about 50 instances where the time doesn't increase monotonically. These have to be edited out otherwise there are problems later in the processing sequence. To find the glitches - load the file into MATLAB obtain the matrix of month, day, hour, mins and seconds convert to secs (using date2sec) create a vector d=diff(secs); find the indices of secs where d<0 print

out the date for these points edit the *_nohead.dat file to remove the 4 extra lines at the times given above

- NOTE - this step might actually be incorporated into despike.m if I have time

(Another note - there are still some time glitches - where the time leaps ahead by 2 seconds rather than sampling at 0.5 second intervals - I'm ignoring these for the time being).

STEP 3 - remove spikes from the data

The MATLAB routine despike.m can be used to remove the major spikes from the data, although this is still somewhat dependent on the datafile and should be edited each time to make sure it does the right thing. Basically one or more of the Vx, Vy or Vz readings will have a large value in it and this can be used to pick out spikes. The spike is replaced by the average of the two adjacent values. A second set of spikes is also present - finding the Vz<0 instances usually locates these which occur in sets of 3. These are located and replaced with the average of the points either side of the 3 spikes. The end result of despike.m is saved to cd100_*_nospike.dat.

STEP 4 - smooth the data

Prior to subsampling the data are filtered (or smoothed) using a running mean boxcar filter of length 120, assuming they are going to be subsampled at 60 second intervals. This is achieved using the MATLAB routine smooth.m. The result is saved to cd100_*_smooth.dat.

STEP 5 - subsample the data

The filtered data are subsampled to 60 second intervals to match the navigation data provided by Bob. Awk is used for this picking out the rows where the seconds column is zero.

awk -f subsample.awk cd100_*_smooth.dat > cd100_*_TOBI.dat

STEP 6 - convert the magnetic data to nT

The matlab routine raw2nt.m is used to convert the magnetic data from volts to nT, applies the manufacturer's calibrations and changes the coordinate system. It also calculate the total field intensity and plots the total field and three components against elapsed seconds since the start of the run. The resulting matrix is saved to cd100_*_nT.dat.

STEP 7 - add the navigation data to the magnetics data

The matlab routine addnav.m is used to add TOBI navigation information to the magnetics data. There are still some problems with time glitches here but the matlab routine now removes any offending lines. This should be alright in later processing as I think there is an interpolation done before any inversions. Output is saved to cd100_*_navmag.dat and has the following columns - month, day, hour, mins, tsecs, navlat, navlong, utmx, utmy, Fx, Fy, Fz, Total, altitude, depth

This completes the initial processing sequence as identified by Simon Allerton in CD99. At this stage it is possible to plot the individual components and total field data against latitude or longitude.

Further steps that need to be carried out are - (1) correction for the magnetic effect of the TOBI vehicle and other pitch, heading type corrections

(2) removal of IGRF to give magnetic anomaly data

(3) inversion to give crustal magnetization.

Programs exist for these steps and have been included in the directory of magnetic processing programs. They are total_field_corn.f - which needs to be modified for CD100 data filter_mag.m - which probably won't be used invert_mag.m - which calls the following programs parkhues.m detrend.m border3.m border2.m upwcon.m newsyn2d.m newinv2d.m magfd85.m newskew.m bandpass.m

The matlab program magfd85.m uses a file sh.mat which is also included in the programs directory. The data for the total_field_corn program to correct for the TOBI vehicle is in the file hdg.tcor0.1t10 located in the sub-directory tobi_turns.

5.2 SIMRAD Processing

5.2.1 Bathymetry *(E. Avgerinos & S. Mello)*

The EM12 data was automatically stored on hard disk by the Simrad MERMAID logging system as a series of Raw format files (denoted by the prefix *.allí). The operation was constantly monitored by watchkeepers and set manually to start a new file every hour. GPS navigation data were logged and processed in parallel by the RVS 'ABC'system.

Some post-processing of the bathymetry data was performed on board by RVS personnel using the Simrad Neptune processing system (a suite of programs running on Sun Unix platforms). Prior to using the Neptune system, the 'Raw' format data files were converted to Simrad 'survey' format files (using the 'handleMessage' utility); at this stage additional 'survey' format position files were generated from the 'ABC' processed navigation data and merged with the bathymetric data.

The Neptune processing consisted of removing major spikes from the data, prior to gridding. The gridded files (*.ASCXYZ and *.ASCGRI) were exported via the computer network of the RRS Charles Darwin Cruise 100 on a daily basis. These files were gridded with 50 m grid cell size and the coordinates are in UTM.

The *.ASCGRI files were then converted to a xyz format using the routine `irap2xyz` to remove the header of the files and utilise them with GMT (Generic Mapping Tool). The data are then regridded using the UTM command `xyz2grd` and a grid cell size of 100 m. Bathymetric contour maps were produced at a scale of 1:50,000 using the UTM commands grdimage and grdcontour. The full script generating the maps resides in directory /local/disk2/CD100/simrad/bathy/ps_scripts.

Regridding with 50 m grid cell size introduced considerable noise in the final product, mainly at the elongated stripes where survey lines are overlapping, due to the shipís different navigation along each line. Also noise was introduced at

areas with data gaps due to low multibeam coverage. To overcome these problems a grid cell size of 100 m was considered optimum.

5.2.2 Sidescan (*Eddie McAllister*)

SIMRAD sidescan processing was simply carried out by taking the xyz ascii data as supplied by RVS, and then calclulating the minimum, maximum and the average backscatter amplitude value within a desired grid spacing. Thsi uses a program called `bin_xyz_data` written by Neil Mitchell. The three files were then gridded using the nearest-neighbour gridding program nearneighbor which is part of the GMT suite of programs. The following script was used routinely to produce sidescan maps:

```
#Create a SIMRAD sidescan map
# To run: make_simrad_ss <input_filename> <output_filename>
<grid_space>

set gloc = `head -15 $1 | awk '{if (NR == 8) lmin = $3; if (NR == 9) lomin =
$3; if (NR == 10) lmax = $3; if (NR == 11) lomax = $3; if (NR == 12) print "-
R"lomin"/"lomax"/"lmin"/"lmax}' `

set loc = `head -15 $1 | awk '{if (NR == 8) lmin = $3; if (NR == 9) lomin = $3;
if (NR == 10) lmax = $3; if (NR == 11) lomax = $3; if (NR == 12) print "-
W"lomin,"-E"lomax,"-S"lmin,"-N"lmax}' `

cat $1 | bin_xyz_data -M3 -H15 $loc -X$3 -Y$3 -O > temp.xyz

nearneighbor temp.xyz $gloc -S0.002 -V -N1 -I$3 -Ggrd/$2 -ENaN

grdimage grd/$2 -Jm1:100000 -C106_gray.cpt -Ba5m -P | pageview -w 15 -h 30
```

This script is located in the simrad/ss/script directory which lies below CD100

5.3 Navigation (*Bob Janssen*)

5.3.1 Ship Navigation

Position throughout the cruise has been logged by a Trimble 4000AX GPS receiver. Sampling interval is 1-2 seconds. The receiver typically locks on to three or four satellites that are over a certain elevation over the horizon. GPS satellites transmit a radiosignal onto which a binary code is modulated. This code contains the time of transmission as well as the position of the satellite. The receiver determines the time elapsed between the emission from the satellite and reception of the signal at the receiver's antenna and therewith the range to the satellite. Ranging to two, preferably more satellites produces a position on earth. Single point fixes are exact within 100m. Precision and reliability increase when position is logged over prolonged periods of time.

However, when satellites disappear or appear under/over the horizon, the geometry changes and jumps (typically < 35 m) in position occur on the log. These jumps must be removed. On the computer screen, latitudes and longitudes are continuously displayed along with constellation changes and position jumps. This allows for a visual discrimination between more and less reliable data. Data

blocks that are deemed less reliable are given a lower status (lower statistic weight). Satellite count and PDOP can be used to support this somewhat subjective editing. Subsequently, an interpolation between higher quality fixes is carried out using dead reckoning (from ship speed and gyro heading). This process simultaneously corrects the ship's speed and heading. Standard deviation is typically <5m for datablocks with a constant satellite configuration. Finally, a 10 minute wide tapered averaging window smooths and resamples data to 10 second intervals complying with the Simrad sampling rate.

The results of this processing are stored in a file bestnav that is continuously maintained by RVS. The C-shell script bestnav_extract extracts a record per minute, containing time-stamp., latitude and longitude. The data are written to a file *ship_navigation.dat* in the format required for TOBI side-scan processing.

5.3.2 Tobi Navigation

The following is based on Javier Escartin's section in the CD99 cruise report. I slightly modified his Matlab and C-shell scripts to further automate the procedure and take into account the different setup of the computer network and file organisation.

A Matlab script (*navega.m*) calculates the location of TOBI using simple trigonometric approximations. Input is wire-out, ship-position and TOBI-depth. *Navega.m* computes TOBI position every 10 minutes and produces datafiles used to plot track charts, WHIPS side-scan processing, and replotting side-scan sonar at 1:50000 ("millimeters").

Output is written to respectively *tobixyz_lis.dat*, *tobixyz_sca.dat* and *tobixyz_lis.dat.*

Input files

TOBI data are supplied on CD-roms. A contiguous TOBI survey may be recorded on several CD's. The C-shell script navega_extract compiles the data that are needed for subsequent processing. It requires start and end time as well as the appropriate filenames.

Wire out data.

Wire out is inaccurately logged by TOBI. Therefore, we use the wire-out that is manually logged every ~10 minutes. File *cd100wireout.dat* contains readings in the following format that is readable by Matlab:

julian day	hour	minute	wire-out
106	16	40	1855
106	16	50	2105
106	17	00	2320
106	17	14	2569
106	17	20	2567

Navege_extract copies the data covering the appropriate time window into file *wire*.

5.3.3 TOBI depth

TOBI depth is extracted from the magnetics files (typically called *cd100_xyz_tobi.mag* where *xyz* is the number of the corresponding magneto-optical). Depth is logged every 0.5 second. *Navega_extract* extracts a reading every 10 minutes.

The time span over which TOBI positions are computed is equal to the time span over which wire-out data are provided (generally shorter than TOBI's mag files). Wire-out, TOBI-depth and ship's position are not necessarily sampled at the same rates and times. Navega.m performs an interpolation to obtain a matrix of time, wire-out, ship-position and TOBI-depth. The interpolation requires that the time window for the wire readings $(T_{w1} - T_{wn})$ fits within the depth readings window $(T_{d1} - T_{dn})$.

5.3.4 TOBI track calculation

TOBI navigation is computed by navega.m. Input files are the aforementioned *wire, ship_navigation.dat and tobi_nav.dat*. This program is based on positioner5.m by Stefan Hussenoeder (WHOI).

Wire is assumed to be straight so that TOBI lag behind the ship is

$$lag = \sqrt{wire^2 - depth^2} + 200$$

The lenght of the umbilical connectiong the depressor weight and TOBI is 200 m. For the purpose of this calculation, the umbilical is supposed to be straight and parallel to the wire. The (horizontal) wire angle is calculated at time *t=n*. The angle depends on the previous position of TOBI at *t=n-1*, ship's position at *t=n-1*, *n* and *n+1*, and a "viscosity" factor. This "viscosity factor" produces a smooth TOBI track . TOBI latitude and longitude are calculated from ship's position, lag and wire angle (**Figure 5.8**)

5.3.5 Processing Problems.

A small number of problems related to the format of the cd100_xyz_tobi.mag files occurred, these are detailed below, with reference to the data formating structure (Table 5.2 on page 111:,

cruise	run #	date	time	sec	alt	wire	depth	magnetics						
CD100		960415	1610	290	999	971	-5	104448.4	-98932.3	-105029.8	178124.4	-20.00	-20.00	0.00

Table 5.1

xyz is the number of the magneto-optical disk.
'date' in year, month, day;
'time' in hours, minutes,
'sec' in tenths of a second.
'alt' altitude in meters
'wire' wire-out in meters
'depth' TOBI depth in meters

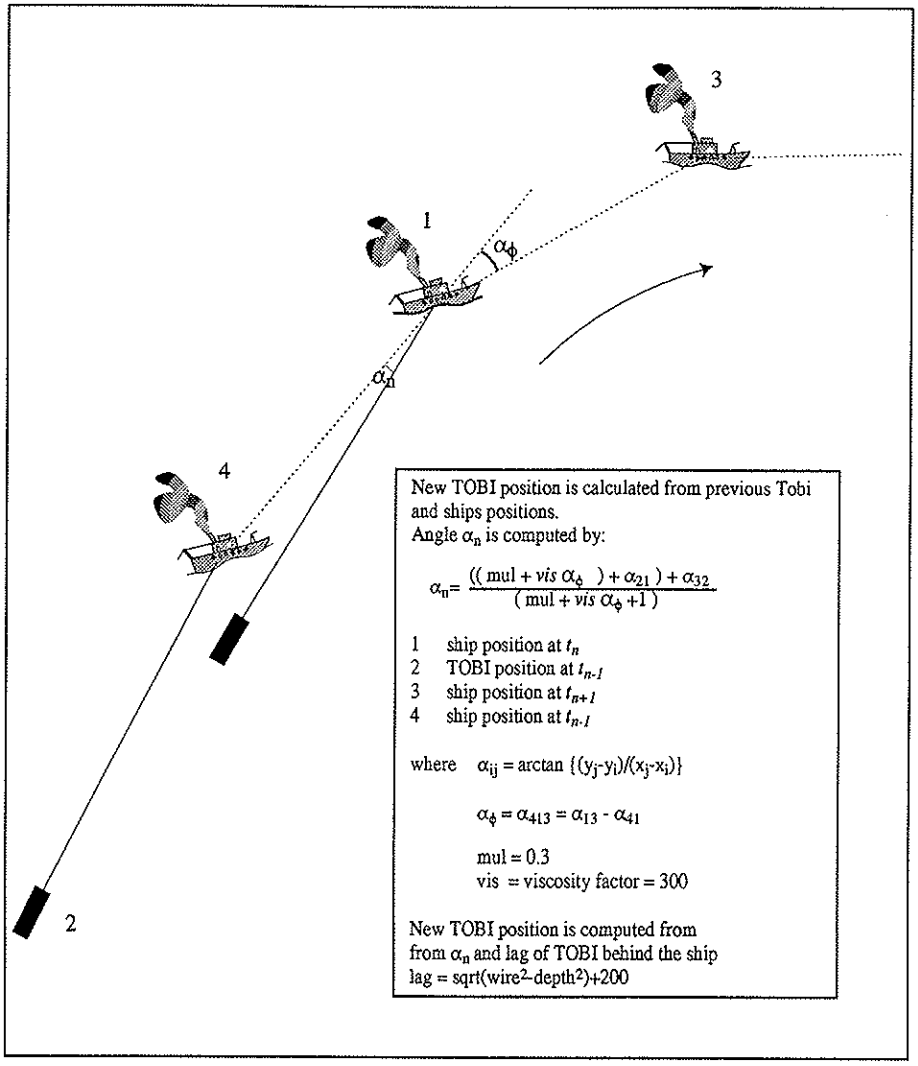

Figure 5.8 TOBI position calculation with respect to the ship on turns

At various occasions, the first column was written 'CD 100', creating a supplementary column. This confuses the awk-script navega_tobi.awk in navega_extract. Occurrences of 'CD 100' were subsequently replaced by 'CD100'.

A more serious matter is the occurrence of a sign change in the .mag files when TOBI depth exceeds -2^15/10 meters (-3277 m). If this (or any other unexpected jumps) occurs, navega.m will plot the read TOBI depths and then shift them to their correct position.

The time stamping in the .mag files are not in the correct ascending order (see below!). At irregular intervals, time readings jump back. This does not affect

navega.m because it automatically re-assigns correct corresponding times to depth readings.

			date	time	sec	alt	wire	depth						
CD100	run	#	960415	1900	370	637	2048	2026	25946.4	-8765.2	31820.0	41982.8	0.62	0.94	196.00
CD100	run	#	960415	1900	375	637	2048	2026	25959.3	-8787.2	31805.4	41984.4	0.62	0.78	196.00
CD100	run	#	960415	1900	380	637	2048	2026	25977.7	-8780.7	31793.8	41985.6	0.78	0.78	196.50
CD100	run	#	960415	1900	385	637	2048	2026	25972.0	-8769.9	31799.7	41984.2	0.47	0.47	196.50
CD100	run	#	960415	1900	390	637	2048	2026	25958.8	-8757.6	31814.3	41984.6	0.62	0.62	196.50
CD100	run	#	960415	1900	395	637	2048	2026	25959.1	-8747.4	31815.3	41983.4	0.78	0.94	196.50
CD100	run	#	960415	1900	380	642	2050	2026	25974.2	-8691.6	31818.1	41983.3	0.62	0.62	196.50
CD100	run	#	960415	1900	385	642	2050	2026	25980.3	-8665.1	31819.8	41982.9	0.47	0.47	196.50
CD100	run	#	960415	1900	390	642	2050	2026	25981.1	-8658.4	31820.4	41982.4	0.47	0.62	196.50
CD100	run	#	960415	1900	395	642	2050	2026	25974.0	-8701.0	31817.9	41985.0	0.47	0.47	196.50

Table 5.2

Navega.m converts latitude-longitude positions into cartesian UTM coordinates to predict TOBI positions. Coordinates pertain to a particular UTM zone depending on longitude. In one occassion (magneto-optical disc number 447-449) some of the eastern-most longitudes are in zone 23 which leads to a major shift in UTM coordinates. This problem was bypassed by imposing that all positions are situated in UTM zone 24.

compact disc	julian day	date	time	processed file
431	**106**	**4/15**	**16:11**	**tobi431_432_whp.dat**
	106	**4/16**	**08:06**	
432	**106**	**4/16**	**08:19**	
	106	**4/16**	**16:38**	
435_436	**115**	**4/24**	**23:37**	**tobi435_436_whp.dat**
	116	**4/25**	**10:35**	
436b	**116**	**4/25**	**10:35**	
	117	**4/26**	**00:46**	
437	**117**	**4/26**	**14:38**	**tobi437_443_whp.dat**
	118	**4/27**	**06:46**	
438	**118**	**4/27**	**06:46**	

Table 5.3

Time period that each navigation file overs together with a start and end time for all the Tobi sidescan sonar discs.

compact disc	julian day	date	time	processed file
	118	**4/27**	**22:55**	
439	**118**	**4/27**	**22:55**	
	119	**4/28**	**15:04**	
440	**119**	**4/28**	**15:04**	
	120	**4/29**	**07:14**	
441	**120**	**4/29**	**07:14**	
	120	**4/29**	**23:23**	
442	**120**	**4/29**	**23:23**	
	121	**4/30**	**15:35**	
443	**121**	**4/30**	**15:35**	
	121	**4/30**	**20:20**	
443_2	**122**	**5/01**	**10:55**	**tobi443_2_444_whp.dat**
	122	**5/01**	**22:36**	
444	**122**	**5/01**	**22:36**	
	123	**5/02**	**13:29**	
445	**125**	**5/04**	**17:49**	**tobi445_446_whp.dat**
	126	**5/05**	**09:58**	
446	**126**	**5/05**	**09:58**	
	127	**5/06**	**01:14**	
447	**127**	**5/06**	**04:43**	**tobi447_449_whp.dat**
	127	**5/06**	**20:46**	
448	**127**	**5/06**	**20:46**	
	128	**5/07**	**12:56**	
449	**128**	**5/07**	**12:56**	
	129	**5/08**	**03:32**	

Table 5.3 Time period that each navigation file overs together with a start and end time for all the Tobi sidescan sonar discs.

5.4 Underway Geophysics

No data processing has be carried out on the underway gravity and magnetics data.:

5.5 Directory structure used for CD100.

All cruise data were stored below the directory CD100 located with /local/disk1 on the Sun Ultra halmir. The hierarchy of directories is listed below:

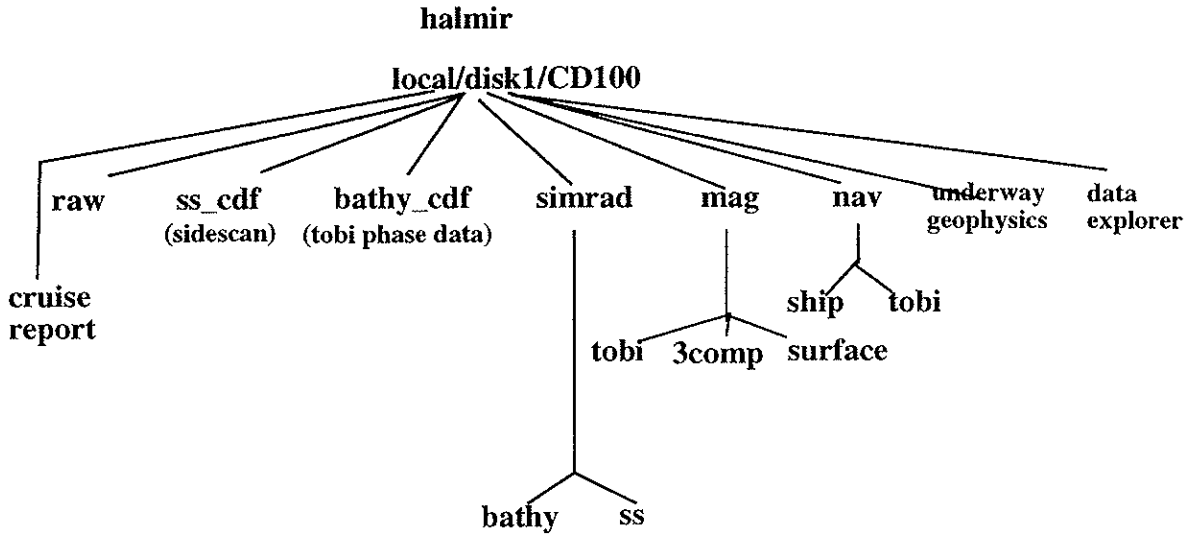

A complete backup of the directory was made on to two Dat tapes called Final backup1 and Final backup2. Final backup1 contains all the files listed below ss_cdf. Final backup2 contains all the simrad files and all other directories.

5.6 Data store

Several Dat tapes were made at regular periods throughout the cruise to retain copies of the raw data. The following table lists the Dat tape name and the contents of the tape

Name	Contents	File number	Data format
TOBI tape 1	Raw TOBI data CD#'s 431,432,435-436,436b,437,438	1	binary
TOBI tape 2	Raw TOBI data CD#'s 438, 439, 440, 441, 442	1	binary

Table 5.4 Dat tape contents

Name	Contents	File number	Data format
TOBI tape3	Raw TOBI data CD#'s 443a, 443b, 444	1	binary
TOBI tape 4	Raw TOBI data CD#'s 445, 446	1	binary
TOBI tape 5	Raw TOBI data CD#'s 447,448,449	1	binary
Raw SIMRAD Data	Raw simrad files days: 0001-120496-140741 to 0300-250496-030001	1	binary
Raw SIMRAD Data	Raw simrad files days: 0301-250496-040000 to 0600-070596-130000	2	binary
SIMRAD TAPE	Bathymetry and sidescan in both gri and ascxyz format JD 106-118	1	ascii
CD100 software	Copy of all software used to process TOBI data	1	binary & ascii

Table 5.4 Dat tape contents